8312353

Hubickyj, E. Olenka

THE EFFECT OF OPACITY ON THEORETICAL MODELS OF RR LYRAE STARS

City University of New York PH.D. 1983

University
Microfilms
International 300 N. Zeeb Road, Ann Arbor, MI 48106

PLEASE NOTE:

In all cases this material has been filmed in the best possible way from the available copy. Problems encountered with this document have been identified here with a check mark ✓.

1. Glossy photographs or pages _____
2. Colored illustrations, paper or print _____
3. Photographs with dark background _____
4. Illustrations are poor copy _____
5. Pages with black marks, not original copy _____
6. Print shows through as there is text on both sides of page _____
7. Indistinct, broken or small print on several pages ✓
8. Print exceeds margin requirements _____
9. Tightly bound copy with print lost in spine _____
10. Computer printout pages with indistinct print _____
11. Page(s) _____ lacking when material received, and not available from school or author.
12. Page(s) _____ seem to be missing in numbering only as text follows.
13. Two pages numbered _____. Text follows.
14. Curling and wrinkled pages _____
15. Other _____

University
Microfilms
International

THE EFFECT OF OPACITY ON THEORETICAL MODELS OF RR LYRAE STARS

by

E. OLENKA HUBICKYJ

A dissertation submitted to
the Graduate Faculty in Physics
in partial fulfillment of the requirements
for the degree of Doctor of Philosophy,
The City University of New York

1983

To my father, who never knew ...

To my mother, who may not have understood but strongly supported me ...

To my sister, Chrystyna, who taught and encouraged me to dream and explore the heavens.

To my friend Jeffrey, who taught and encouraged me to dream on the ground.

This manuscript has been read and accepted for the Graduate Faculty in Physics in satisfaction of the dissertation requirement for the degree of Doctor of Philosophy.

JAN. 28, 1983
date

Richard Mathews
Chairman of Examining Committee

Feb 14, 1983
date

Executive Officer

Supervisory Committee

The City University of New York

Abstract

THE EFFECT OF OPACITY ON THEORETICAL MODELS OF RR LYRAE STARS

by

E. Olenka Hubickyj

Adviser: Professor Richard Stothers

The RR Lyrae instability strip is investigated with computer models that were calculated using Carson opacities. A nonlinear computer program was applied to fundamental and first overtone modes of pulsation (*ab*- and c-type, respectively). Comparison of the models with observed surface light and velocity curves showed good agreement in phase of the secondary bump on the velocity curve (ϕ_v ~1.6) and light amplitude for M/M* = 0.60 - 0.65 log (L/L*) ~ 1.7, and Y = 0.25. A linear computer program was used to examine the location of the blue edges of the instability strip as mass and chemical composition varied. The results of the linear survey showed: 1) no substantial change in the PTLM relation due to opacity; 2) similar blue edges to those in previous studies that employed the Los Alamos opacity series are calculated with the Carson models for a lower helium abundance and with masses more consistent with evolutionary tracks. Several comparison tests of the models with observations showed good agreement. The overall linear results indicated a mass of 0.70 ± 0.05 M* and a helium content of 0.25 ± 0.04.

ACKNOWLEDGEMENTS

In the past few years there have been many people who encouraged my studies as well as nurtured my existence. It is time to give recognition and my thanks:

To Dr. Richard Stothers for suggesting this project on RR Lyrae instability strip, his guidance, and patience.

To Dr. Sastri Vemury for his guidance through the intricacies of the nonlinear pulsation computer program as well as for his moral support.

To the rest of the members of my committee, Professors V. Canuto, C. W. Chin, and C. Yuan, for discussions, encouragements, and "hasslings", (whether I needed it or not); also, the members of the CCNY Physics Department, particularly, Professors T. Boyer, H. Soodak, and M. Tiersten, who are primarily responsible for my pursuit of a career in Physics.

To Dr. Robert Jastrow and Dr. James Hansen, the past and present Directors of the Goddard Institute for Space Studies, who granted me the use of the Institute's computer and other facilities.

To everyone at GISS for their encouraging words and actions at a time when I needed it most and even at times when I didn't.

To the operations and systems groups; namely, Thomas Larkin and Kevin "O'Reilly'' Hopkins for making the machine work for me whenever I really needed it (which was all the time!), for miraculous turn-around on my

programs, for "Okie", and friendship greatly appreciated; to David Soll who helped by explaining IBMisms to me in English and doing it in less than 5,000 words (or 40 minutes, which ever came first).

To Ronnie Maddalena for being insightful and/or helpful at the strangest times; to Mike Miller for my wonderful cheesecake; to Chris Brest, who traded research horror stories and made me realize the "hazing-rights"; to Bill Rossow for encouragement and installments of confidences often needed; and to Philip Yacos for conversations that sometimes came to a point and sometimes didn't, but were always timely, kind, and sensitive.

To my family for carrying on without me (and sometimes with me), particularly, my aunt Leontyna and my cousin Lydia for always being there, ready to feed me, keep me company, and who were always ready to cry, laugh, and get angry at the world with me.

To Marilyn, for her kindness, tranquility, and for accepting me and letting me enjoy the Steiner family: Kristi, Jacqui, and Nicky, and of course, Jeffrey.

To Daria Zahorodny whose kindness and caring was and is boundless; to Micheal Chakansky whose friendship I couldn't and wouldn't do without; to Lilly Del Valle who helped me stay sane at times when insanity was the rule; and to Leonard Stein who has always been there in the "pinch", readily providing much needed support and help.

TABLE OF CONTENTS

Page

LIST OF TABLES

LIST OF FIGURES

CHAPTER 1: INTRODUCTION

Pulsating stars have been observed since about 1600. These pulsations are now known to derive from periodic oscillations of stellar envelopes which are driven by hydrogen and helium ionization reactions. There are several types of pulsating stars: Cepheid, RR Lyrae, and other Cepheid-like stars whose mechanisms are relatively well known, and δ Scuti, T Tauri and other variables that remain problematic (see Cox 1974 for a general review). RR Lyrae stars comprise a group having periods of from several hours to a day. They have absolute magnitudes that range from 0 to +1 mag. Luminosity, temperature, and radius fluctuations have been extensively modeled for these stars based on radial pulsation assumptions (Baker and Kippenhahn 1962, Christy 1966). These results will be tested in this thesis with new opacities computed by Carson (1976).

Opacities are tabulations of effective absorption coefficients which are arrived at through atomic models for various species interactions. They are used in classical stellar structure equations as implicit theoretical parameters (Cox and Guili 1968). Opacities represent the energy absorption and atomic scattering properties of stellar envelopes. They effectively damp or enhance energy transfer, as discussed further along.

While important in stars of all evolutionary stages, they are particularly important in the pulsation stages of stars. Most stars evolve through a relatively brief period of pulsation. The ramifications of considering pulsation periods include the possibility of estimating helium abundances and ages in galaxies, and in particular, that of the Milky Way.

Recent theoretical attention has been focused on determining stellar characteristics within the instability strip on the H-R diagram. The RR Lyrae instability strip has been examined by using Carson opacities in a general survey of linear and nonlinear pulsation models, complementing pioneering studies of Christy (1966).

1.1 Historical Background: Observational Data

Bailey, in the early 1900's, cataloged RR Lyrae light curves and divided them into three types : type *a* stars possess an asymmetrical light curve with an amplitude close to one magnitude; type *b* stars have a relatively smaller amplitude, a more symmetric but less smooth light profile, with a hump in light intensity on the ascending side and a corresponding shoulder on the descending branch; and type *c* stars which have comparatively symmetrical light curves and amplitudes of about one-half a magnitude. Many RR Lyrae stars have subsequently been found to undergo modulation of their light curves. RR Lyrae itself manifests a type *a* light curve but later in its 41-day cycle, evolves type *b* characteristics (Ledoux and Walraven 1958). The resultant suggestion that intrinsic variability ranges between an *ab* set (believed to

be pulsating in the fundamental mode) and a *c* set (believed to be pulsating in the first overtone mode) of curves is supported by the studies of RR Lyrae variables in globular clusters where there is a sharp distinction between the two sets.

Based on the Bailey classification, the observations of RR Lyrae stars were logged into stellar catalogs. Oosterhoff (1939) and others demonstrated that RR Lyrae variables in globular clusters fell into two distinctive groups, I and II, based on the mean period. Group I variables have a mean period of $0^d.55$ for *ab* stars and $0^d.32$ for *c* stars; group II variable stars have mean periods of $0^d.65$ and $0^d.37$ for *ab* and *c* types, respectively. Later, Kinman (1959) refined the Oosteroff groups in terms of metal abundances: group I metallic spectral lines are notably weak relative to the solar abundance, and group II are very weak. By means of theoretical investigations of RR Lyrae stars, the chemical composition of globular clusters can be estimated and in turn that of the associated galaxy, the Milky Way.

1.2 Historical Background: Theory

For as long as variable stars have been studied observationally, explanations for pulsation mechanisms have been made. Ideas on fluctuation range from those related to the precessing motion of presumed ellipsoidal star forms to periodic sunspot formation (Ledoux and Walraven 1958). The theories became much more sharply focussed as more became known about the nature of stars.

As an explanation for variability in stars, radial

pulsations were first proposed by A. Ritter in the 1880's. It was Eddington who set up a firm foundation for pulsation theory in Cepheid-like stars (1926, 1941, 1942) by using adiabatic energy equations. In a series of papers spanning a few decades Eddington presented a heat engine analogy to explain Cepheid type pulsation. A portion of the heat budget was related to gravitational mechanisms, and another portion was proposed to derive from the kinetic energy of hydrogen ionization. The numerical calculations of Zhevakin (1952 as reviewed in 1963) substantiated the hydrogen (and later the helium) ionization concept. Later workers, including Baker and Kippenhahn (1962,1965) refined the nonadiabatic model, and established helium ionization as the major factor supplying energy for driving Cepheid-like stellar pulsations.

In a region where an abundant element is undergoing ionization, the adiabatic gradient, (Γ_3-1), is small and the variation in temperature for the region is small. Since the luminosity varies with the temperature, the flow of radiation is decreased. At maximum compression, therefore, the energy that would otherwise have increased the thermal energy of the layer goes into ionization. Clearly, this absorption of energy at maximum compression can produce driving of stellar pulsation provided that its effects outweigh those of dissipation elsewhere in the star. This process is referred to as the "γ-mechanism".

A further enhancement of the driving region occurs if the opacity law is of the form $\kappa \sim \rho^n T^{-s}$, $(n,s>0)$. Then the variation of opacity is

$$\frac{\delta\kappa}{\kappa} \sim n\,\frac{\delta\rho}{\rho} - s\,\frac{\delta T}{T}$$

At maximum compression, in the region of decreasing (Γ_3-1), the reduced temperature variation will cause an increase in opacity. The radiation is thus "dammed up" and even more energy is absorbed. This process is called the "κ-mechanism". A more extensive and detailed discussion is available in Cox (1980J).

Christy (1966) greatly expanded and redirected the theory to fully include nonadiabatic, but still essentially heat engine based heat transfer equations, and nonlinear dynamical equations. The combined Baker-Kippenhahn (linear) and Christy (nonlinear) models successfully describe the structural parameters of pulsating stars. Numerous investigators, notably Iben and his coworkers, have examined the linearized properties of RR Lyrae stars, emphasizing the blue edge of the instability strip. In this and related work, parameters aside from opacities (Cox and Stewart 1965) were systematically varied. Carson and Stothers (1976) introduced the Carson opacities as the most recent restructuring of the BK/Christy model.

CHAPTER 2: APPROACHING THE PROBLEM

The theoretical studies of RR Lyrae variable stars have ranged from rough order of magnitude calculations to detailed computer modeling. The result of these endeavors is a formulated method of study that incorporates a linear approximation to the pulsation equations and a time evolved nonlinear solution of the same equations.

With these methods previous investigators have attempted to theoretically reproduce the observed periods, light and velocity curves, and boundaries of the RR Lyrae instability strip. All reasonable parameters available to the theoretician's control were varied: the star's mass, the chemical composition, the surface boundary conditions, and even the method of interpolation of the opacity tables (Tuggle and Iben 1972). It wasn't until the independently developed Carson opacities were introduced (Carson, Mayers, and Stibbs 1968, and Carson 1976) that the astronomer could finally realistically examine the effects of opacity on stellar structure.

The purpose of the present survey is to investigate the influence of the Carson opacities on the pulsation properties of RR Lyrae stars and to compare the results with observations and earlier studies. The period and blue edge investigations of the RR Lyrae instability strip

are performed by using a computer program based on the linearized approximation to the pulsation equations. Full amplitude, nonadiabatic, nonlinear models are also needed in order to compare the theoretical light and velocity curves with those observed.

2.1 The Linear Survey Description

The amplitudes of the pulsators near the blue edge of the RR Lyrae instability strip are small compared with those further into the strip. As a result, a linear, non-adiabatic computer program study can reliably determine the location of the blue edge on the H-R diagram. This same program can dependably calculate periods of theoretical RR Lyrae models since the nonlinear effects on the period are minimal (Stellingwerf 1975).

The basic structure of the linear computer model survey was designed to study the dependence of the blue edge on mass and chemical composition. A series of models calculated for a particular stellar mass and chemical composition all had the following luminosities: log L/L_* = 1.4, 1.6, 1.7, 1.8, 2.0. The effective temperature was varied so that the blue edges for the fundamental, first, and second overtone modes of pulsation were well determined. Extra models were calculated across the instability strip for two reasons. One reason was to get a good representation of the period variation across the instability strip. Another reason was the behavior of the blue edge of the second overtone mode. In calculating the models, it was noticed that this blue edge began to curve over to lower luminosities at very cool effective

temperatures. For the purpose of carefully mapping out this extended blue edge models were computed with appropriate luminosities and temperatures.

In this manner seven series of models were calculated using Carson opacities and varying stellar parameters. The opacity was obtained using the method of spline interpolation of the opacity tables. A series of models was also calculated using the less accurate method of linear interpolation of the Carson opacity tables in order to examine the difference in the blue edges due to the method of interpolation. A direct comparison of the effect of opacities themselves was made possible by calculating a final series of models with the most recent Los Alamos opacity tables (kindly supplied to R. Stothers by A. Cox).

Three different masses were chosen to examine the variation of the results with mass: 0.4 M*, 0.6 M*, 0.8 M*. The main reason for this range of values is that given by Bohm-Vitense, Szkody, Wallerstein, and Iben (1974). Theoretical evolutionary studies have demonstrated that 0.4 M* is the probable lower limit to the mass of the helium core of a red giant star. The upper limit of 0.8 M* is that mass for which a star presently evolving off the main-sequence will reach the horizontal branch without prior mass loss.

Examining changes of pulsation characteristics due to chemical composition called for a wide range of assumed helium and metal abundances. The composition parameters used were the following: (Y,Z) = (0.25,0.00), (0.25,0.005), and (0.24,0.021), for metal content

variation studies; (Y,Z) = (0.25,0.00), (0.50,0.00), and (0.75,0.00), for helium content variation studies.

Table 1 contains a summary of the series of models comprising the linear computer model survey. For purposes of comparison series #1 was chosen as the standard. The mass and helium content of 0.6 M* and 0.25, respectively, seem to be the best mean values given by the recent published studies of RR Lyrae stars (Stothers 1981, Cox, Hodson, and Clancy 1983).

Figure 6a in the paper by Carson, Stothers, and Vemury (1981) illustrates the Z-dependence of the type II Cepheid model blue edges calculated with Carson opacities. Extrapolating downward to luminosities valid for RR Lyrae stars, one observes the blue edges to converge. Since other authors (Iben and Huchra 1970, Iben 1971b, Tuggle and Iben 1972) have also discussed this minimal dependence on the metal parameter, the Z = 0.00 value in the standard model is considered an adequate choice.

2.2 The Nonlinear Survey Description

The nonlinear survey consists of a series of computer models of stars in the fundamental and first overtone modes of pulsation. Stothers (1981) reported the results and analysis of the theoretical models pulsating in the fundamental mode. On the basis of the conclusions in that study a grid was chosen for the theoretical first overtone mode oscillators.

From the previous work on the Cepheid variables it was shown (Carson, Stothers, and Vemury 1978,1981) that the phases of the secondary bumps on the surface light and

TABLE 1

PARAMETERS FOR THE LINEAR SURVEY MODELS

Series	M/Mx	Y	Z	Comments
1	0.6	0.250	0.000	
2	0.6	0.250	0.005	
3	0.6	0.240	0.021	
4	0.4	0.250	0.000	
5	0.8	0.250	0.000	
6	0.6	0.500	0.000	
7	0.6	0.750	0.000	
8	0.6	0.250	0.005	Los Alamos Opacity
9	0.6	0.250	0.000	linear interpolation

velocity curves were sensitive indicators of opacity. Regardless of the type of Cepheid (classical or type II) the phases calculated with Carson's opacities differed substantially from those using the Cox-Stewart or the new Los Alamos opacities. The agreement of the phases with observations in the case of the Carson models was doubly advantageous because the masses predicted for these Cepheid variables corresponded well with those masses predicted from evolutionary tracks.

The grid for the nonlinear fundamental mode models was designed to determine the mass and the helium content of RR Lyrae stars. This was done, as in the case of the Cepheid variables, by comparing the theoretical light and velocity curves with the observed ones. Two important determining factors were the phase of the secondary bump on the surface velocity curve and the phase differences between the light and velocity curves. Barring the slightly oversized predicted phase lag between the light and velocity curves, the full amplitude fundamental mode models reported by Stothers (1981) exhibited the same kind of agreement with observation and evolutionary track studies that was demonstrated by the Carson model Cepheids. It would be beneficial if the first overtone full amplitude models had some special characteristics so that there would exist independent means to corroborate the conclusions of the fundamental mode models.

Preston and Paczynski (1964) measured the phase lag between the light and velocity curves of observed RR Lyrae stars of both *ab* and *c* types. This phase lag is defined as

$$\delta\varphi(\text{mean}) = \varphi(\langle V\rangle) - \varphi(\langle v_{rad}\rangle)$$

where $\varphi(\langle V\rangle)$ is the phase of the time averaged mean visual magnitude on the rising branch of the light curve and $\varphi(\langle v_{rad}\rangle)$ is the phase of the time averaged radial velocity on the falling radial velocity curve. For the c-type pulsators the phase of mean velocity was found to lag mean light by about ~ 0.15 P. Detailed models of theoretical first overtone pulsators have not been extensively published. Therefore, a determination of whether this phase lag could be reproduced theoretically, as well as be an indicator of the physical nature of the RR Lyrae variables, was a prime objective in the examination of the first overtone pulsator models.

.Considering the amount of time involved in reaching full amplitude pulsation using the nonlinear computer program, the grid for the fundamental and first overtone models must be economical. The mass variation of the full amplitude fundamental mode model stars was studied by using the masses: 0.377 M*, 0.578 M*, 0.679 M*. The reason for these choices is basically the same as discussed in the description of the linear survey. All but one theoretical model was calculated with a helium abundance of Y = 0.25; the other model had Y = 0.49. This allowed an examination of helium dependence. The metal abundance was taken to be Z = 0.005 since the metal content is believed to be small in globular clusters. All the models were calculated using this value because the choice of Z is unimportant (Carson, Stothers, and Vemury 1981). Two luminosities used were: log L/L* = 1.578, 1.800. These luminosities

were chosen to compare with earlier surveys; the lower luminosity model was to be compared with Christy's work (the 5g F model star) and the higher luminosity model with that of Stellingwerf (1975). The effective temperatures coincide with those used by Stellingwerf: log T_e = 3.792, 3.813, and 3.833.

The stellar masses used for the first overtone model grid did not vary as much as for the fundamental mode models. The two masses used, 0.578 M* and 0.679 M*, are within the reasonable range of masses predicted by previous studies (Stothers 1981). Only one chemical composition was used: (Y,Z) = (0.25,0.005), since the helium dependence was examined adequately in the fundamental mode investigation. The luminosities and effective temperatures were chosen so that the periods of pulsation would fall into a period range of $0^d.3 - 0^d.4$, as quoted by van Albada and Baker (1973) to be the typical range of c-type RR Lyrae variables in globular clusters. The luminosities used were log L/L* = 1.585 and 1.700. The effective temperatures were log T_e = 3.813, 3.851, 3.869. The parameters for all the models of the nonlinear computer survey are summarized in Table 2.

2.3 Numerical Methods

Numerical sophisticated computer modeling has become "de rigeur" to the theoretical astronomer. The success of the early linearized computer models (Zhevakin 1952, Cox 1963, Baker and Kippenhahn 1965) in predicting the observed periods and demonstrating the driving mechanism for pulsation was enhanced by Christy's (1966) nonlinear,

TABLE 2

PARAMETERS FOR THE NONLINEAR SURVEY MODELS

Fundamental Mode Models

Series	M/Mx	Y	Z	log L	log T
1	0.377	0.250	0.005	1.585	3.813
2	0.578	0.250	0.005	1.585	3.813
3	0.679	0.250	0.005	1.585	3.813
4	0.578	0.250	0.005	1.800	3.792
5	0.578	0.250	0.005	1.800	3.813
6	0.578	0.250	0.005	1.800	3.833
7	0.578	0.490	0.020	1.585	3.813

First Overtone Mode Models

Series	M/Mx	Y	Z	log L	log T
1	0.578	0.250	0.005	1.585	3.813
2	0.578	0.250	0.005	1.585	3.851
3	0.578	0.250	0.005	1.585	3.869
4	0.578	0.250	0.005	1.700	3.851
5	0.578	0.250	0.005	1.700	3.869
6	0.679	0.250	0.005	1.585	3.813
7	0.679	0.250	0.005	1.700	3.851

nonadiabatic computer model survey. Both methods provide the astronomer with powerful means by which he/she can develop a full and detailed picture of variable stars.

Both the linear and nonlinear computer models require the solution of the radial differential equations of spherical stellar structure :

$$\frac{\partial M}{\partial r} = 4\pi r^2 \rho \qquad (1)$$

$$\frac{\partial^2 r}{\partial t^2} = -\frac{GM\rho}{r^2} - \frac{\partial P}{\partial r} \qquad (2)$$

$$T * \frac{\partial S}{\partial t} = -\frac{\partial L}{\partial M} \qquad (3)$$

$$\frac{\partial T}{\partial r} = -\frac{3}{4ac}\,\frac{\kappa\rho}{T^3}\,\frac{L}{4\pi r^2} \qquad (4)$$

To be added are equations of state and opacity. The equation of state, involving the Saha ionization equation, is applied to a mixture of radiation and non - degenerate gas. The gas consists of hydrogen, helium, and an average metal all of which are in various degrees of ionization. This gas mixture is assumed to be fully ionized for temperatures greater than log T = 5.5. Carson opacities and the method of calculation employed in the computer programs will be discussed in the next section.

In solving for the small amplitudes of the physical variables, the equations of structure and motion are linearized by expanding the functions in a Taylor series about the equilibrium model values. If f is the general representation of any variable, the equations are then

rewritten by substituting for each parameter the expression $(f_0 + \delta f)$, where f_0 is the equilibrium value and δf is a small perturbation comprised of space and time components. Only first order terms are retained. Since the pulsation follows simple harmonic motion a time dependence of the form of $e^{i\omega t}$ is used where ω, the frequency of the oscillation, is complex $(\omega=\omega_R+i\omega_I)$. When the the second order terms are no longer negligible, amplitudes must be obtained by a nonlinear technique.

(a) Carson opacities and methods of calculation

The development of the Carson opacity tables is discussed by Carson (1976). One of the earliest applications of these new opacities was reported by Stothers (1974) who did an opacity comparison study for homogeneous stellar models with two Population I chemical compositions. However, it is pulsation theory that provides the best testing ground for opacity calculations (Carson and Stothers 1976). By means of the explicit presence of the opacity and its derivatives in the pulsation equations a thorough investigation of the various opacity tables may be performed.

The hot Thomas-Fermi model of the atom for all the elements heavier than hydrogen and helium was utilized in constructing the Carson opacity tables. The series of Los Alamos opacity tables (Cox and Stewart 1965) were developed using the "hydrogenic" model of the atom. Figure 1 illustrates comparative plots of the Carson and the new Los Alamos opacities for the chemical compositon

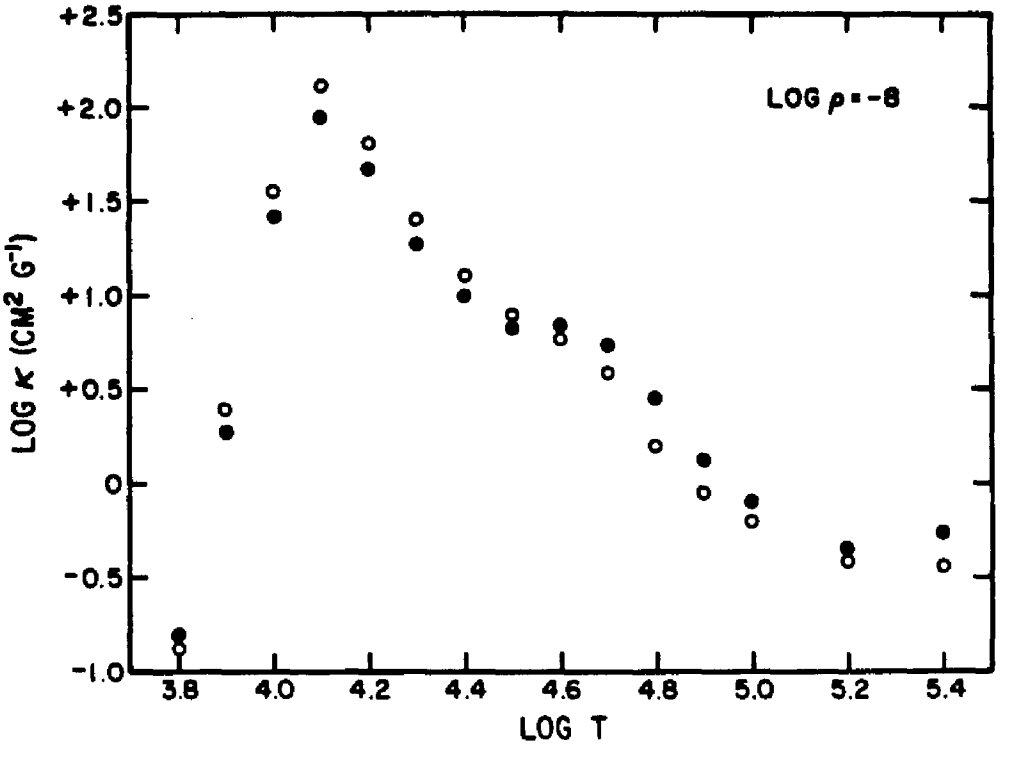

FIGURE 1

COMPARISON OF CARSON AND NEW
LOS ALAMOS OPACITIES

of (Y,Z) = (0.25,0.005). The peak at log T ~ 4.1, in the hydrogen ionization temperature region, is slightly smaller for the Carson opacity. A prominent bump occurs in the second helium ionization temperature range (centered around log T ~ 4.6) in the Carson opacities. The same feature for the new Los Alamos opacities is slightly more than an inflection in the curve. There is another bump in the Carson opacity at temperatures associated with CNO ionizations (about log T ~ 5.6). The Los Alamos opacities are flat at this same temperature. However, this has little effect on the pulsating model envelopes since this temperature occurs well within the envelope where the amplitudes of pulsation are very small.

All but one of the linear series of models were calculated using Carson opacities. The new Los Alamos opacity table was used for the last series of models to investigate directly the effect of varying the opacity on the linear pulsation results. All but one of the linear series of models used a spline interpolation method for calculating the opacity from the tables. A 4-point linear interpolation scheme that was used for all of the nonlinear model calculations was applied to one series of linear models. In this manner the effect of varying the methods for calculating the opacities could be examined.

Rood (1971) reported that errors due to linear interpolation in opacity tables were not negligible and that they may be large enough to negate any physical improvements in the opacity tables. Switching to multipoint interpolation methods greatly enhanced the accuracy of his stellar model calculations. Tuggle and

Iben (1972) calculated the opacities for their RR Lyrae linear models using the spline interpolaton method by which they demonstrated substantial improvements in their results. The method of cubic splines used in this survey is the technique described in Young and Gregory (1972) as applied to the scheme described in Tuggle and Iben (1972). The advantage of the spline method is the built-in continuity of the interpolated values as well as of their first and second derivatives.

Three model envelopes were calculated (in a manner to be described in the next section) differing mainly in the method of interpolating the opacity. The stellar parameters correspond to those of Christy's 5gF model ($M = 0.578\ M*$, $\log L/L* = 1.585$, $\log T_e = 3.813$). The Carson opacity table for the chemical composition $(Y,Z) = (0.25, 0.005)$ is used for two of the models and Christy's (1966) analytical opacity formula approximating the Cox and Stewart (1965) opacity tables was applied to the third model. The opacities and their first derivatives, $(\partial \ln\kappa/\partial \ln T)_\rho$, that were calculated in the model using the method of spline interpolation are plotted in Figure 2a. The same quantities calculated by means of the 4-point interpolation scheme are graphed in Figure 2b. Discontinuities in the derivatives are clearly visible. Figure 2c illustrates the resulting values of the Christy approximating opacity formula.

There do not appear to be significant differences in the opacity values other than intrinsic ones (i.e. Carson vs. Cox-Stewart). Careful examination of Figures 2a and 2b demonstrates that both methods of interpolation provide

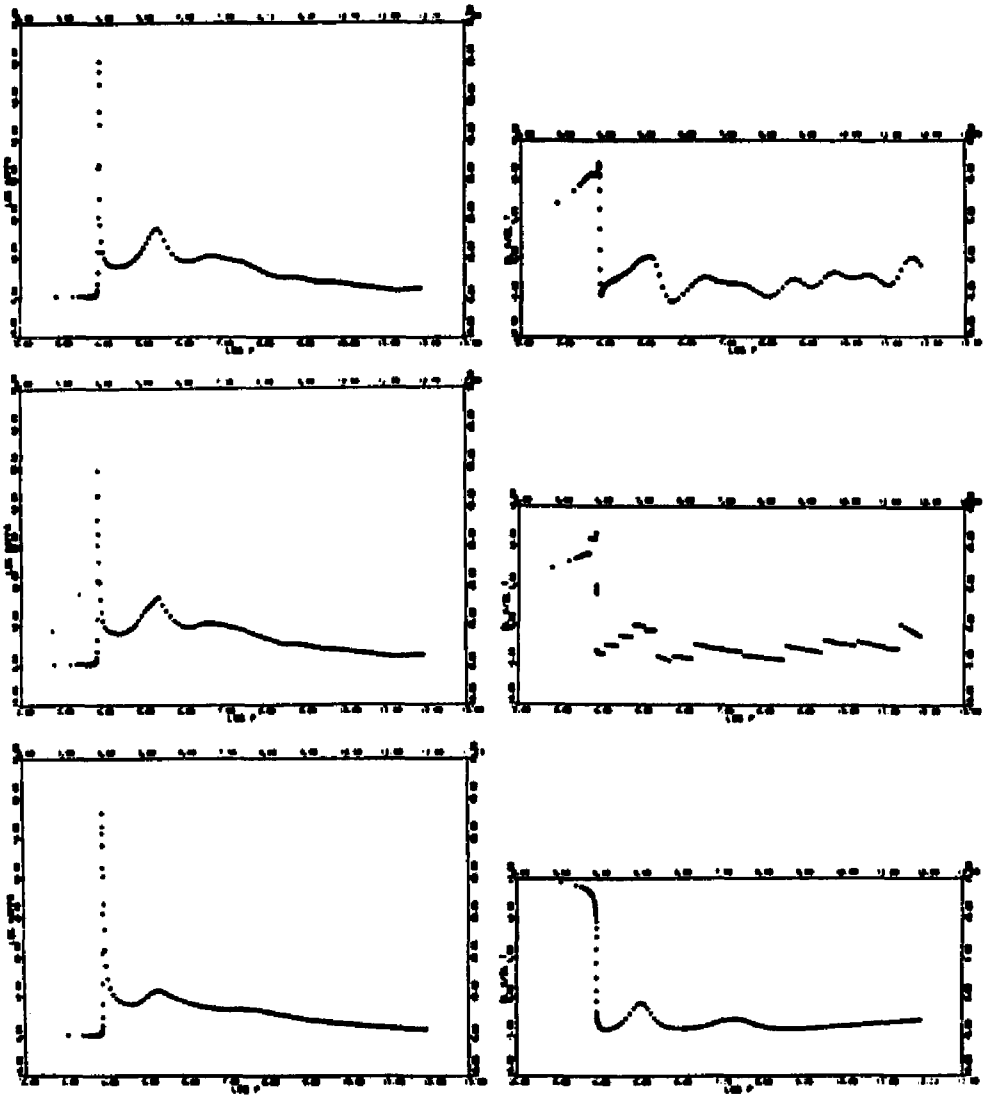

FIGURE 2

OPACITY AND $(\partial \ln \kappa / \partial \ln T)$ FOR DIFFERENT METHODS OF CALCULATION OF THE OPACITY

similar and continous values for the opacity. This should not be surprising since there is rather fine zoning of the shells in these envelope models. However, the distinction in method is quite obvious in the plots of the first derivatives. Though the shape of the curve is basically the same, the continuity in the spline-determined values clearly illustrates the advantage of this method over the linear interpolation scheme. It should be noted of course that the cubic spline method enhances the accuracy of calculations within the table, not the accuracy of the opacity table itself.

In light of the above discussion the use of the 4-point interpolation method in the nonlinear calculations should not be considered unreasonable. The nonlinear model envelopes are calculated with about 40 mass zones. Therefore, the 4-point linear interpolation method is more than adequate for this roughly zoned nonlinear stellar envelope.

(b) The linear computer program.

The solution of the linearized pulsation differential equations is basically an eigenvalue problem (Baker and Kippenhahn 1962, 1965). The Castor (1971) scheme was chosen because it is a straightforward method for calculating the eigenvalues and eigenfunctions. The stellar structure equations (1)-(4) are first integrated using Heun's numerical integration method (Kaplan 1964). Pressure, the fastest changing variable, is taken to be the independent variable. A fine mesh of pressure layers is calculated and the other associated stellar variables are

used to evaluate parameters in the set of finite-difference equations appropriate for a static shell model.

The boundary conditions are the same as used by Iben (1971a) and Castor: a stationary inner boundary is placed at the bottom of the stellar envelope and there is assumed to be no variation in the energy supply ($\delta L = 0$); each wave of pulsation is reflected at the outer surface boundary and the pressure is calculated from radiative transfer theory.

Using a form of the Baker and Kippenhahn (1965) linearized pulsation program Iben and Huchra (1971) tested many variations in stellar parameters. They showed that the blue edges, particularly the first overtone edges, were essentially identical whether or not convection was explicitly considered. Carson and Stothers (1976) have also pointed out that near the blue edge the size of the convection zone is much smaller in the hydrogen ionization region on account of the Carson opacities. As a result convection is considered unimportant in establishing the blue edges and is not incorporated into the stellar structure equations.

Pulsations involve the envelopes of stars. The calculation of the mechanical and thermodynamic variables at each pressure level of the equilibrium model is initialized at the top of the atmosphere set at optical depth $\tau = 0.005$. The numerical integration continues inward to the inner boundary, defined by the radial position of about 20% of the total radius of the star. A restriction on the temperature change in the integration includes an iteration process so that the following

relation between consecutive thermal layers is satisfied:

$$\frac{T_{i+1} - T_i}{T_i} = 0.01$$

where the i^{th} layer is the one closer to the surface. This proves to be important, considering the magnitude of the temperature differential across the hydrogen ionization zone. Typically, equilibrium model envelopes contain 700 - 800 layers.

This first cycle of the integration process also yields also the mass levels within the envelopes. To arrive at a static model envelope convenient for later pulsation calculations, the pressure layers are combined in groups of a set number. Typically, there are seven layers to one shell. The shell finite-difference equations require the mass to be the independent variable. By combining these pressure layers, the mass of each shell and initial guesses for other stellar parameters neccessary for the next cycle of integration are obtained.

The finite-difference equations used to numerically integrate the model envelope in the Castor scheme are as follows:

$$\frac{\partial^2 r_l}{\partial t^2} = - \frac{GM_l}{r_l^2} - 4\pi r_l^2 \frac{P_l - P_{l-1}}{DM2_l} \qquad (5)$$

$$T_l \frac{\partial S_l}{\partial t} = \frac{L_l - L_{l+1}}{DM1_l} \qquad (6)$$

$$V_l = \frac{4\pi}{3} \frac{r_{l+1}^3 - r_l^3}{DM1_l} \qquad (7)$$

$$L_l = \frac{4\sigma}{3} (4\pi r_l^2)^2 \frac{T_{l-1}^4 - T_l^4}{0.5(\kappa_l DM1_l + \kappa_{l-1} DM1_{l-1})} \qquad (8)$$

The subscript l is the shell index for which l = 1 is the stationary inner-most boundary and l = N refers to the surface. The thermodynamical variables are evaluated within the shell and range from l = 1 to l = N. The mechanical variables (r_l, M_l) are evaluated at the interfaces of the shells and therefore range from l = 1 to l = N + 1. The mass of shell l is $DM1_l = M_{l+1} - M_l$, and $DM2_l = 0.5(DM1_{l+1} + DM1_{l-1})$ is the mass of the l^{th} interface. The intershell temperature variation is now held at less than 6% (easily achieved because of the initial 1% condition). The final model envelope contains about one hundred mass zones.

When the shell difference equations (5)-(8) are linearized the time differentials are replaced by factors of $i\omega$, the eigenfrequency. These equations then provide for all the unknown physical variables to be expressed in terms of only the radius variation, δr_l, and the entropy variation, δS_l. Full information about the linearized pulsating model is obtained once the eigenvalue, ω, and the eigenfunctions, δr_l and δS_l, are known.

Subsequent steps in the Castor methodology will be briefly outlined since a detailed description may be found in his paper. The first step is to solve for the adiabatic properties, which is accomplished by setting $\delta S_l = 0$ in

the equations. The resulting eigenfrequency, ω_0, and eigenfunctions, (δr_1) and (δS_1) are real. The adiabatic quantities are now applied to initialize the process of calculating the nonadiabatic eigenvalue. First order perturbation theory is employed. The correction to the adiabatic eigenfrequency produces an initial guess to the imaginary part of the nonadiabatic eigenvalue. The final solution involves an iterative process of upgrading the eigenquantities. With the value obtained from perturbation theory a quick convergence to the final solution of the nonadiabatic equations is ensured.

Once the eigenquantities are known it is a simple task to evaluate the period and the radial fluctuations of the stellar parameters (temperature, luminosity, etc.). In addition, other related quantities such as growth rates and the kinetic energy of the pulsation are easily calculated. In this manner full information about linearized pulsations for the fundamental, first, and second overtone modes was acquired.

(c) The nonlinear computer program

The full amplitude models for the fundamental and first overtone modes were calculated using the nonlinear computer program described by Vemury and Stothers (1978). The method of solution of the nonlinear, nonadiabatic equations has been published fully by Christy (1964, 1967), who was first to develop a successful scheme, as well as by Stobie (1969). It is left to the interested reader to study these papers for details of the numerical methods. In the present discussion will primarily report

that part of the process involved in the actual running of the computer program to reach full amplitude pulsation.

The process of calculating the static model envelope is similar to that in the linear computer program. Differences that exist are due to restrictions ensuring physical and mathematical continuity. On the average there are about 40 zones to a model which is a much smaller quantity than the hundred or so zones typically found in the linear model envelopes. Once a suitable static model envelope is calculated, a superimposed velocity profile sets the model star into pulsation.

The results of the theoretical fundamental mode models are presented and discussed by Stothers (1981). Calculating these models was a relatively uncomplicated process. Full amplitude pulsation was reached with frequent artificial amplifications of the pulsation velocity (as described in Vemury and Stothers 1978) whether or not a careful and precise velocity profile was introduced. Almost all the models were initiated into motion with an initial velocity profile of

$$v_0 = -10x^5 \text{ km/sec} , \quad x = (r/R)$$

as suggested by Christy (1964).

In the case of the first overtone mode models a suitable initial velocity profile was difficult to find. Christy's (1964) suggestion of

$$v = (-20x^{10} + 6x^5) \quad \text{km/sec} ,$$

produced unreasonable values for inducing pulsation in my models. (By unreasonable, I mean that there was significant scatter in the period and velocity amplitude in the first 6 periods.) A suitable velocity profile was established by fitting a polynomial of the form

$$v = ax^{p1} + bx^{p2}$$

to the linear ($\omega_R \delta r$) profile, in a manner similar to that of Stobie (1969). It is important to choose a velocity profile so that only the mode to be studied is present. Since the growth and decay rates for RR Lyrae stars are on the order of 10,000 periods it is obvious that any contamination by an extraneous mode is a strong disadvantage. Repeated attempts to find such a velocity distribution were unsuccessful in picking out a pure first overtone mode. However, the effects of the fundamental mode and higher overtones appeared to be slight and with frequent artificial amplifications a satisfactory full amplitude first overtone model was achieved.

As the computer program evolves the pulsating model star the period, velocity amplitude, and maximum kinetic energy of the pulsation as well as a few other quantities are monitored. The criterion for reaching full amplitude pulsation is a zero growth rate of the maximum kinetic energy. Once the maximum kinetic energy has leveled off the calculation is continued for a few more periods so as to allow all the quantities to settle down, at which point the computation is terminated. However, it turns out that a few more periods are not sufficient sometimes for the

final full amplitude values to converge. By averaging these values over a few periods an adequate final result is obtained and the need for further computation is avoided. One of the models was calculated to such a large number of periods that all the cycles repeated exactly. Application of the averaging process to earlier period values for this model confirmed the validity of this averaging method in obtaining satisfactory full amplitude results for the other models.

The surface and interior zonal plots for the models were graphed after full amplitude was attained. A simple smoothing process of the data described by Carson, Stothers, and Vemury (1981) was used when the surface velocity and light curves were graphed. With the combined numerical results listed in the tables and with the graphical illustrations a full comparative study with previous surveys, and more importantly, with observations may be accomplished.

CHAPTER 3: PRESENTATION AND DISCUSSION OF THE LINEAR SURVEY RESULTS

3.1 Periods

The period of a variable star is related to its mean density as :

$$P \left(\frac{\rho}{\rho_*}\right)^{0.5} = Q$$

where Q is the so-called pulsation constant by which different types of variable stars are characterized. Any stellar system undergoing harmonic motion as a result of its gravitational forces obeys this relationship (Ledoux and Walraven 1958). By applying the Stefan - Boltzmann radiation law this equation may be rewritten in terms of observable stellar parameters as :

$$\log P = -3.0 \log T_e + 0.75 \log L - 0.5 \log M + \text{const} \quad (9)$$

The luminosity and mass are in solar units. The data for the fundamental mode in this linear survey has been fitted to this same form of the equation with the result

$$\log P_0 = -3.43 \log T_e + 0.835 \log L - 0.86 \log M + 11.318 \quad (10)$$

Exact agreement of the coefficients, in the strict sense,

does not exist but the essence of the two equations is the same; namely, the sign and the order of magnitude of the coefficients agree. Similar fitted equations have been presented by van Albada and Baker (1971) and Tuggle and Iben (1972 - hereafter TI).

The suitability of equation 10 in connection with data of series 1, Table 1, is illustrated for a constant mass of 0.6 M* and constant luminosity in Figure 3a (for (Y,Z) = (0.25,0.00). The same data are shown in comparison with the corresponding van Albada and Baker equation (Figure 3b) and TI equation (Figure 3c). Present data are most consistent with equation 10 represented in Figure 3a, but fair consistency is shown throughout. Therefore, the opacities, which differ in the three cases, (Carson opacities for the lines of Figure 3a, Christy's approximating formula to the Cox-Stewart opacities for the lines of Figure 3b, and the Cox-Stewart opacity tables interpolated using the spline method for the lines of Figure 3c) are not a sensitive parameter for the period.

The period of a variable star depends on its physical structure which indirectly depends on opacity. But opacity does not correlate with the period, as demonstrated by Figure 3. Carson and Stothers (1976) have shown that the opacity will not manifest itself to any great degree on the theoretical structure appropriate to these variables. Plots of Figure 3 simply underscore this finding.

Similar plots for the rest of the series in Table 1 reveal a slight dependence on metal content. The other calculated values of the periods based on equation 10 were

a)

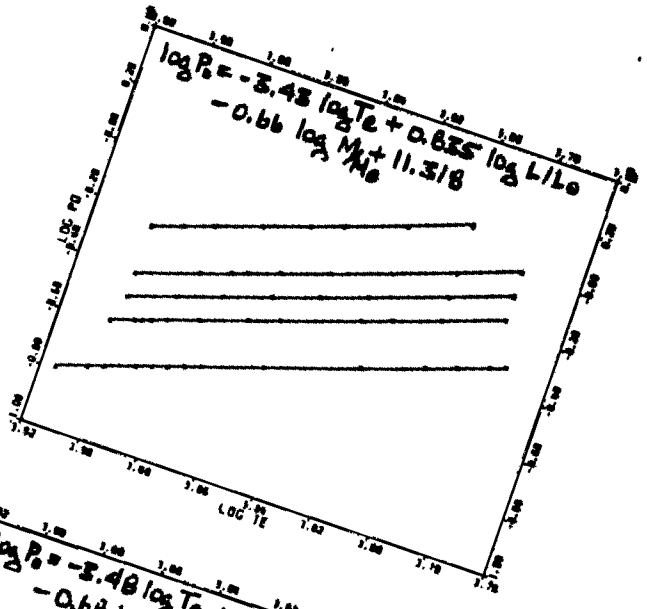

b)

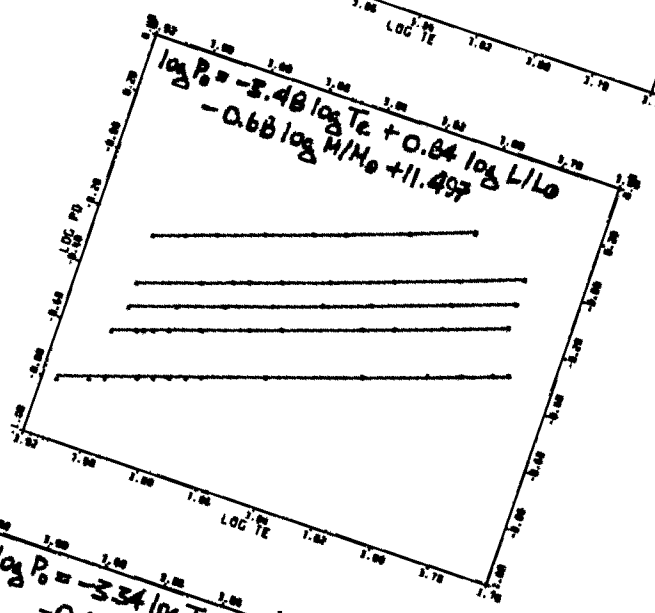

c)

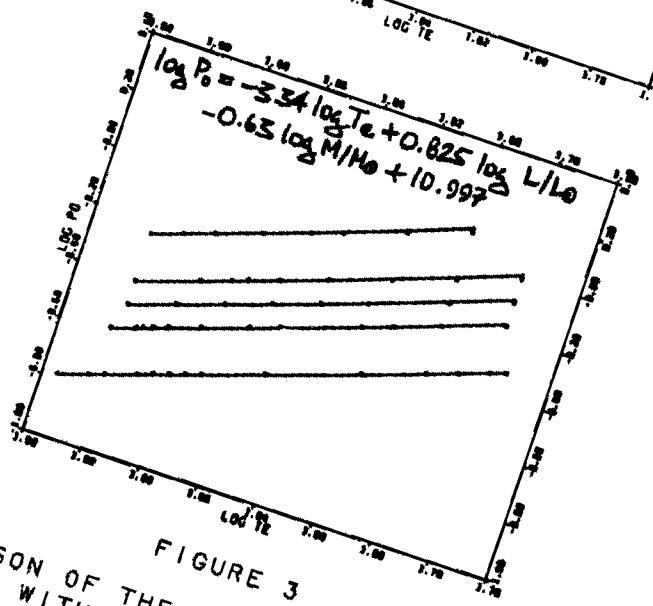

FIGURE 3

COMPARISON OF THE THREE DIFFERENT PTLM RELATIONS WITH DATA OF THE LINEAR SURVEY

always well within 1% of the data values. But those series for which metal abundances were varied (series #2 and #3) showed about a 2% variation from the fitted formula. However, compared with the variation in period due to luminosity, temperature, and mass, the metal content exerts a negligible effect.

The effects of higher overtones on pulsational properties are frequently characterized by taking the ratio of the period of the overtone to the fundamental period, P_1/P_0. The linearity of the relationship P_1/P_0 to P_0 has been discussed and accepted in the literature (see Cox, King, and Hodson 1980, Figure 2, as a recent example). Guided by this and the equation derived by Stothers (1981) for his linear data on RR Lyrae stars, the data of the present linear survey were fitted to

$$P_1/P_0 = -0.059P_0 + 0.067\log(M/M*) + 0.03Y^{0.6} - 0.06Z^{0.4} + 0.776$$

The differences between the values calculated using the above equation and the actual data values range from -0.001 to +0.001. In finding the best fit the process seemed hampered by the sensitivity to the luminosity. The two ratios, P_1/P_0 and P_2/P_0, are plotted in Figure 4 for the theoretical models of mass 0.6 M* and chemical abundance of (Y,Z) = (0.25,0.00). Though the linearity is more than acceptable, especially in the period range of 0.4-0.9 day, it should be noted that there exists a modest spread in the ratio due to luminosity.

In order to verify this scatter the linear data

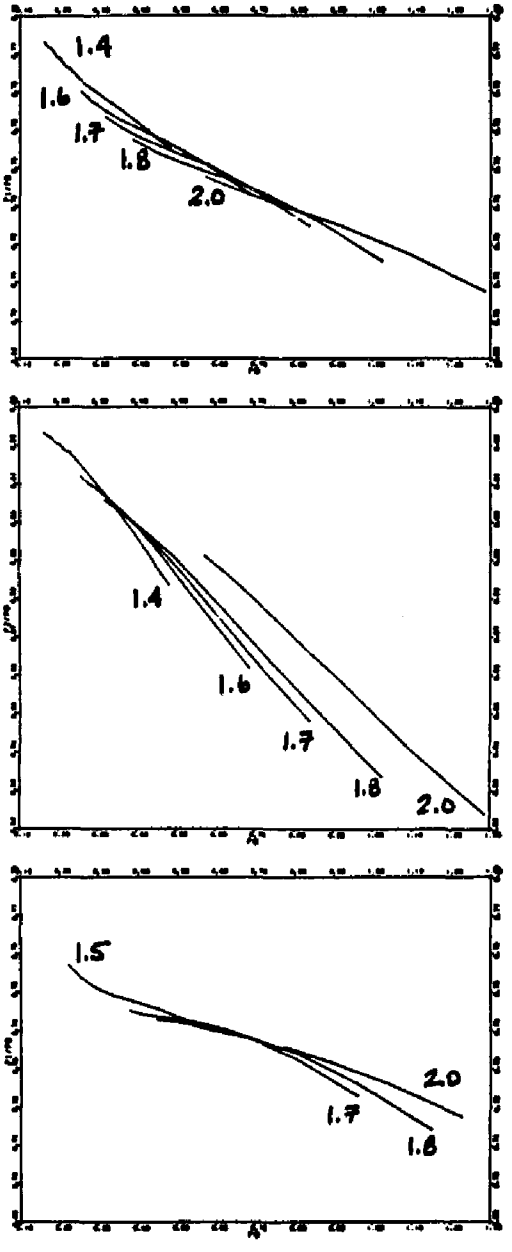

FIGURE 4

PERIOD RATIO FOR THE FIRST AND SECOND OVERTONE MODES

presented by Stellingwerf (1975) are plotted in Figure 4c. The mass of the model star is 0.578 M* and the opacity is calculated from a formula fitted to the King 1a opacity table with a composition of (Y,Z) = (0.299,0.001). The luminosities for which he calculated the model stars were log L/L* = 1.5, 1.7, 1.8, and 2.0. It is evident from Figure 4c that the same scatter exists. The difference in slopes may be due to three factors: the mass, the helium content, and the opacity. The mass is ruled out since there is little difference between 0.6 M* and 0.578 M* . If $P_1/P_0 - P_0$ plots for my series of models that vary in the helium content are examined it is found that an effect on the slope of the line does exist. However, it is not until Y = 0.75 that a significant change from the lower helium abundance models can be discerned. Since this difference in slope occurs at such an extreme value of helium content it seems reasonable to attribute the difference in slope between my models and Stellingwerf's to the different opacities used in the calculations.

3.2 Effects on the blue edge

The blue edge of the instability strip for a theoretical RR Lyrae model is a point of zero amplitude growth. Growth rates, computed from the computer model-generated eigenfrequencies, are defined as

$$\eta = -4\pi \frac{\omega_i}{\omega_R}$$

and change sign at the instability strip boundary. Sets of models with slow growth rates were computed by using

steps of 0.005 in log T_e; otherwise $\Delta \log T_e$ increments were in the range 0.010 - 0.015.

Blue edges calculated with models using Carson opacities exhibit a qualitative similarity to the edges that result from Cox-Stewart opacity models, but show certain quantitative differences. The present survey will examine the differences in the two blue edges attributable to differences of mass, chemical composition, and method of opacity calculation. Foremost among these factors is the helium content.

(a) Mass variation

The results of varying the mass in the models using Carson opacities are plotted in Figures 5 and 6 and tabulated in Table 3. These models, with masses of 0.4 M*, 0.6 M*, and 0.8 M*, were calculated with the same chemical abundances, (Y,Z) = (0.25,0.00). As seen in Figure 5, the first overtone blue edge is more sensitive to mass than is the fundamental blue edge. Furthermore, the difference in log T_e is relatively constant for the fundamental blue edge, whereas the first overtone blue edges with the masses varied fan out with increasing luminosity.

The difference in log T_e for the fundamental blue edges is greater between the 0.4 M* and 0.6 M* edges ($\Delta \log T_e \sim 0.007$) than for the 0.6 M* and 0.8 M* edges ($\Delta \log T_e \sim 0.004$) at all luminosities. The first overtone edges do not have a constant difference but vary as follows: $\Delta \log T_e \sim 0.005$ at log L/L* = 1.4 to ~0.061 at log L/L* = 2.0 when the mass is changed from 0.4 M* to

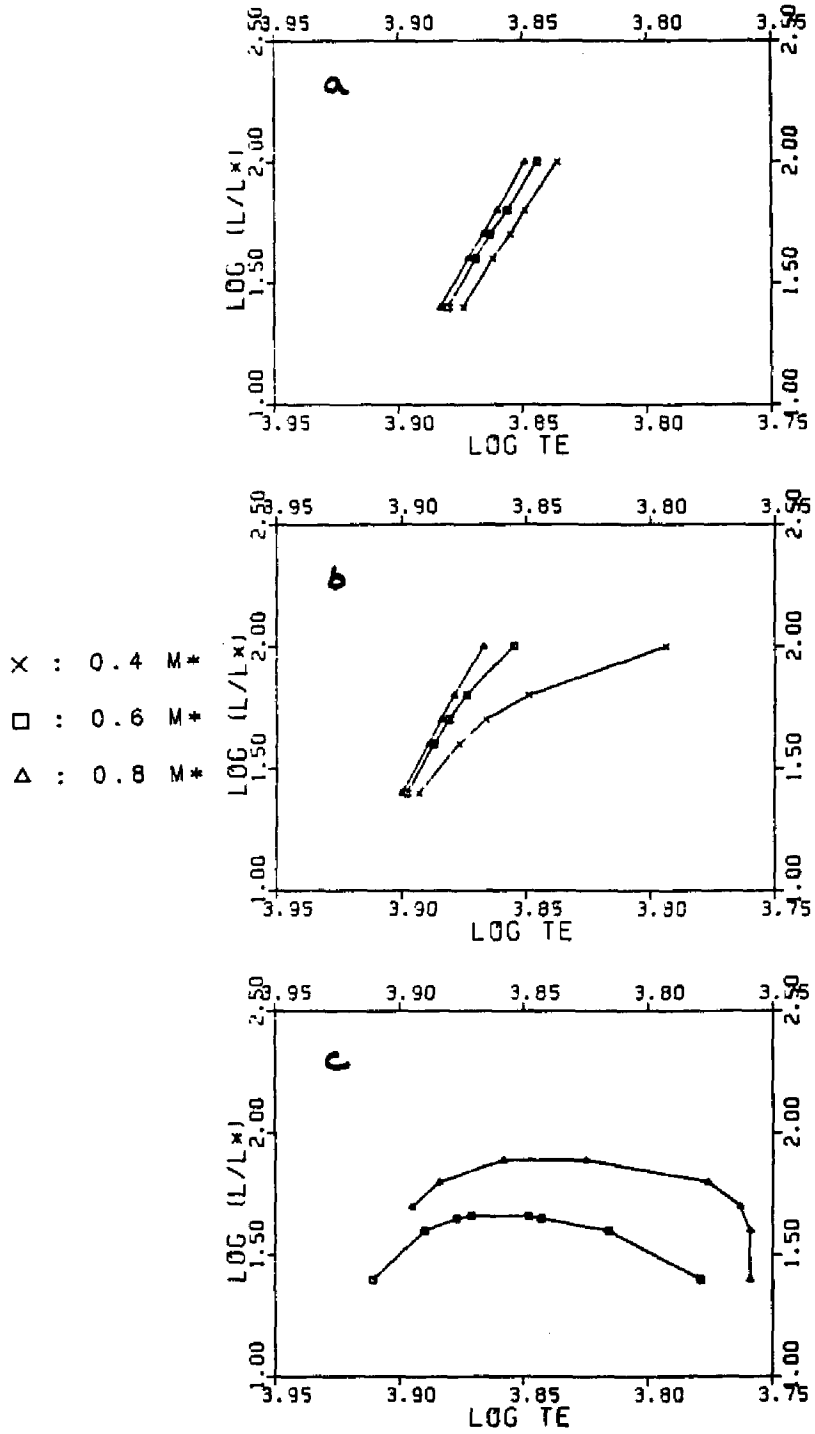

FIGURE 5

VARIATION IN LOCATION OF THE BLUE EDGES WITH MASS

TABLE 3

BLUE EDGE DATA FOR LINEAR MODELS WITH VARYING MASS HAVING (Y,Z) = (0.25,0.00)

Fundamental Mode

log L/L⊙	0.4 M⊙	0.6 M⊙	0.8 M⊙
1.4	3.874	3.880	3.883
1.6	3.862	3.869	3.872
1.7	3.855	3.863	3.866
1.8	3.849	3.856	3.860
2.0	3.836	3.844	3.849

First Overtone Mode

log L/L⊙	0.4 M⊙	0.6 M⊙	0.8 M⊙
1.4	3.893	3.898	3.900
1.6	3.877	3.887	3.889
1.7	3.866	3.881	3.884
1.8	3.849	3.874	3.879
2.0	3.794	3.855	3.867

0.6 M*. The corresponding $\Delta \log T_e$ values for the variation of mass from 0.6 M* to 0.8 M* is 0.002 at log L/L* = 1.4 and 0.012 at log L/L* = 2.0 .

As mentioned earlier, the second overtone blue edge for some calculated series takes the form of a closed region, within which the models are found to be pulsating in the second overtone mode. Figure 5c illustrates the mass dependence of this feature. The overall trend is an expansion of the region with increasing mass. Noticeably absent is a second overtone blue edge for model stars calculated with a mass of 0.4 M*. These were all found to be stable against pulsation ir the second overtone mode. As the mass is increased and instability in the second overtone appears, the peak luminosity increases and shifts to cooler temperatures as the range in temperature of this region becomes slightly wider.

It should be noted that the fundamental and first overtone modes of the computer models also had the tendency to curve over but the peak luminosities were much higher than those relevant to RR Lyrae stars and the cooler temperature boundaries were much too red to be worth considering, in view of the neglect of convection in the models.

The fundamental and first overtone blue edges are plotted together for the three masses and presented in Figure 6. The intersection of the two modes occurs only for the 0.4 M* model star. It appears that the blue edges of the 0.6 M* model star calculations will intersect, but beyond the range of values relevant to RR Lyrae stars. A constant separation of $\Delta \log T_e = 0.018$ characterizes the

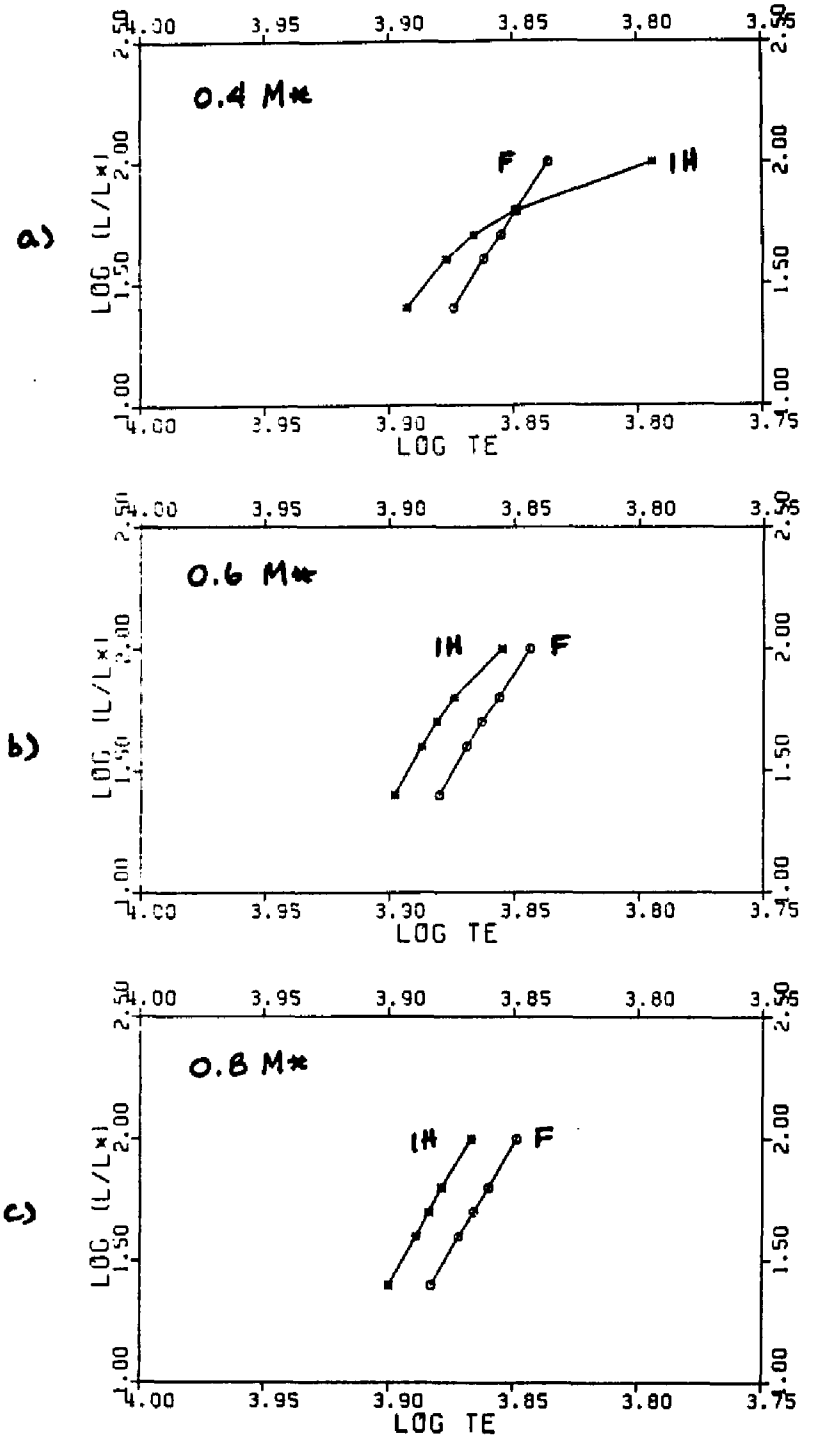

FIGURE 6

VARIATION OF THE FUNDAMENTAL
AND FIRST OVERTONE BLUE EDGES WITH MASS

blues edges of the 0.8 M* model stars. This lack of an intersection will be further discussed when comparisons to other linear surveys are made.

(b) Metal content variation

The variation in the blue edge due to the metal content was studied for a series of models with a mass of 0.6 M* and chemical compositions of (Y,Z) = (0.25,0.00), (0.25,0.005), and (0.24,0.021). The results of the calculations are plotted in Figures 7 and 8 and are listed in Table 4.

An interesting feature is the cross-over of the blue edges for both the fundamental and first overtone modes (Figure 7a and 7b). The fundamental mode has a pivoting set of blue edges as the metal content increases, around a point near log $L/L*$ ~ 1.7 and log T_e ~ 3.893. The first overtone mode is similar, and it is interesting that the angular spacing in the range Z = 0.00 to 0.005 is almost the same as in the range Z = 0.005 to 0.021, for both modes. The pivotal point for the first overtone blue edges occurs at log $L/L*$ ~ 1.5 and log T_e ~ 3.893. By inspecting Tables 3 and 4 as well as Figures 5 and 7 it seems at first glance that the $\Delta \log T_e$ values for the metal content variations are comparable with those due to mass variations. The one important difference is the change in slope of the theoretical blue edge in Figure 7. Whereas the blue edge is simply displaced blueward as the mass increases, the edges seem to rotate toward the blue with increasing Z. Therein lies the main significance of the metal abundance. The effects of the mass, the helium

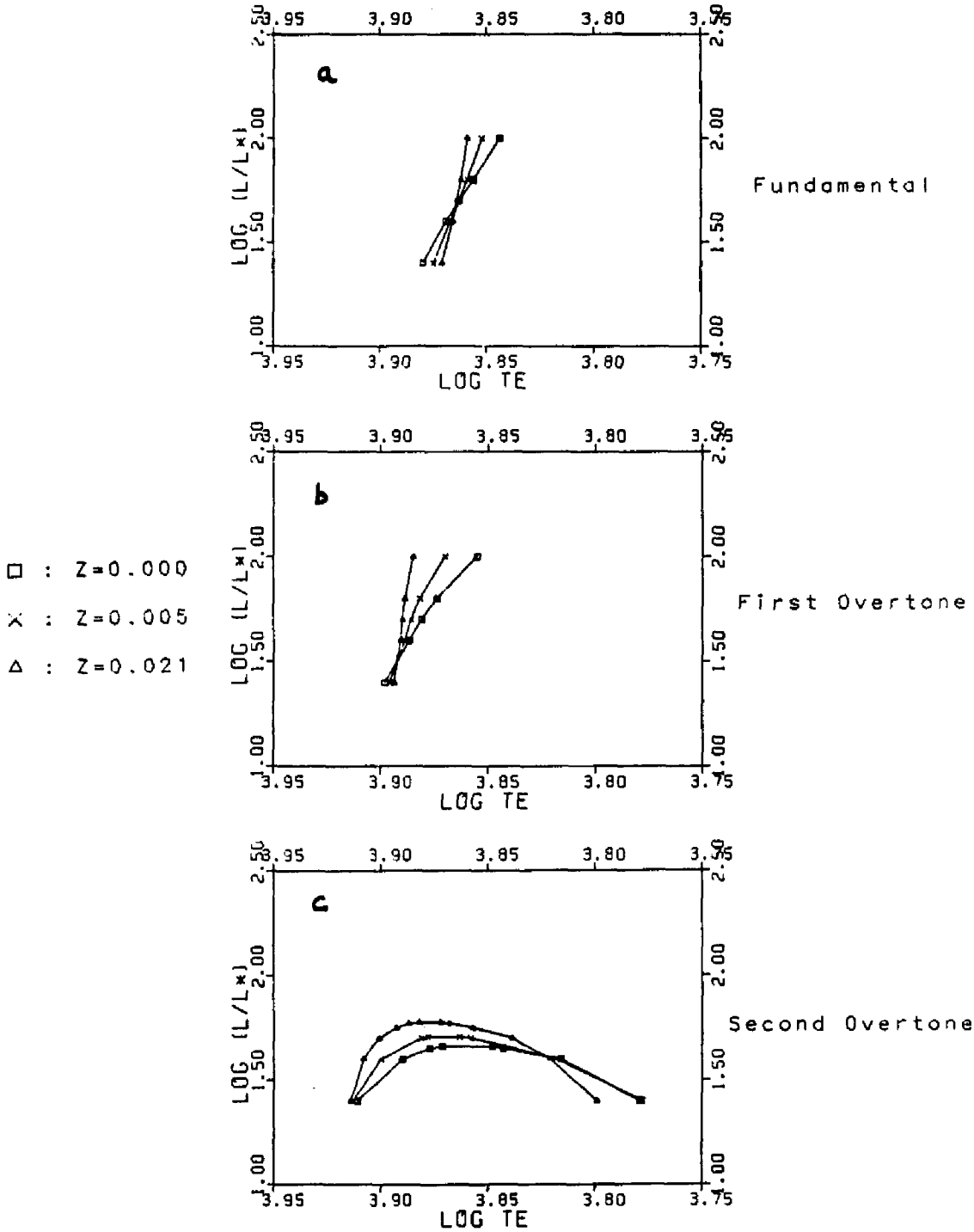

FIGURE 7

VARIATION IN LOCATION OF THE BLUE EDGES
WITH METAL CONTENT

TABLE 4

BLUE EDGE DATA FOR LINEAR MODELS
WITH VARYING METAL CONTENT AND M = 0.6M*

Fundamental Mode

	Z		
log L/L*	0.000	0.005	0.021
1.4	3.880	3.875	3.871
1.6	3.869	3.867	3.866
1.7	3.863	3.863	3.864
1.8	3.856	3.852	3.859
2.0	3.844	3.852	3.859

First Overtone Mode

	Z		
log L/L*	0.000	0.005	0.021
1.4	3.898	3.896	3.894
1.6	3.887	3.889	3.891
1.7	3.881	3.886	3.890
1.8	3.874	3.882	3.889
2.0	3.855	3.870	3.885

content, and the opacity appear to be to displace uniformly the blue edge in the HR diagram. The slope of the theoretical instability strip appears to be controlled by the Z variable.

For the second overtone blue edge the bell shape feature is again encountered. Increasing the metal abundance has a minimal effect. The peak luminosities are log L/L* = 1.66, 1.70, 1.77 for the three different Z values (increasing in value) used in the calculation of the models. The range of log T_e for the region does not change in going from Z = 0.00 to 0.005 and decreases by about $\Delta \log T_e \sim 0.02$ when Z increases from 0.005 to 0.021 at log L/L* = 1.4. Contrary to the trend found in the mass variation, the peak luminosity moves to hotter temperatures as the metal content is increased.

Illustrated in Figure 8 are the blue edges for the two lowest modes for the three Z values of this study. The first overtone blue edge is displaced from that of the fundamental mode by $\Delta \log T_e \sim 0.018$ for Z = 0.00 and this displacement increases as Z increases: $\Delta \log T_e \sim 0.022$ for Z = 0.005 and $\Delta \log T_e \sim 0.025$ for Z = 0.021. The promise of an intersection point is evident in Figure 8a and 8b but this point would be out of range of accepted values for RR Lyrae stars.

(c) Helium content variation

By far the largest effect on the blue edge is produced by the helium content of the model stars. The derived values of luminosity and effective temperatures of the blue edge are listed in Table 5. This sensitivity of

a)

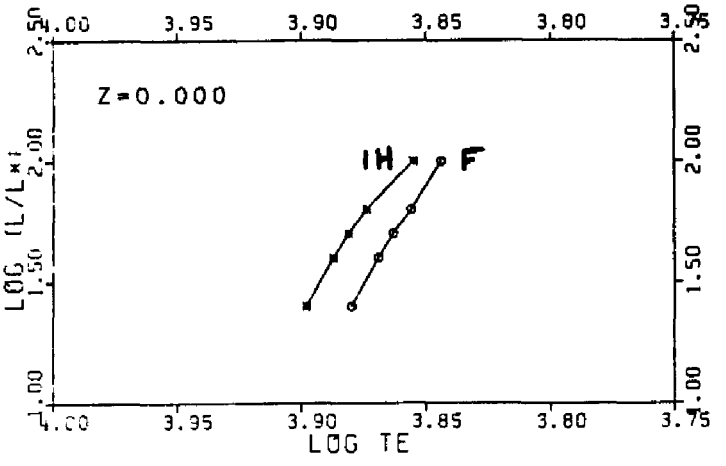

b)

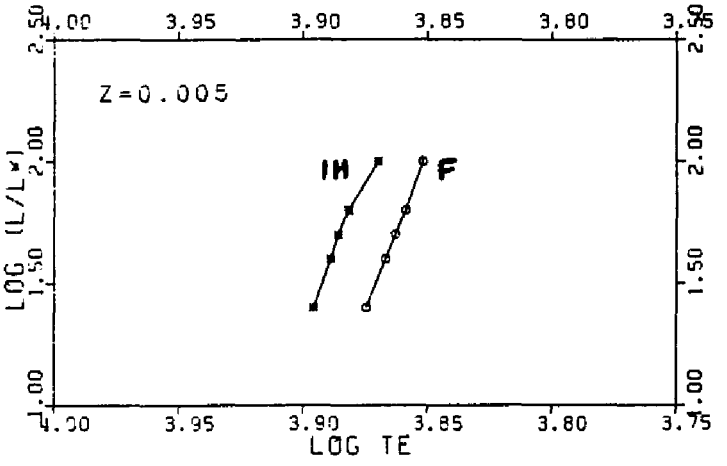

c)

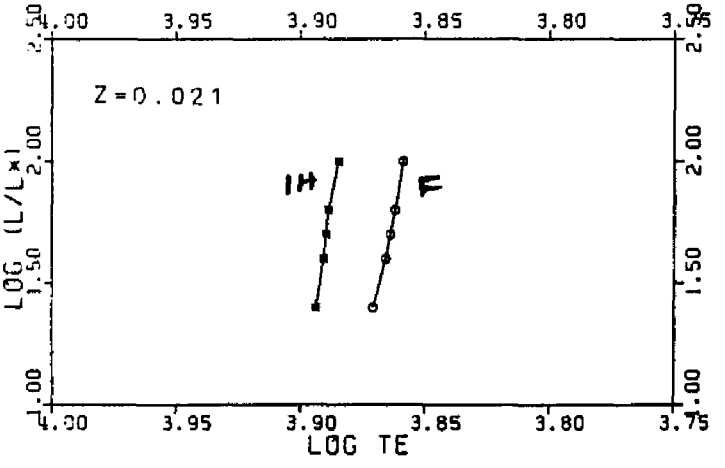

FIGURE 8

VARIATION OF THE FUNDAMENTAL AND
FIRST OVERTONE BLUE EDGES WITH METAL CONTENT

TABLE 5

BLUE EDGE DATA FOR LINEAR MODELS
WITH VARYING HELIUM CONTENT
HAVING M = 0.6M* AND Z = 0.00

Fundamental Mode

	Y		
log L/L*	0.250	0.500	0.750
1.4	3.880	3.901	3.909
1.6	3.869	3.890	3.899
1.7	3.863	3.884	3.895
1.8	3.856	3.879	3.890
2.0	3.844	3.868	3.881

First Overtone Mode

	Y		
log L/L*	0.250	0.500	0.750
1.4	3.898	3.922	3.934
1.6	3.887	3.913	3.924
1.7	3.881	3.909	3.920
1.8	3.874	3.905	3.917
2.0	3.855	3.896	3.910

the blue edge to the helium content, having been established early in the theoretical study of RR Lyrae stars, is used to estimate the helium abundances of the RR Lyrae variables and therefore of the globular clusters in which they are found.

To study the effect of helium on the blue edge using Carson opacities, model stars were calculated with a mass of 0.6 M*, Z = 0.00, and Y = 0.25, 0.50, and 0.75. The result of the calculations is shown in Figures 9 and 10. Increasing the helium content caused both the fundamental and the first overtone blue edges to shift towards higher temperatures. When the helium abundance was changed from Y = 0.25 to 0.50, the fundamental blue edge was displaced blueward by a little more than $\Delta \log T_e \sim 0.02$; the shift in the first overtone edge was larger and not constant, with a range of $\Delta \log T_e \sim 0.024$-$0.041$. The increase of Y from 0.50 to 0.75 caused less of a shift: $\Delta \log T_e \sim 0.01$ and $\Delta \log T_e \sim 0.012$ for the fundamental and the first overtone modes, respectively.

The effect on the second overtone blue edge is striking. Increasing the helium content in the models causes the peak luminosity to go beyond log L/L* = 2.0, and the closed region found for Y = 0.25 becomes a separated double edge for Y = 0.50 and 0.75.

The spread of log T_e between the fundamental and first overtone blue edges compares well with that found for the variation in metal content. Figure 10 illustrates the two blue edges when Y is varied. Comparison with Figure 8 shows a slight structural difference but the displacement of the first overtone blue edge from that of

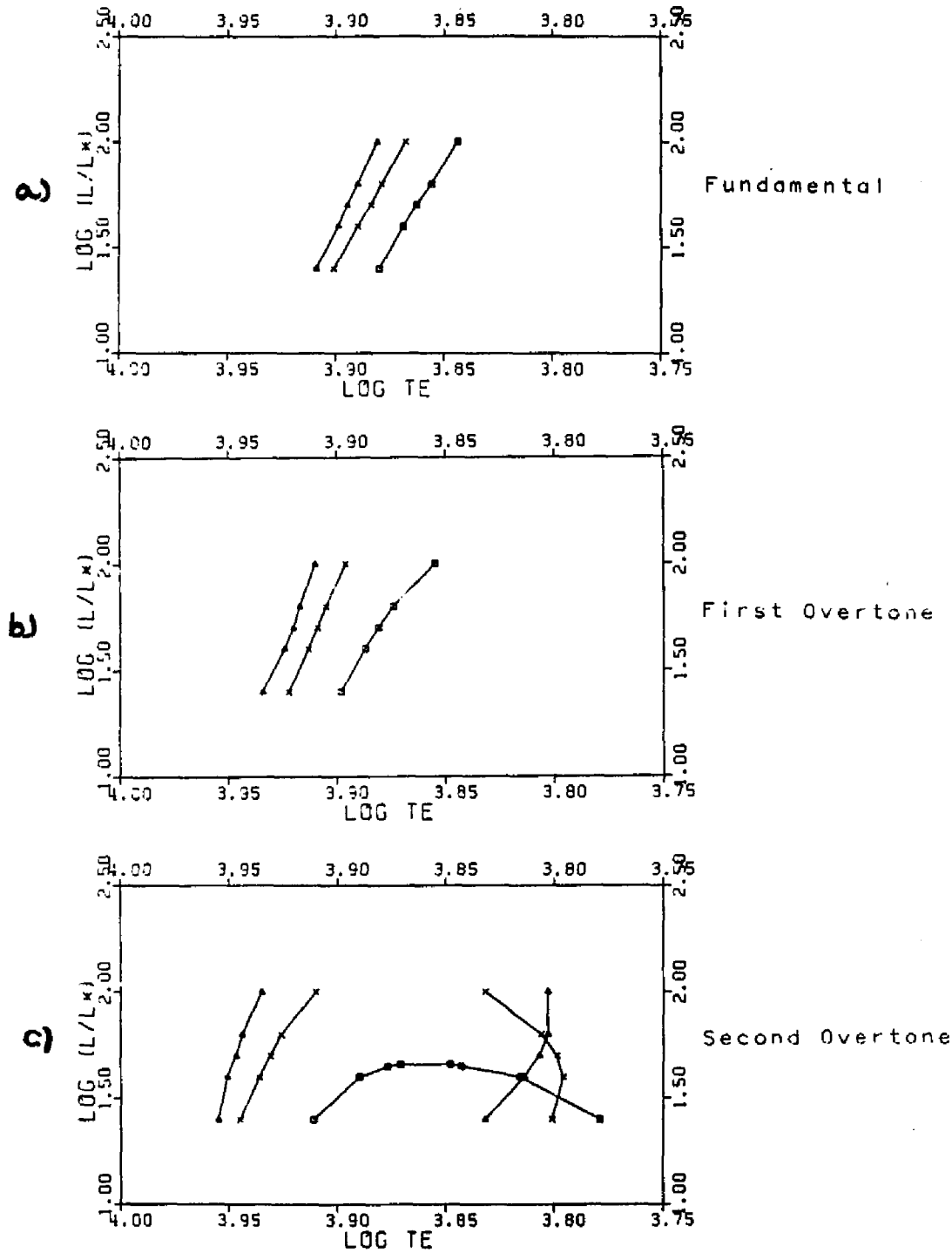

FIGURE 9

VARIATION IN LOCATION OF THE BLUE EDGES
WITH HELIUM CONTENT

□ : Y=0.25 × : Y=0.50 △ : Y=0.75

a)

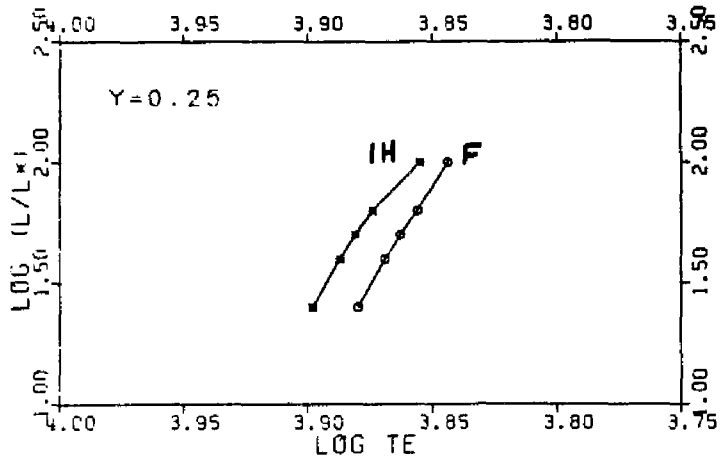

b)

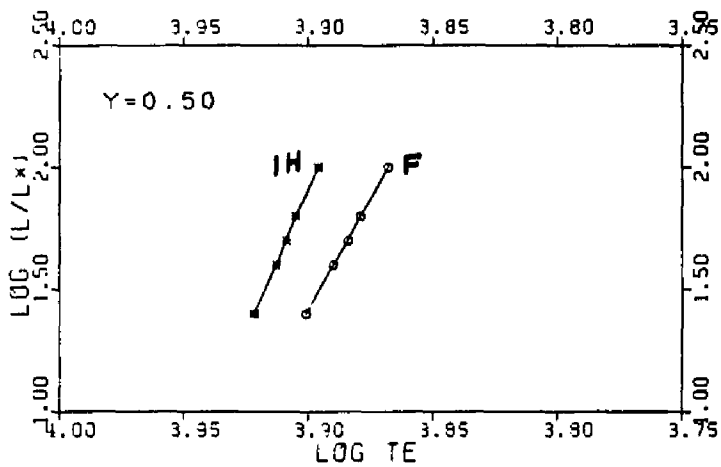

c)

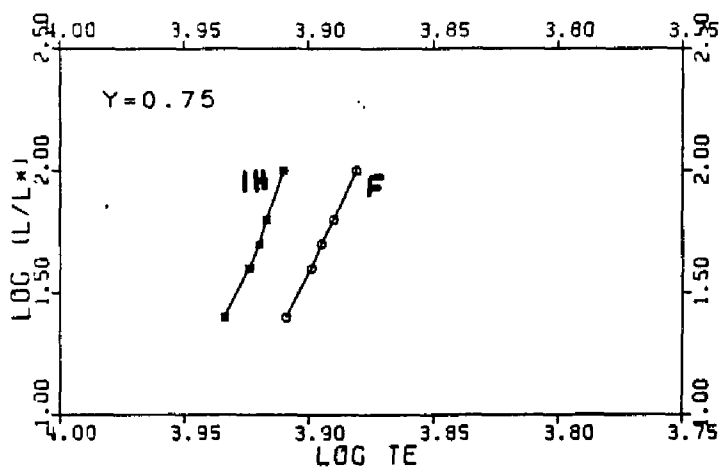

FIGURE 10

VARIATION OF THE FUNDAMENTAL AND
FIRST OVERTONE BLUE EDGES WITH HELIUM CONTENT

the fundamental one seems to be governed by the chemical composition more than the mass (Figure 6).

(d) Opacity variation

(i) New Los Alamos opacities vs. Carson opacities

After having investigated the variation of the stellar parameters with the use of the Carson opacities it remains to examine the effect of the opacity itself. The new Los Alamos opacity table for the chemical composition (Y,Z) = (0.25,0.005) was used to calculate a series of models necessary to determine the blue edges. These were compared with the series for the same chemical composition using the Carson opacity (series #2 in Table 1). The results are plotted in Figures 11 and 12 and tabulated in Table 6.

There are several noteworthy features in Figure 11. The calculated blue edges using Carson opacities for both fundamental and first overtone modes are bluer than those using the new Los Alamos opacities. The fundamental blue edge is displaced blueward from that calculated with the Los Alamos opacity by about $\Delta \log T_e \sim 0.01$-$0.015$. More important are the first overtone blue edge differences since it is this edge that is most easily compared with observations. The differences in $\Delta \log T_e$ range from 0.02 for log L/L* = 1.6 to ~0.046 at log L/L* = 2.0.

A substantial distinction between the two opacities is illustrated by the second overtone blue edge. A second overtone region exists for both opacities but for all practical purposes the second overtone mode is stable against pulsation when the new Los Alamos opacities are

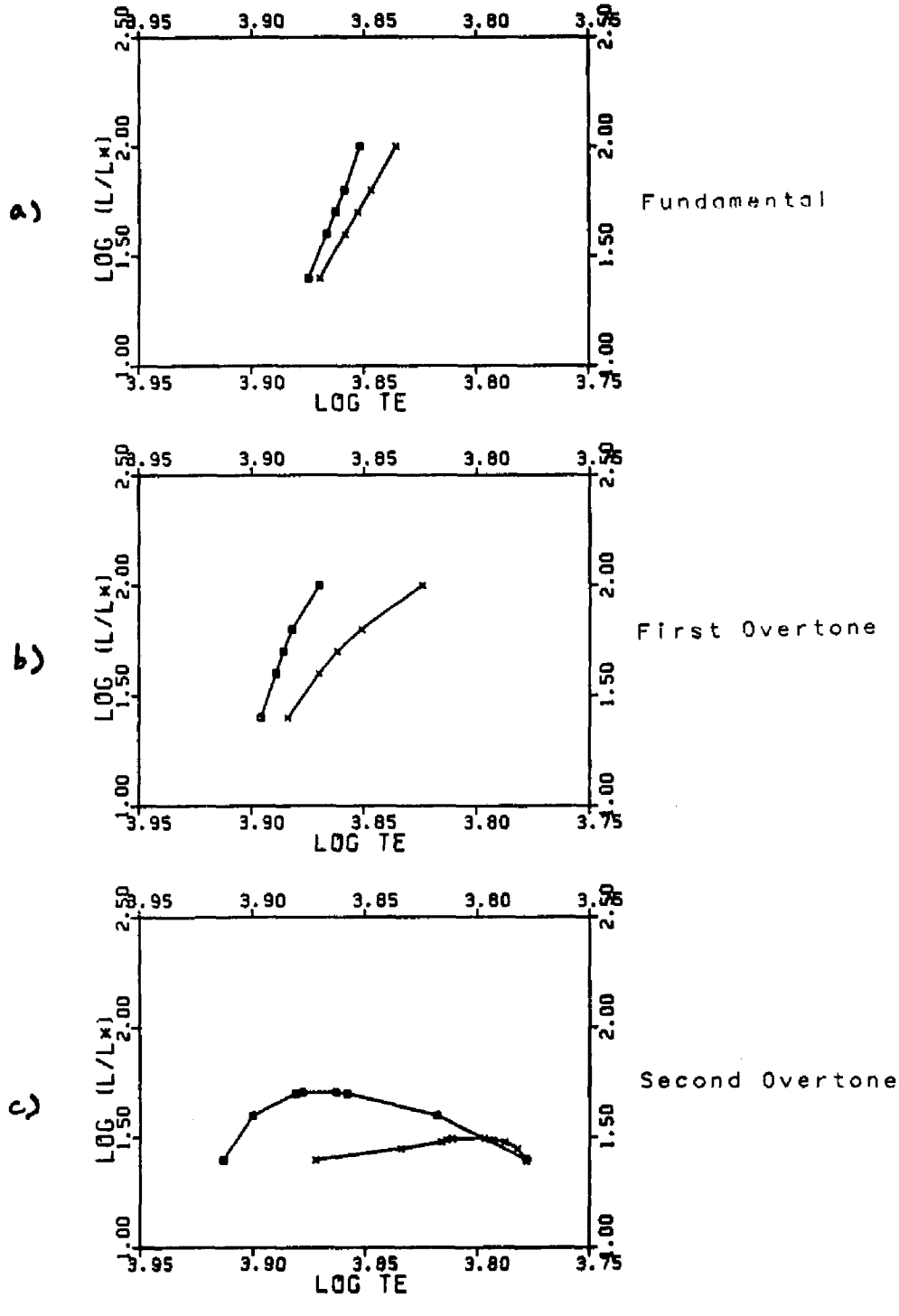

FIGURE 11

VARIATION IN LOCATION OF THE BLUE EDGES
WITH DIFFERENT OPACITIES

× - New Los Alamos □ - Carson

TABLE 6

BLUE EDGE DATA FOR THE LINEAR MODELS
WITH VARYING OPACITY AND HAVING
M = 0.6M⊙ AND (Y,Z) = (0.250,0.005)

Fundamental Mode Models

log L/L⊙	Carson	Los Alamos
1.4	3.875	3.870
1.6	3.867	3.859
1.7	3.863	3.853
1.8	3.859	3.847
2.0	3.852	3.836

First Overtone Mode Models

log L/L⊙	Carson	Los Alamos
1.4	3.896	3.884
1.6	3.889	3.870
1.7	3.886	3.862
1.8	3.882	3.851
2.0	3.870	3.824

used since the luminosity is very low (log L/L* = 1.4) and temperatures are far too red.

Two final points of interest are illustrated in Figure 12. Plotted are the fundamental and first overtone blue edges for both opacities. The intersection of the two edges when the Los Alamos opacities are used does not exist when the edges are calculated using the Carson opacities. In addition, the first overtone blue edge is always significantly further away from the fundamental edge for the Carson models. The average value of the difference is $\Delta \log T_e \sim 0.022$. For the new Los Alamos opacities the largest separation occurs at log L/L* = 1.4 and has a value of $\Delta \log T_e \sim 0.014$.

(ii) Method of Interpolation (i.e. spline vs 4-point linear)

The method of interpolating the opacity tables will affect the position of the blue edge in the H-R diagram. Before TI introduced the spline method of interpolation, use of Christy's approximating formula fitted to the Cox-Stewart opacity tables was prevalent. In studying the effect of varying the method of opacity interpolation, Iben (1971a) compared a 4-point linear interpolation scheme with Christy's formula. He found the edges associated with the linearly interpolated opacities to be shifted blueward by $\Delta \log T_e \sim 0.005$-$0.01$ from those edges derived from models using Christy's formula. Further investigation by TI found the edges to be shifted by $\Delta \log T_e \sim 0.03$ blueward of Christy's edges when the opacities were calculated using the method of spline

a)

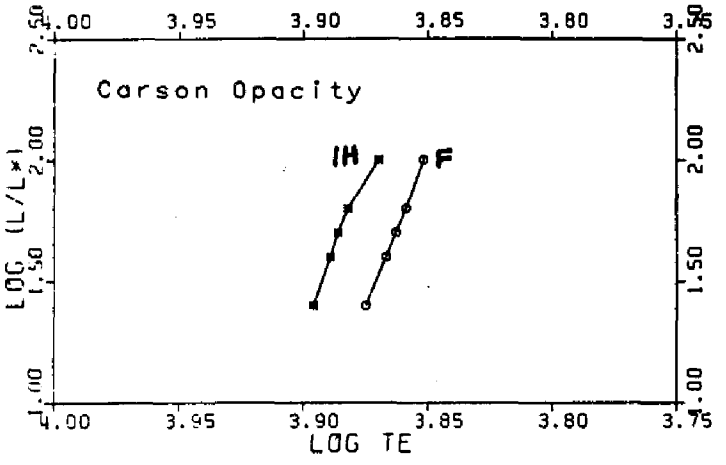

b)

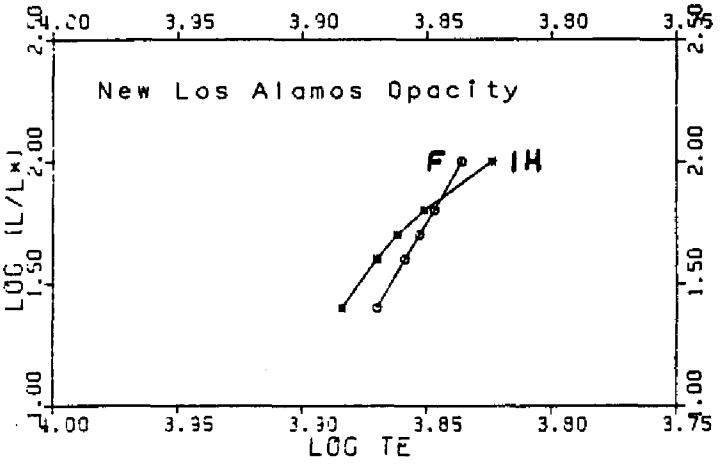

FIGURE 12

VARIATION OF THE FUNDAMENTAL AND
FIRST OVERTONE BLUE EDGES WITH OPACITY

interpolation. The implication of these two studies is that the method of spline interpolation of the opacity tables will shift the blue edge by roughly $\Delta \log T_e \sim 0.02$ blueward of that calculated using linearly interpolated opacities. The data of Iben (1971b) and TI are plotted in Figure 13 and are presented here to illustrate the shift of the edges caused by the method of opacity interpolation and will be further discussed in a later section.

One final series of models was calculated with Carson opacities for a model star of mass 0.6 M* and a chemical composition of (Y,Z) = (0.25,0.00). The opacities were derived by means of a 4-point interpolation scheme. The words of caution voiced by Iben (1971b) and Carson and Stothers (1976) were well borne out. The irregularity of the interpolated opacity derivatives produced very ragged growth curves, and determining the blue edges was challenging, to say the least. Specifying the blue edges calculated from the spline interpolation method was unambiguous and well defined. But the decisiveness of the blue edge determination was curtailed by the frequent sign changes in the growth rate curves for the linear interpolation opacity models.

The results of the calculations are presented in Figure 14 and Table 7. There appears to be little difference in the fundamental blue edges. The irregularity of the fundamental edge calculated with the models using the linearly interpolated opacities can be attributed to the interpolation method itself. The differences in the first overtone blue edge are of the order quoted by TI. Again the irregularity of the first

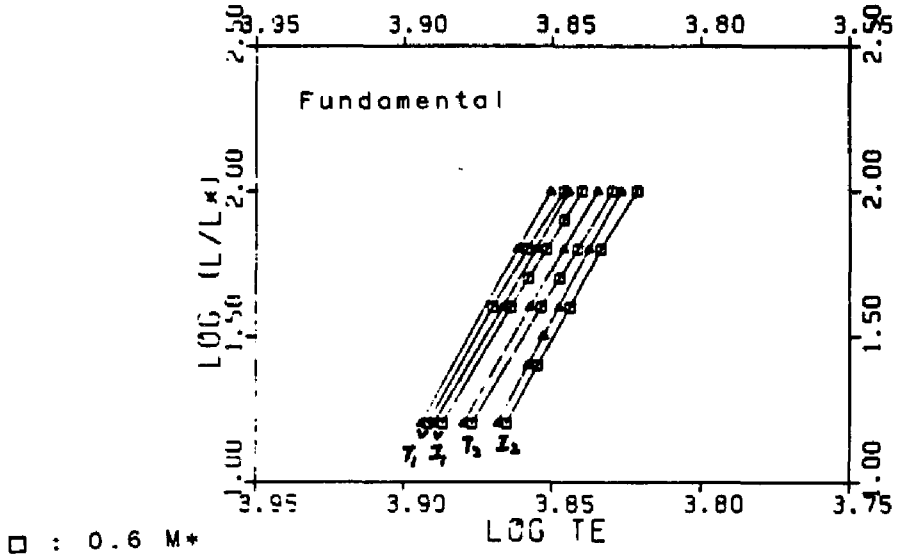

□ : 0.6 M*

△ : 0.8 M*

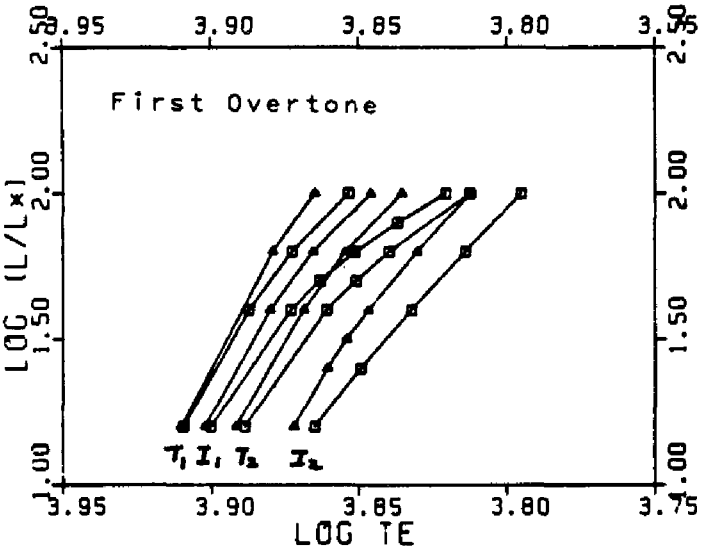

T1 - Tuggle (Y=0.296)
T2 - Tuggle (Y=0.199)

I1 - Iben (Y=0.30)
I2 - Iben (Y=0.20)

FIGURE 13

COMPARISON OF RESULTS OF IBEN (1971b) AND TUGGLE AND IBEN (1972)

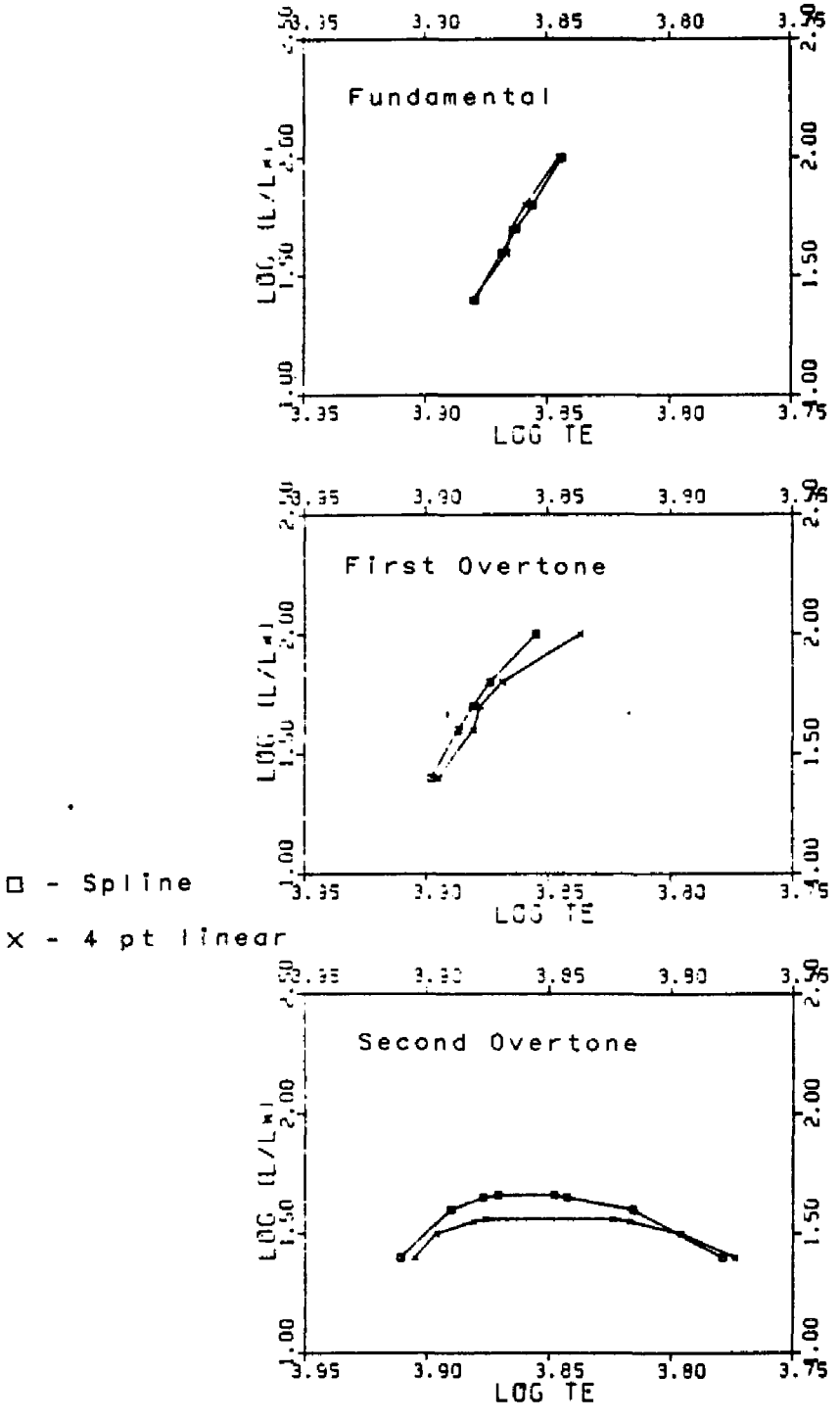

FIGURE 14

CHANGE IN THE LOCATION OF THE BLUE EDGES AS THE METHOD OF INTERPOLATING WITHIN THE OPACITY TABLES IS VARIED

TABLE 7

BLUE EDGE DATA FOR LINEAR MODELS HAVING
M = 0.6M⊙ AND (Y,Z) = (0.25,0.00)
WITH DIFFERENT METHODS OF INTERPOLATION
IN THE OPACITY TABLES

Fundamental Mode Models

log L/L⊙	Spline	4-pt linear
1.4	3.880	3.881
1.6	3.869	3.867
1.7	3.863	3.865
1.8	3.856	3.859
2.0	3.844	3.845

First Overtone Mode Models

log L/L⊙	Spline	4-pt linear
1.4	3.898	3.895
1.6	3.887	3.881
1.7	3.881	3.878
1.8	3.874	3.869
2.0	3.855	3.837

overtone edge corresponding to the linear interpolation scheme is attributed to the method.

3.3 Comparison with previous surveys

The earlier linear surveys by Iben and Huchra (1971, hereafter IH), Iben (1971a,b), and TI provide a full range of possible comparisons with the present survey, particularly with regard to opacities and methods of interpolating the opacity. The boundary conditions used by the above mentioned authors are similar to those used by the present calculations. Convection is neglected by all. IH and Iben (1971a,b) used the Christy (1966) formula approximation to the Cox and Stewart (1965) opacities. The TI data were calculated by using a spline interpolation method for the Cox and Stewart (1971) opacity tables.

In Figure 15 the blue edges calculated from the data of IH are plotted for M = 0.6 M*, Y = 0.3 with varying Z values: 0.01,0.001, and 0.0001. These were graphed to compare with the edges calculated for M = 0.6 M*, Y = 0.25, and the varying Z values of 0.00, 0.005, and 0.021 used in the present survey. That the helium content is different will have little bearing on the present discussion.

The claim by these investigators of a negligible metal dependence of the blue edges can be easily seen in the figure; especially for the change from Z = 0.0001 to 0.001 for the first overtone blue edge. The cross-over found for the Carson blue edges is not present when Christy's approximation to the Cox-Stewart opacities is

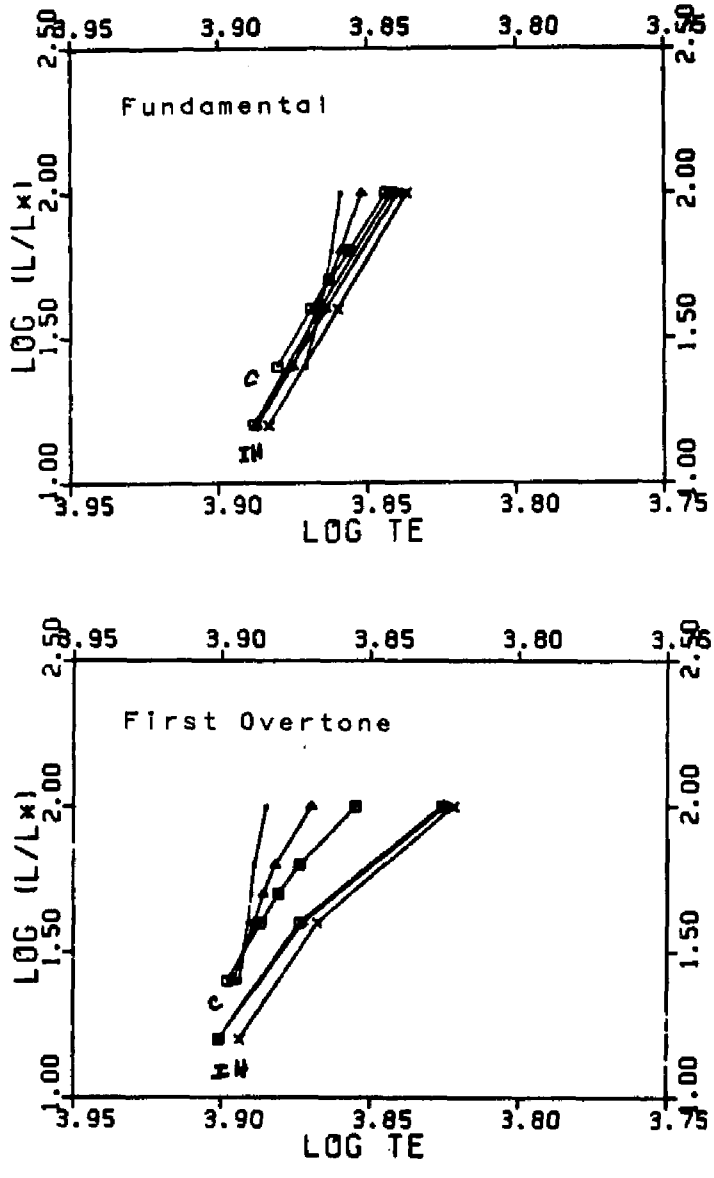

Carson: (Y=0.25)

□ - Z=0.000

Δ - Z=0.005

· - Z=0.021

Iben and Huchra: (Y=0.30)

□ - Z=0.0001

Δ - Z=0.001

× - Z=0.01

FIGURE 15

Z DEPENDENCE OF THE BLUE EDGES FOR THE CARSON MODELS AND THOSE OF IBEN AND HUCHRA (1971)

used. In fact, the Cox-Stewart edges show a parallel displacement toward the blue edge with decreasing metal content for the full range of luminosities. The range of displacement of the Carson edges is greater than the Cox-Stewart edges. This is especially evident in the first overtone blue edges. The curvature remains constant for the IH Cox-Stewart blue edges but not so for the Carson blue edges. In fact, it appears that the Carson first overtone blue edge approaches linearity as the metal content increases. One also notices that the slope of the Carson fundamental blue edge increases with increasing Z whereas the Cox-Stewart blue edge slope remains the same. This sizable variation in the Carson blue edges is fortunate in the case of the first overtone blue edge since this may be a fine tuning mechanism in fitting this theoretical edge to observations.

It is noteworthy that the IH blue edges are displaced toward cooler temperatures as Z increases. The opposite is true for the Carson blue edges above the cross-over point. Since the cross-over point for the first overtone blue edges occurs at a luminosity of log $L/L_* \sim 1.5$, which is possibly a lower limit of luminosity for most RR Lyrae stars, it is a valid consideration that the overall effect of increasing Z on the first overtone blue edge is opposite for the two different opacities.

The comparison of the mass and helium content dependences of the Carson blue edges with those calculated by Iben (1971a,b) and TI are plotted in Figures 16 and 17, respectively. Masses of 0.6 M_* and 0.8 M_* were graphed It is obvious that the mass dependence is similar, whether

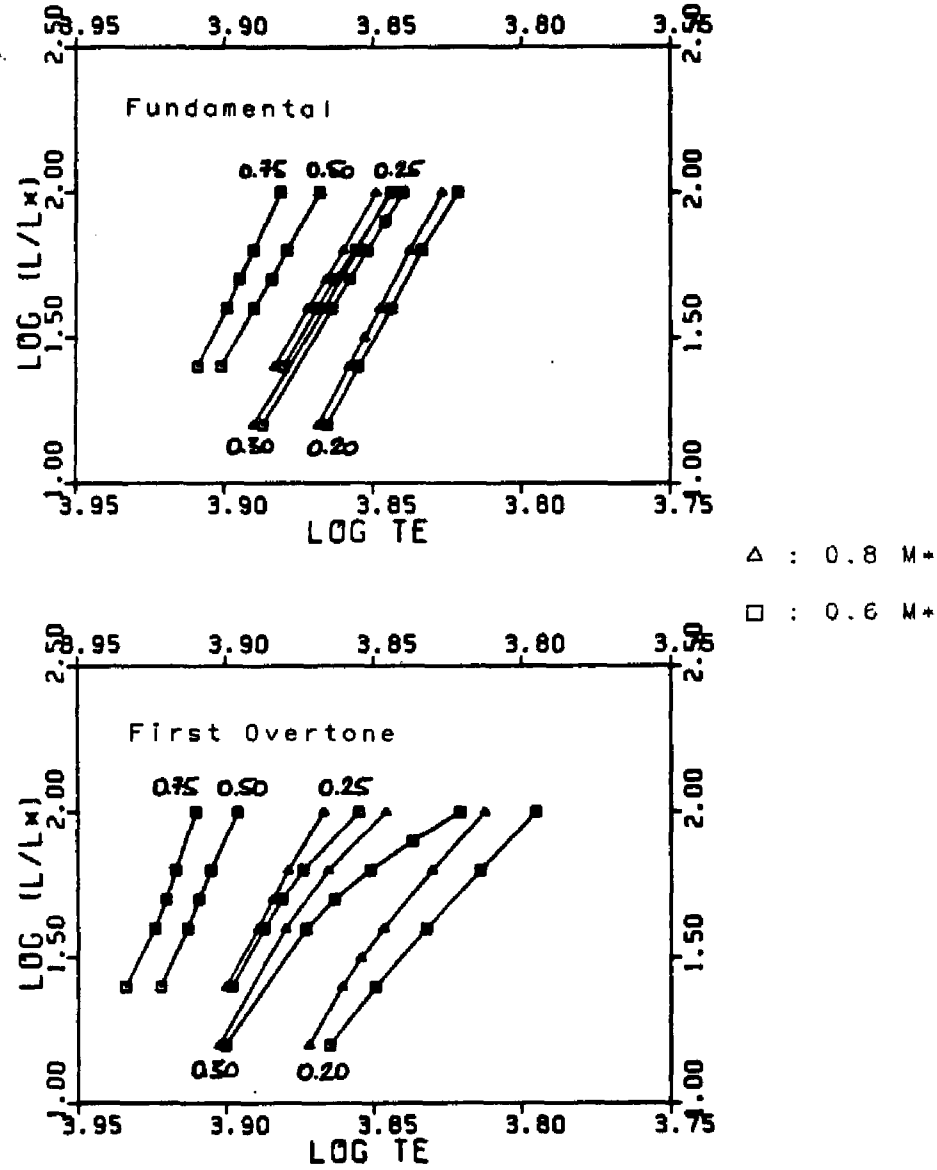

FIGURE 16

MASS AND HELIUM DEPENDENCE OF BLUE EDGES FOR THE CARSON MODELS AND THOSE OF IBEN (1971b)

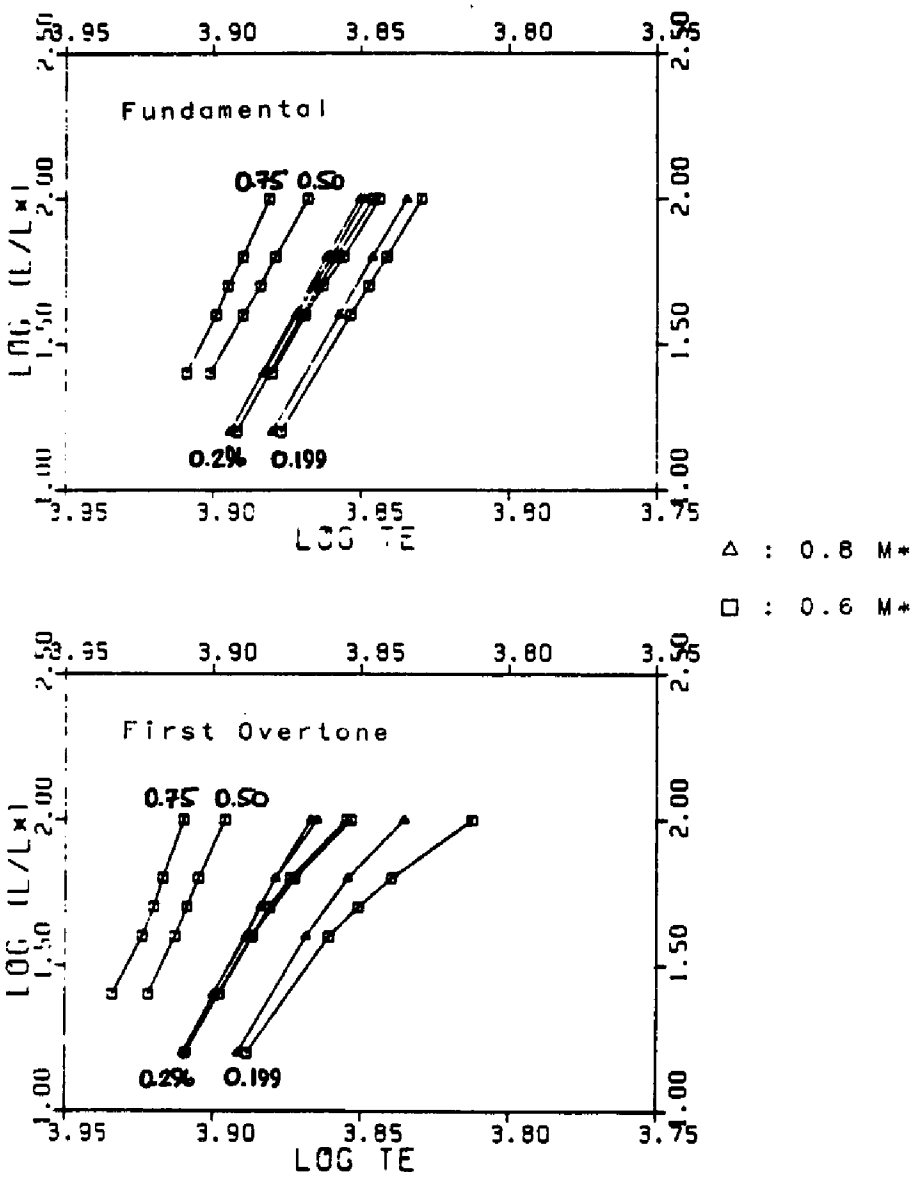

FIGURE 17

MASS AND HELIUM DEPENDENCE OF BLUE EDGES FOR THE CARSON MODELS AND THOSE OF TUGGLE AND IBEN (1972)

Carson opacities are applied or Cox-Stewart opacities are applied, and whether calculated with the Christy fitting formula or the spline interpolation method. One notices in Figure 16 that the first overtone blue edge changes less with mass for the case of Carson opacities than when Christy's formula is used to derive the opacities. The corresponding plot in Figure 17b for the TI data shows that the edges coincide with those of Carson while Iben's edges are to the red of Carson's. (The fact that Y is different in the two cases is unimportant in this discussion because we are comparing relative positions of the edges here.) This may be caused by the method of interpolating the opacities. Referring back to Figure 13 one sees that the edges for both modes for the same mass and chemical composition in the case of the TI data are bluer than in the case of the data of Iben (1971a,b). The divergence at higher luminosities may also be explained in terms of the spline method. In Figure 13 the TI blue edges for Y = 0.3 are less divergent than those of Iben. The general impression is that the difference in opacities does not affect the relative mass dependence of the blue edges as much as the opacity interpolation method itself does.

The major effect of the different opacities is on the helium content dependence of the blue edges. This is evident in both Figures 16 and 17. As demonstrated in Figure 16, the same blue edges using the Cox-Stewart opacities may be obtained with a lower helium content using Carson opacities. The changes in the blue edges due to changes in the helium abundance are less for the case

of the Carson opacities. For the fundamental mode the Carson blue edge becomes bluer by $\Delta \log T_e \sim 0.02$ for Y changing from 0.25 to 0.50. As the helium content is altered from Y = 0.2 to 0.3 the blue edge for the TI models shifts to the blue by $\Delta \log T_e \sim 0.016$. For the first overtone the TI models yield $\log T_e \sim 0.02$-0.04 for $\Delta Y = 0.1$ whereas with Carson's opacity $\Delta Y = 0.25$ for the same range in $\log T_e$. Apparently, the blue edges calculated with Carson opacities vary less with helium abundance than when the Cox-Stewart opacities are applied.

Stellingwerf (1975) used the King Ia opacity tables for the chemical composition (Y,Z) = (0.299,0.001) in his linear survey of RR Lyrae models. The mass, 0.578 M*, corresponds to that used in the nonlinear part of his study. Figure 18 superimposes his calculated blue edges onto those calculated using Carson opacities with varying mass and helium content values. A similar plot with varying metal content values is graphed in Figure 19. Since the effect of varying the mass on the blue edges has been shown to be similar, regardless of opacity, there should be no surprise at the close agreement of the blue edges for M = 0.6 M*. Likewise, as with the previous comparisons, the Carson blue edges are as blue as the Stellingwerf edges for a smaller helium content. The metal content comparison plot, Figure 19, shows exact agreement with the Carson first overtone blue edge for Z = 0.00 and a lower value of Y, and a slight displacement toward the blue from the Carson fundamental blue edge for the same metal content.

The blue edges derived from the Carson linear models

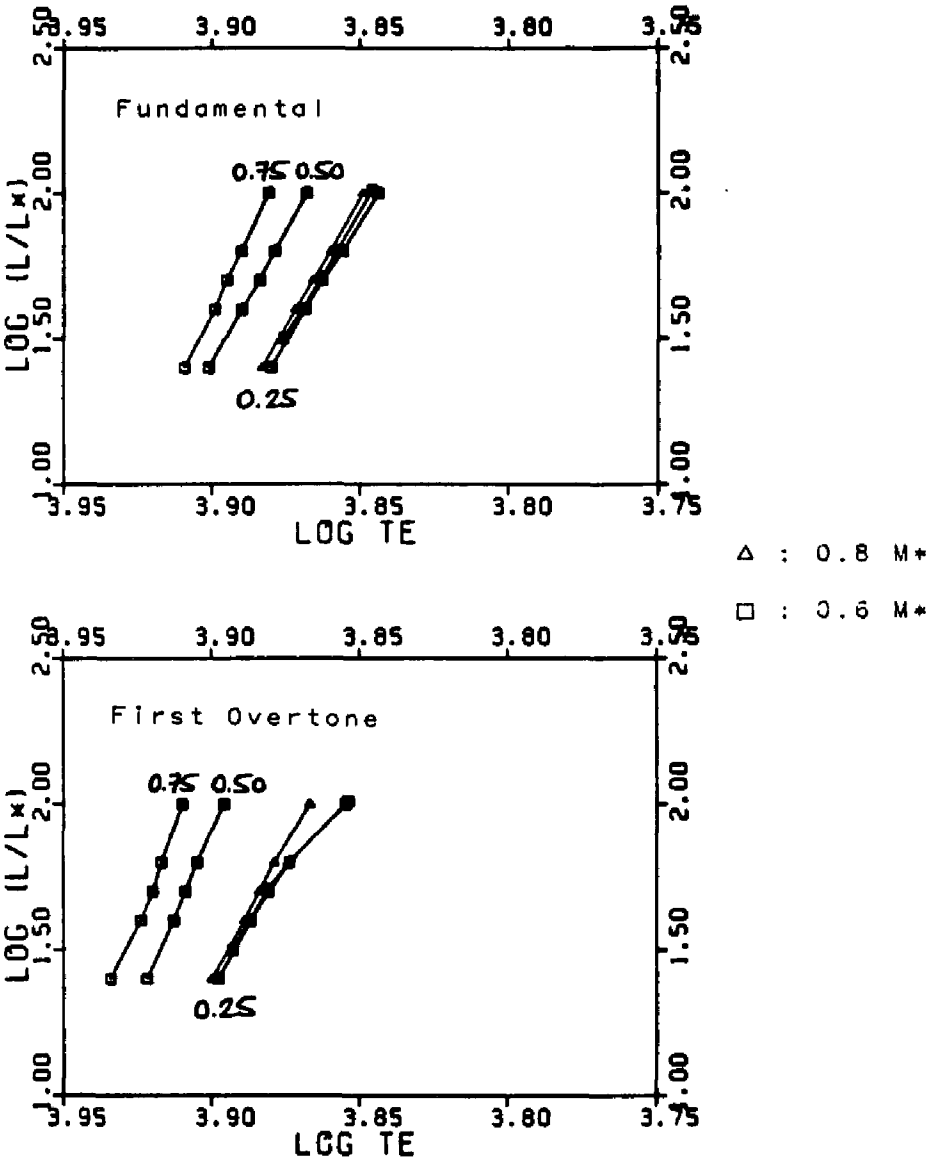

FIGURE 18

MASS AND HELIUM DEPENDENCE OF BLUE EDGES FOR THE CARSON MODELS AND THOSE OF STELLINGWERF (1975)

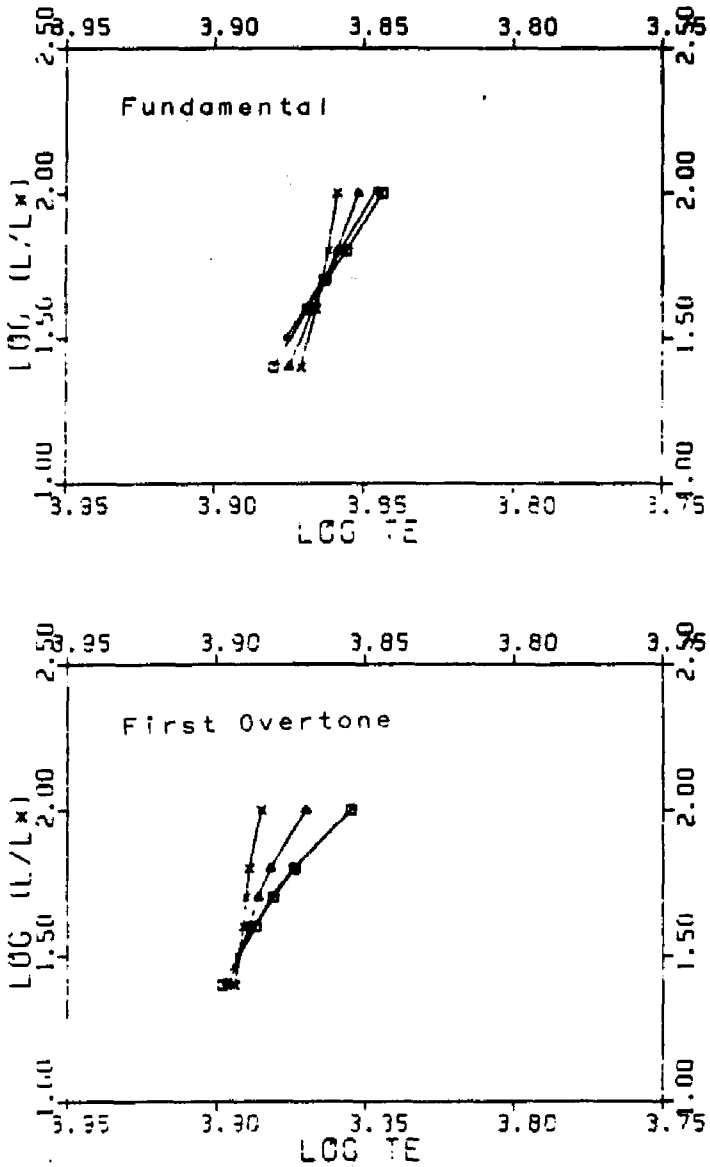

· : Stellingwerf
(Y,Z)=(0.299,0.001)

□ : Carson
(Y,Z)=(0.250,0.000)

△ : Carson
(Y,Z)=(0.250,0.005)

× : Carson
(Y,Z)=(0.240,0.021)

FIGURE 19

Z DEPENDENCE OF THE BLUE EDGES FOR
THE CARSON MODELS AND STELLINGWERF (1975)

for the type II Cepheids (Carson, Stothers, and Vemury 1981) are plotted in Figure 20. The theoretical blue edges for the RR Lyrae models with the same stellar parameters as the type II Cephieds are included. The small discontinuity is most probably due to different boundary conditions used in the type II Cepheid models. These model stars were calculated using the surface boundary conditions of Baker and Kippenhahn (1965). It has been shown elsewhere that the surface boundary conditions used by Iben causes the edges to be bluer than those calculated with Baker and Kippenhahn boundary conditions (Tuggle and Iben 1972). The magnitude and direction are about the same in Figure 20 as what Tuggle and Iben found.

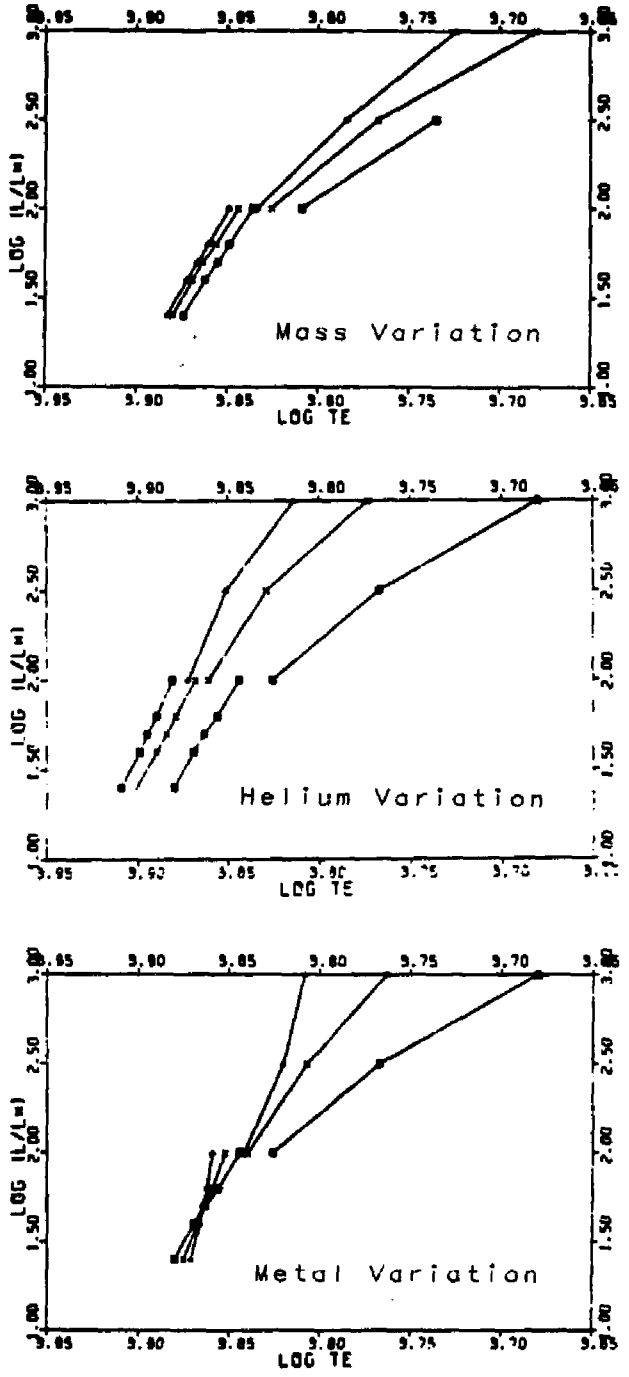

FIGURE 20

BLUE EDGE DATA FOR THE TYPE II CEPHEIDS AND RR LYRAE MODELS WITH VARYING MASS AND CHEMICAL COMPOSITION

CHAPTER 4: PRESENTATION AND DISCUSSION OF THE NONLINEAR SURVEY RESULTS

4.1 Theoretical light and velocity curves

(a) Fundamental mode

Details of the numerics of the fundamental mode models are described and explained in Chapter 2. Table 8 contains the results of the fundamental mode models and the surface light and velocity curves are illustrated in Figures 21 and 22, respectively (these data were incorporated in a recent work by Stothers (1981); several figures from that study appear herein, figures 1, 21-23). For clarification, the symbols involved in Table 8 are briefly explained: K.E., peak kinetic energy; Δ, full (not half) amplitude; *Asymmetry*, time spent on the descending branch of the of the surface velocity (or luminosity) curve divided by the time spent on the ascending branch; φ_v, phase after minimum radius of the secondary bump on the surface velocity curve plus unity; φ(max), phase of maximum luminosity minus phase of maximum velocity at the surface; and φ(mean), phase of mean luminosity (defined by taking one half of the sum of maximum and minimum bolometric magnitude) minus phase of mean velocity during the main rise of luminosity at the surface. The term "surface" refers to a mass layer of the equilibrium model where the optical depth is $\tau \sim 0.2$. The

TABLE 8

FULL AMPLITUDE PROPERTIES OF THE THEORETICAL AB-TYPE RR LYRAE MODELS

Parameter	Model						
	1	2	3	4	5	6	7
$M/M_\odot$	0.377	0.578	0.679	0.578	0.578	0.578	0.578
Y	0.25	0.25	0.25	0.25	0.25	0.25	0.49
$\log (L/L_\odot)$	1.585	1.585	1.585	1.600	1.600	1.600	1.585
$\log T_e$	3.813	3.813	3.813	3.792	3.813	3.833	3.813
$R/R_\odot$	4.87	4.96	4.95	7.01	6.36	5.81	4.95
P(day)	0.732	0.529	0.487	0.964	0.823	0.702	0.542
K. E. (10^{40} ergs)	0.42	0.89	3.60	1.23	1.19	1.02	2.19
$\Delta R/R$	0.19	0.17	0.27	0.15	0.25	0.23	0.17
V_{out} (km s^{-1})	32	39	67	30	40	44	39
V_{in} (km s^{-1})	-46	-44	-47	-44	-47	-40	-41
ΔV (km s^{-1})	78	83	114	74	87	84	80
L_{max} (10^{35} ergs s^{-1})	2.1	2.3	3.4	3.2	4.0	4.1	2.1
L_{min} (10^{35} ergs s^{-1})	0.8	0.8	0.7	1.1	1.1	1.2	0.9
ΔM_{bol}	1.0	1.1	1.7	1.1	1.4	1.3	0.9
Asymmetry (vel.)	4.0	4.1	5.1	3.4	4.2:	4.9	4.2
Asymmetry (lum.)	2.4	5.7	17.2	3.5	6.1	9.0	3.3
ϕ_v	1.62	1.62	1.60	1.58	1.59	1.61	1.61
$\delta\phi$(max)	+0.18	+0.03	-0.05	+0.05	-0.02	-0.04	+0.09
$\delta\phi$(mean)	+0.08	+0.06	+0.03	+0.07	+0.01	-0.03	+0.10

theoretical model star with the stellar parameters M/M* = 0.578, log (L/L*) = 1.585, log T_e = 3.813, and Y = 0.25 (model #2 in Table 8) will be referred to as the standard model since these values are the same as those used by Christy in his 5gF model.

The calculated curves mimic well the observations. Features found in observed stars are all, or in part, evident in the calculated surface plots in Figures 21 and 22. These include the asymmetry in the light curves, the bumps on the descending branches of the light and velocity curves, and even the shock on the ascending part of the light curve.

The phase φ_v of the secondary bump on the surface velocity curve was carefully measured from the original plots used to construct Figure 22. From the listed phase values in Table 8 it is evident that φ_v is sensitive to mass and helium content as parameters, but largely insensitive to the effective temperatures. Most of the models have a measured $\varphi_v \sim 1.6$ which agrees well with that of observed velocity curves. Detailed comparisons of the theoretical results with observations will be discussed in a later section.

The velocity curves for all the zones of the standard model are plotted in Figure 23. In this illustration one can follow the progression of a pressure disturbance which originates in the helium ionization zone. It propagates inward to the bottom of the envelope where it is reflected, and eventually emerges at the surface. The disturbance manifests itself at the surface as the secondary bump. Clearly, this agrees with the Christy echo phenomenon

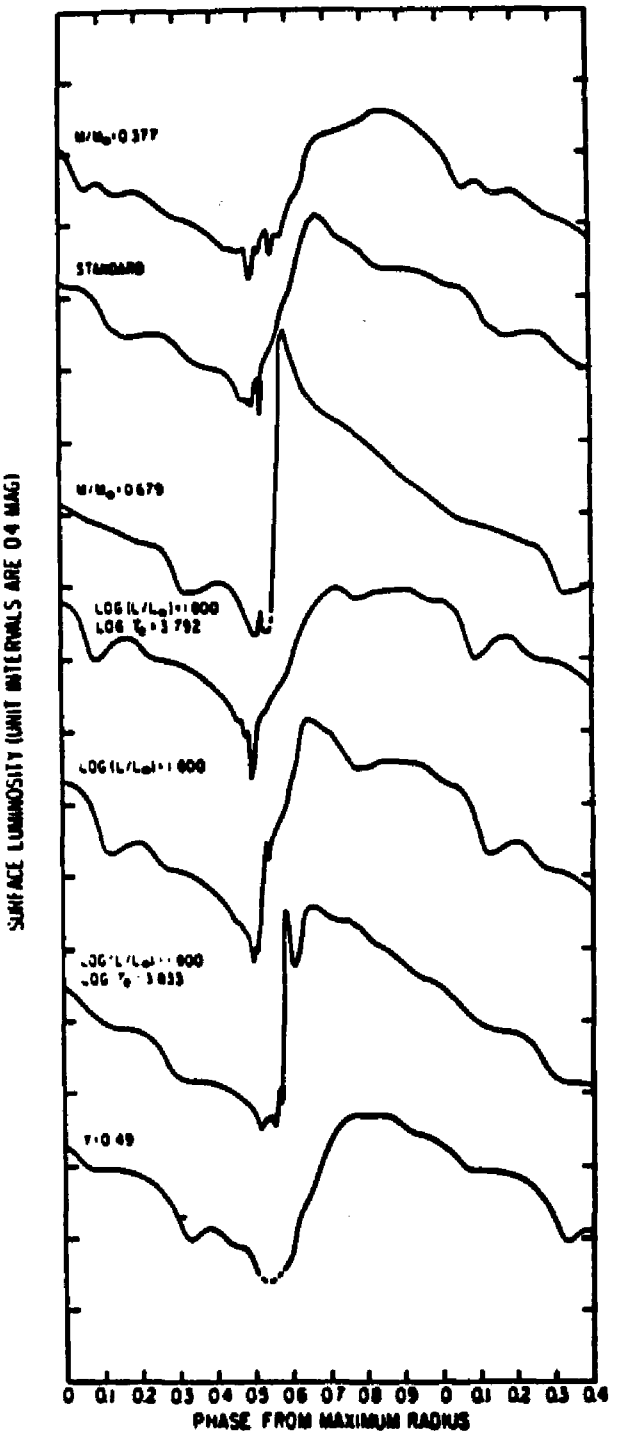

FIGURE 21

SURFACE LUMINOSITY CURVES OF THE NONLINEAR FUNDAMENTAL MODE MODELS

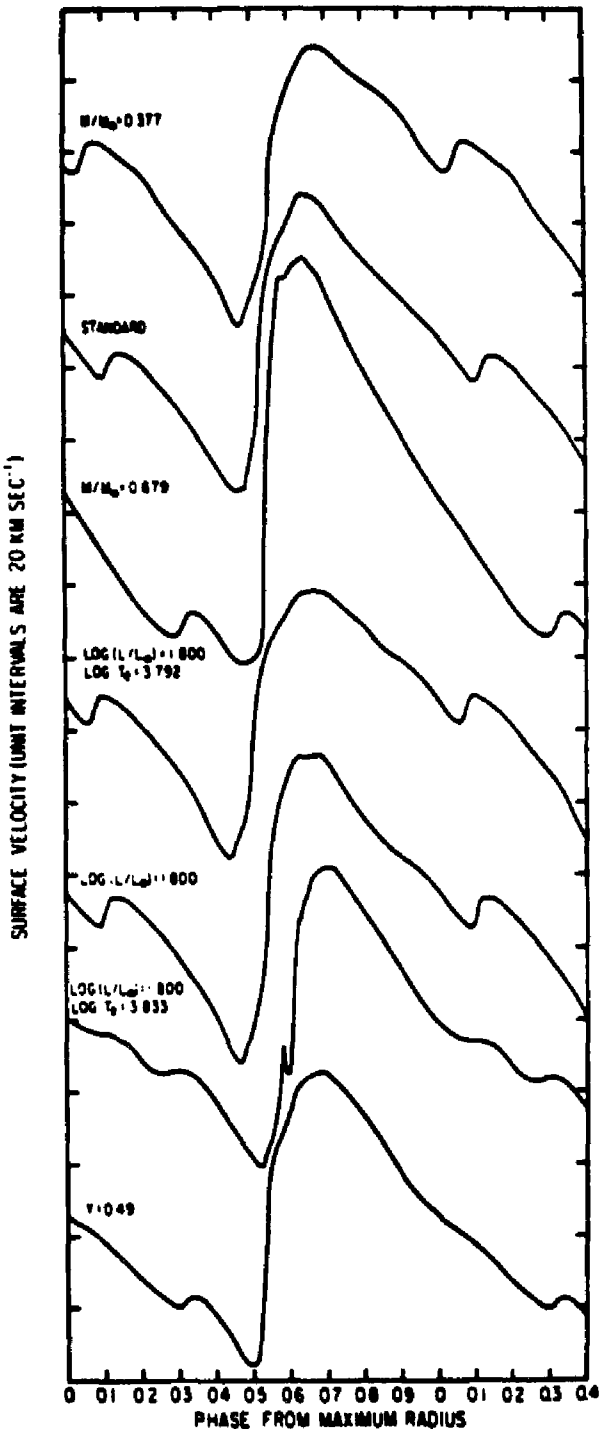

FIGURE 22

SURFACE VELOCITY CURVES OF THE NONLINEAR FUNDAMENTAL MODE MODELS

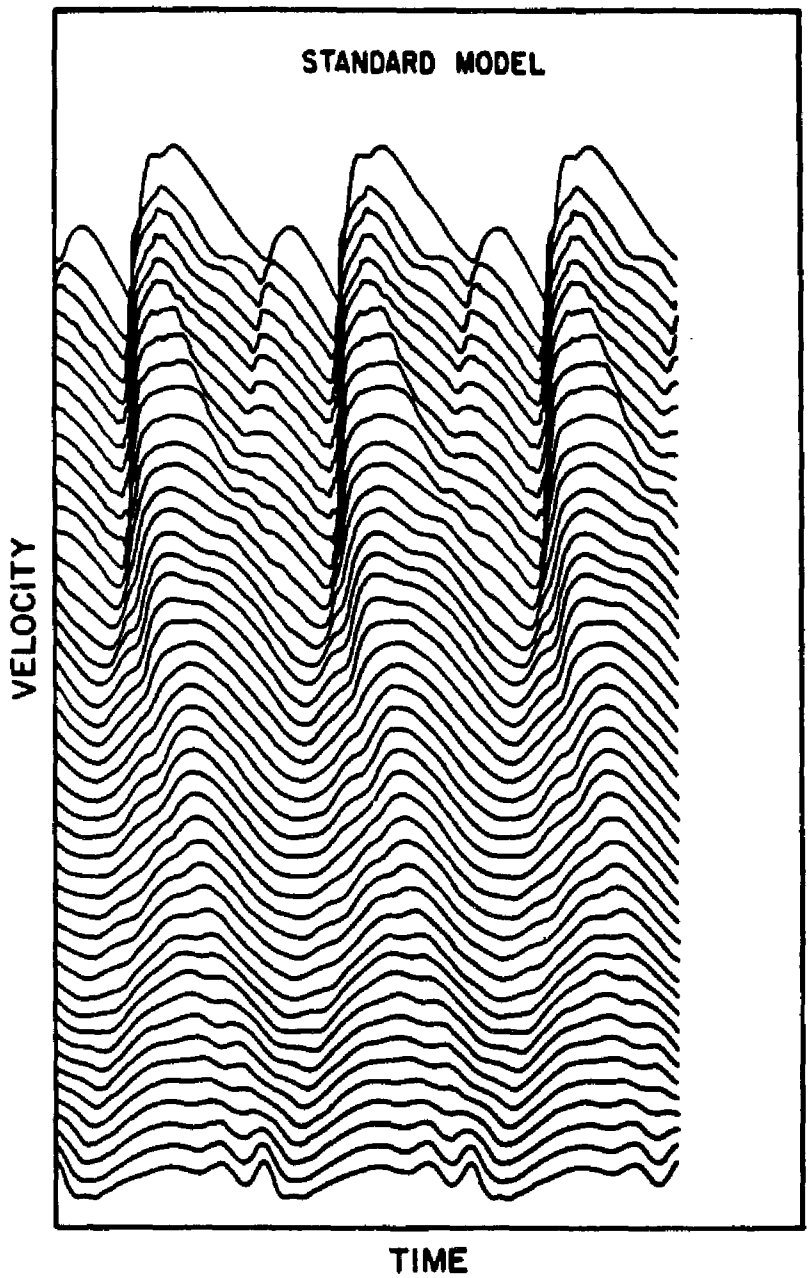

FIGURE 23

VELOCITY CURVES OF ALL THE ZONES FOR THE STANDARD MODEL OF THE FUNDAMENTAL MODE MODELS

(Christy 1966, 1968) as opposed to the resonance effect model proposed by Simon and Schmidt (1976). A further substantiation is found in the period ratios, P_1/P_0 and P_2/P_0, calculated for these models: $P_1/P_0 \sim 0.74$ and $P_2/P_0 \sim 0.58$. These values cannot be accounted for through resonance occurring between the fundamental and the lower overtone modes.

(b) Overtones

Results of the nonlinear calculations for the first overtone models are presented in Table 9 and illustrated in Figures 24 and 25. In keeping with conventions of the previous section the first overtone model for which $M = 0.578\ M_\odot$, $\log (L/L_\odot) = 1.585$, and $\log T_e$ 3.813 is designated as the "standard" model. It should be noted that the word "standard" in this section derives from the selection of parameters and does not indicate a model that is a typical example of a first overtone pulsator. In fact, such is not the case; hence, the use of quotation marks. Further discusson appears later on in the text.

Observed type c stars, almost featureless in comparison to the type *ab* variables, nonetheless, yield distinguishing properties. The theoretical light curves reproduce nicely the symmetry and the double peak at maximum light characteristic of observed c-type stars. The surface velocity curves in Figure 25 satisfactorily resemble published curves. The surface light curves, however, are more instructive in providing a qualitative summation of the parameters of the first overtone mode.

By examination of surface light curves in figure 24,

TABLE 9

FULL AMPLITUDE PROPERTIES OF THE THEORETICAL C-TYPE RR LYRAE MODELS

	MODEL						
parameters	1	2	3	4	5	6	7
$M/M_\odot$	0.578	0.578	0.578	0.578	0.578	0.679	0.679
log $L/L_\odot$	1.585	1.585	1.585	1.700	1.700	1.585	1.700
log T_e	3.813	3.851	3.869	3.851	3.869	3.813	3.851
$R/R_\odot$	4.93	4.14	3.81	4.73	4.35	4.93	4.73
X_{core}	0.46	0.22	0.21	0.20	0.19	0.20	0.20
P (days)	0.378	0.298	0.262	0.371	0.322	0.363	0.338
KE_{max} (10^{40} ergs)	0.197	0.092	0.061	0.093	0.053	0.276	0.149
$\Delta R/R$	0.14	0.07	0.067	0.079	0.06	0.097	0.086
V_{out} (Km/s)	37	28	25	25	22	30	30
V_{in} (Km/s)	-34	-22	-19	-22	-17	-29	-24
ΔV (Km/s)	71	50	44	47	39	59	54
L_{max} (10^{35} erg/s)	1.86	2.1	2.0	2.4	2.44	1.8	2.8
L_{min} (10^{35} erg/s)	0.97	1.0	1.14	1.5	1.54	1.1	1.3
ΔM_{bol}	0.71	0.81	0.61	0.51	0.50	0.53	0.83
$\delta\phi = \phi_{mag} - \phi_{vel}$	0.0	-0.10	-0.12	-0.12	-0.14	0.015	-0.10
P_1/P_0	0.715						
node at x	0.867	0.824	0.815	0.823	0.820	0.832	0.820
# zones	47	39	41	39	41	39	42

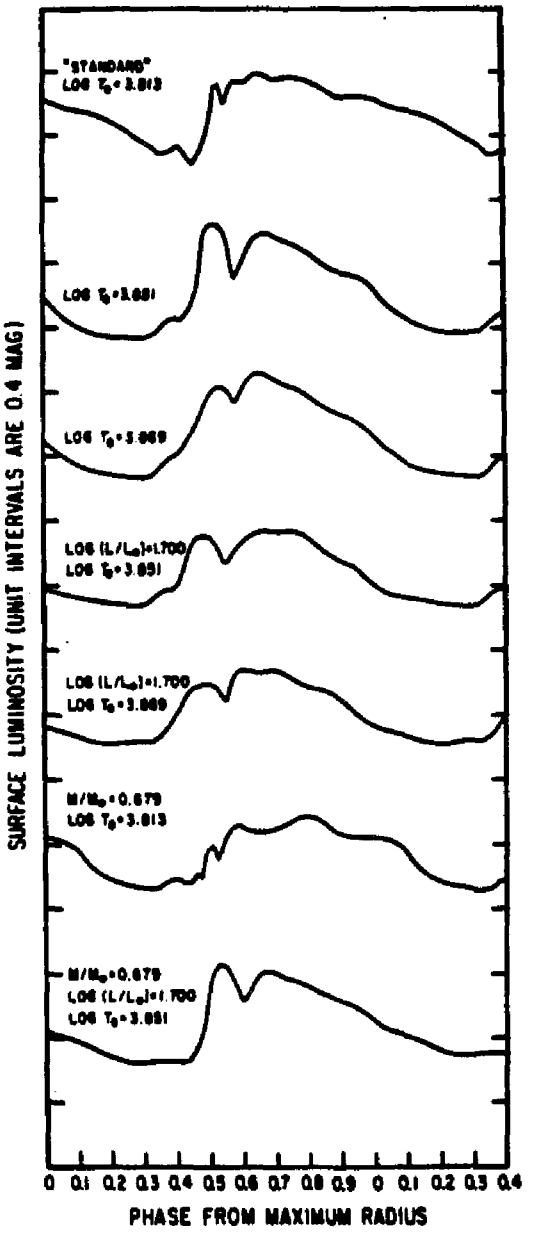

FIGURE 24

SURFACE LUMINOSITY CURVES OF THE NONLINEAR FIRST OVERTONE MODE MODELS

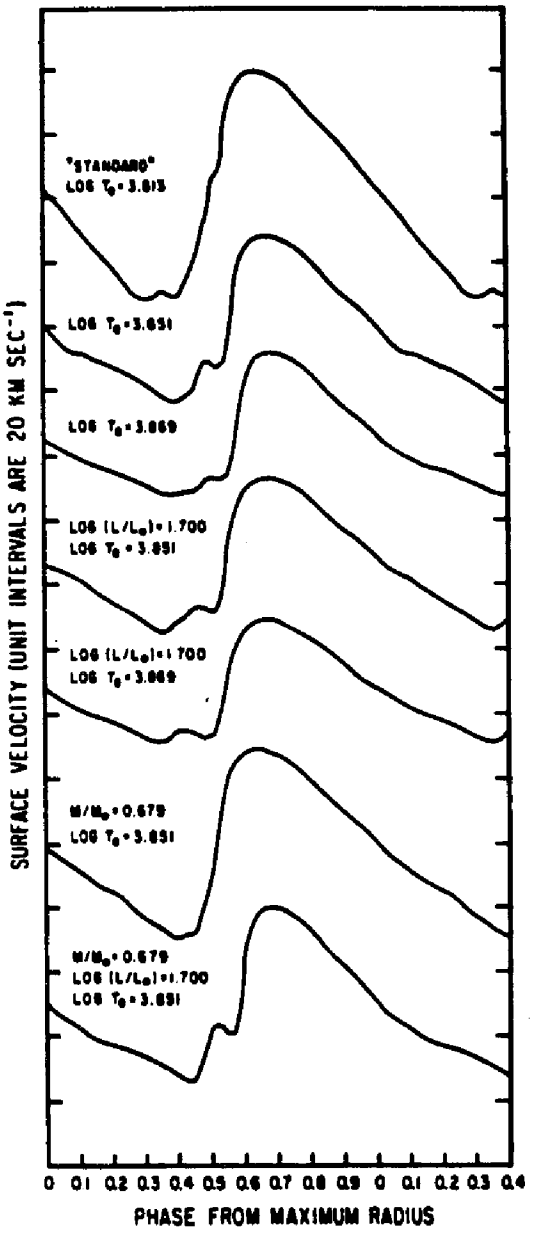

FIGURE 25

SURFACE VELOCITY CURVES OF THE NONLINEAR FIRST OVERTONE MODE MODELS

and phase differences, $\delta\varphi$(mean), in Table 9, some of the input parameters within the grid can be ruled out as having a large effect on the characteristics of type c RR Lyrae stars. Models #1, #2, and #3 differ only in effective temperature. As log T_e increases from 3.813 the phase of mean light changes from a point of coinciding with the phase of mean velocity to leading it by ~0.12 P at log T_e = 3.869. The two models at higher luminosity (models # 4 and #5) show this same increase in $\delta\varphi$(mean) with increasing temperature. An increase in luminosity at constant temperature causes the phase of mean light to occur earlier than it does at the lower luminosity value. It is apparent, however, that the phase difference, $\delta\varphi$(mean), is mainly an effect of temperature. Another qualitative phenomenon stemming from luminosity is also illustrated in Figure 24. For models #2, #3, #4, and #5 one notices that the second peak at maximum light is broadened for the higher luminosity model at a constant temperature. Measurements of relative height and the phase difference between the two peaks at maximum light yielded information of no immediate significance. Altogether, c-type models are very sensitive to effective temperature and only mildly luminosity dependent.

The ascending branch for relatively symmetric model light curves (models 2-5, figure 24) shows satisfactory agreement with c-type stars for the choice of low mass. High mass model stars have both inappropriate light curve geometries and phase differences. In the case of the low temperature models the increase in the mass causes the phase of mean light to lead the phase of mean velocity.

Asymmetry values are not accurately defined for split maxima curves and thus are not considered in the present quantitative work.

Having examined the surface curves related to stellar parameters, we will now discuss the unsuitability of the "standard" first overtone model for an RR Lyrae *c*-type variable. Though the calculated period is within the range of observed values, the asymmetry and the velocity amplitude fall more within the range of *ab*-type variables. Also, the observed phase difference for *c*-type stars, on the order of $\delta\varphi \sim -0.15$, is opposed to that of the "standard" model, which is about ~0.0, verging on the fundamental mode value. Moreover, the log T_e = 3.813 models lie outside the observed effective temperature range. The stellar parameters of *c*-type stars are thus poorly defined by the "standard" model. This further substantiates the conclusions of Cox, Hodson, and Clancy (1983) who report first overtones at higher temperatures, more appropriate to the fundamental blue edge.

Velocity plots for all the zones for the "standard" model and for model #2 are graphed in Figures 26 and 27, respectively. Figure 27 is a typical zonal velocity plot of the first overtone models whose velocity reversal at the node is well illustrated. The sinusoidal behavior of the motion near the node is clearly evident and the independence of the pulsation above and below the node is apparent. On the other hand, the zonal velocity plot for the "standard" model appears more to resemble that of the fundamental mode. There is little evidence in the plot that this is a first overtone model though it is clearly

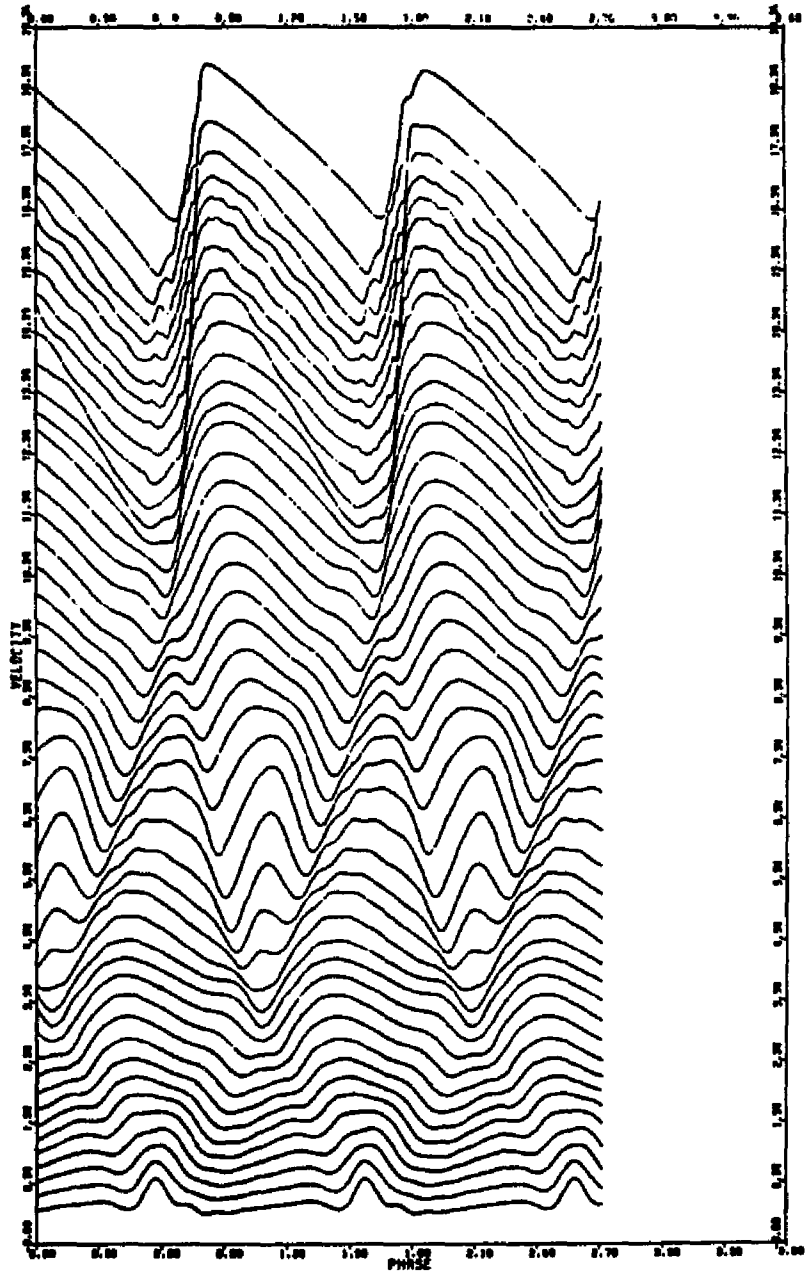

FIGURE 26

ZONAL VELOCITY CURVES FOR THE "STANDARD" MODEL
OF THE NONLINEAR FIRST OVERTONE MODELS

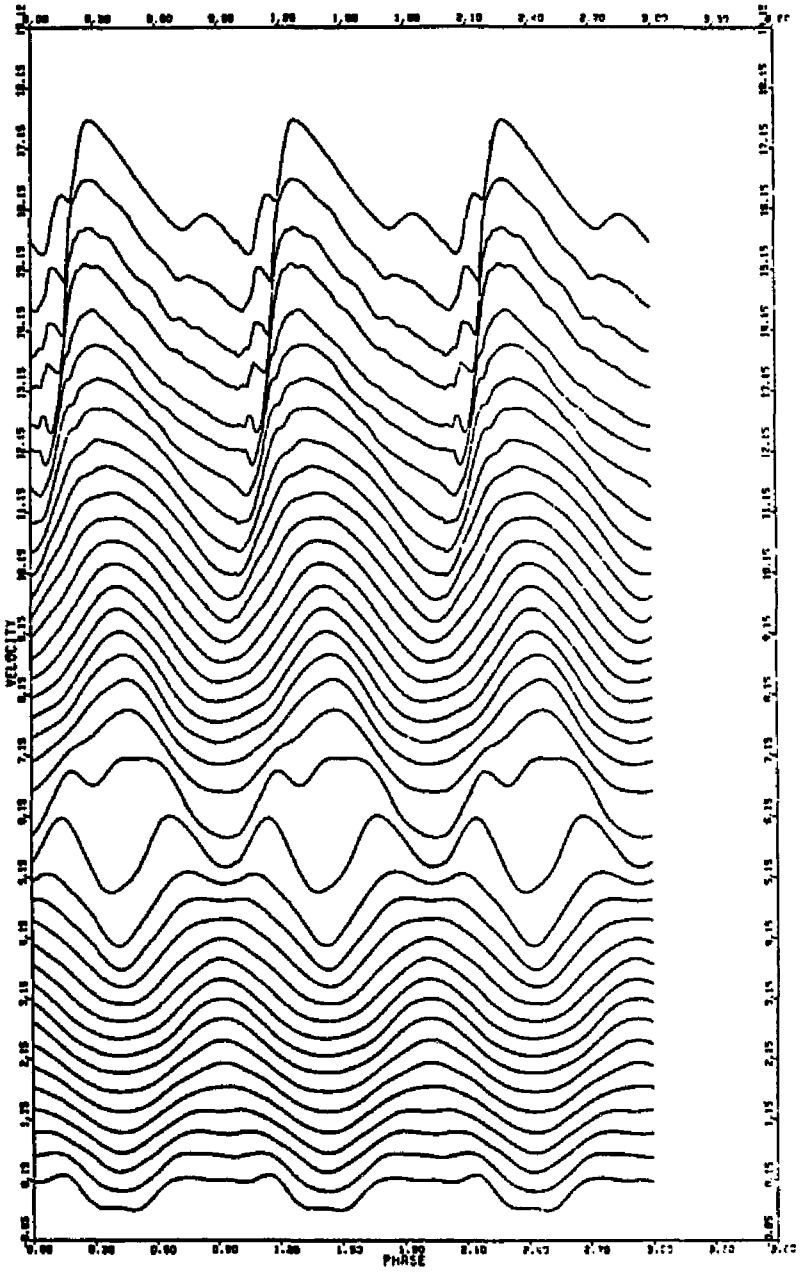

FIGURE 27

ZONAL VELOCITY CURVES FOR A TYPICAL
NONLINEAR FIRST OVERTONE MODEL

indicated as such in the nonlinear model calculations. Most noticeable is what appears to be the Christy echo. In the zonal velocity plots for the typical first overtone model (Figure 27) any disturbance originating from the ionization regions propagates outwardly, only. The zonal velocity plot for the "standard" model shows that the disturbance in this model star produces a Christy-type echo. Apparently, the Christy echo effect is strong enough in some cases to alter the more typical internal structure found for the first overtone models. Careful examination of the "standard" zonal velocity plot shows a gradual change of the reflection of the maximum in velocity above the node into a minimum below the node rather than an abrupt change as in Figure 27. Further investigation of this model would be beneficial.

4.2 Comparison with previous surveys

As mentioned earlier the phase of the bump on the descending branch of the velocity curve for most of the fundamental mode models calculated using Carson opacities is $\varphi_v \sim 1.6$. This same bump for calculations done by other authors (Christy 1966, Baker and von Sengbusch 1969) is ~1.9. Stellingwerf (1975), who calculated his models using the King 1a opacities, measured the bump phase to be ~1.5. Though this latter value for φ_v is roughly comparable to that of the Carson models, Stellingwerf's models were calculated for very shallow envelopes and these results cannot be considered totally reliable. As it was illustrated in Figure 23, the secondary bump is the manifestation of Christy's (1966,1968) echo phenomenon,

and if the envelope is too shallow, as in Stellingwerf's models, the time of the traveling echo is too short.

Other features of the calculated models using the Carson opacities are qualitatively similar to those of other authors. The light amplitude of our standard model is a bit larger than Christy's 5gF but effects due to radiation pressure were ignored in his model. There is little difference in the periods between our results and those of the Christy survey. The fundamental mode periods may be fitted analytically to

$$P_0 \sim 0.022 \left(\frac{R}{R*}\right)^{7/4} \left(\frac{M}{M*}\right)^{-3/4} \quad \text{days},$$

which is the same as that developed by Christy. The scatter in the coefficient is ± 0.0005.

The fundamental standard model was recalculated using the new Los Alamos opacities. The resulting full amplitude pulsation has the following characteristics: P(day) = 0.536; $\Delta R/R$ = 0.29; ΔV(km/sec) = 98; ΔM_{bol} 1.8; *Asymmetry* (vel.) = 4.3; *Asymmetry* (lum.) = 19; and phase φ_v = 1.77. The surface velocity and luminosity curves are plotted in Figure 28. The bump in this model occurs earlier than φ_v = 1.90, the phase of the bump for Christy's 5gF model (as measured from his plot in Figure 15 of his survey paper). However, the phase of this bump in the Carson opacity model is earlier still by 0.15 P. Clearly, the Carson model is a better fit to the observed value of ~1.6. The amplitudes are also larger in the standard model calculated with the Los Alamos opacities.

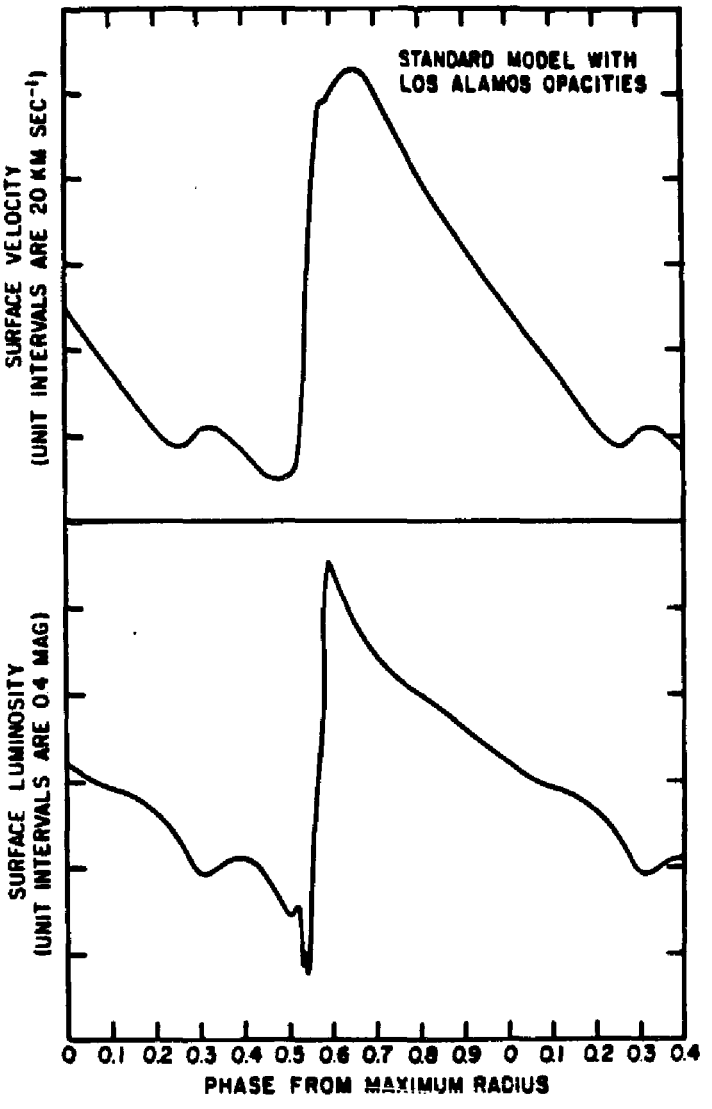

FIGURE 28

SURFACE VELOCITY AND LUMINOSITY CURVES OF THE NONLINEAR MODEL USING THE NEW LOS ALAMOS OPACITIES

Christy demonstrated that a saturation in the helium ionization region will limit the nonlinear amplitudes. Evidently, the larger helium bump in the Carson opacities has little effect on the final amplitudes of the pulsations.

Even though Christy's theoretical calculation of RR Lyrae variables was primarily concerned with the *ab*-type models, his paper provides also an extensive survey of first overtone models. Direct numerical comparison with his results is limited to our "standard" model but the surface velocity and light curves in Christy's Figure 33 furnish enough information to make a suitable comparison with the Carson models.

Stellingwerf's (1975) nonlinear survey included some first overtone models. Two of his models are similar in stellar parameters to models #4 and #5 in the Carson survey. If Christy's (1966 p.152) statement that the pulsation of the first overtone model envelope behaves as if an "immovable boundary" were placed at the node holds true, then the shallow envelopes of the Stellingwerf models should not be completely disregarded in the case of the overtone models. Neither Christy nor Stellingwerf list the position of the nodes in their models. However, there is no reason to assume a substantial difference from that found in the Carson models.

The bottom of the envelope for the Stellingwerf models is $x \sim 0.66$ ($x \sim 0.2$ for the Carson models) and the node is located at $x \sim 0.82$ in the Carson models. In the model corresponding to #4 in Table 9 the periods agree well, which is not surprising. However, the

velocity amplitudes for the Stellingwerf models are larger by 10 km/sec and bolometric light amplitudes by about 0.43 mag. There is closer agreement for the model with log T_e = 3.869 but the magnitude amplitude is still greater by 0.12 mag. It is possible that the difference may be due to opacity since the standard model for the fundamental mode using the Los Alamos opacity also has amplitudes larger than those of the corresponding Carson model. Otherwise, the assumption of an immovable boundary at the node is not valid. Phase lag values are not available for the Stellingwerf models; thus further comparisons cannot be implemented.

Within the range of features available for comparison, the Carson models agree well with the Christy models. The double peak is present in both sets of models but where the first peak appears to get larger with increasing temperature for the Christy models the reverse is true for the Carson models. In relation to phase difference values, Christy defines the phase lag as the difference between the phase of mean light and the phase at which the star is at zero velocity. The phase of mean velocity is used to define the phase difference in the present survey. It turns out that there is a negligible difference between the phases of zero velocity and mean velocity for the Carson models. Accordingly, these values will be considered the same and referred to in this text as $\delta\varphi$.

Christy's wide range of models furnishes a framework which establishes phase lag trends for variations of the stellar parameters. Figure 29 illustrates the mass, luminosity, and helium content variation of the phase

FIGURE 29

VARIATION OF THE PHASE LAG WITH LOG T$_e$ DUE TO CHANGES IN MODEL PARAMETERS

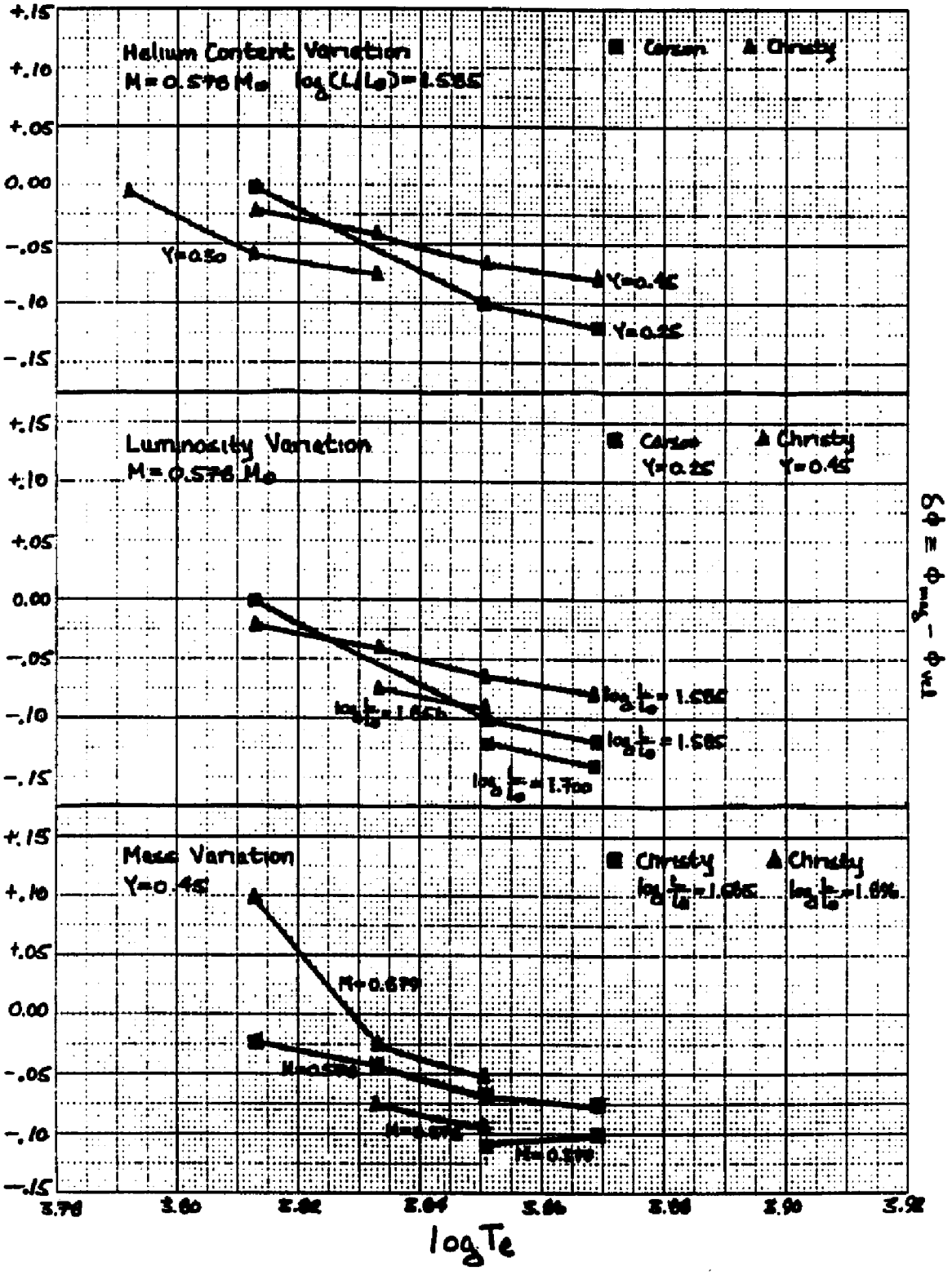

difference in both Christy's and the present surveys of the first overtone mode models. The Carson models were all calculated for one chemical composition, consequently, no composition comparison may be made. However, the behavior is qualitatively the same for the variation with mass and luminosity. Quantitative comparisons are generally unreliable since the trend of helium content variation for the Carson models is unknown. As Figure 29 shows, the phase lag decreases with an increasing luminosity, and increases with mass and helium abundance. This phase lag difference will provide an important connection when these theoretical results are compared with observations.

CHAPTER 5: OBSERVATIONAL COMPARISON WITH THEORETICAL RESULTS AND CONCLUSIONS

5.1 Comparison with observation (nonlinear survey)

The present computational approach outputs a spectrum of usable stellar parameters which can be tested against observations. Some of these represent rather minor additions to an already comprehensive body of work (Christy 1966, Iben 1971), and others seem to be quite new and timely in providing alternative perspectives on observations, or better resolutions of already reasonably well understood parameters, such as mass and helium content. This section attempts to place present results into the historical framework. The overall conclusions are left to the last part of this section.

Few variable stars are realistically suited to a comparison analysis. In particular, the theoretical surface velocity curves are calculated with greater accuracy than the surface light curves. However, it is the light curve which is observed more frequently and in greater detail than the velocity curve. Consequently, the paramters of only four *ab*-type and four *c*-type RR Lyrae stars, listed in Table 10 and 11, respectively, have the appropriate coupling of the light and velocity curves. (YZ Cap is included in Table 11 because its $\delta\varphi$(mean) is important in the comparative analysis.) The radial

TABLE 10

OBSERVED PROPERTIES OF FOUR AB-TYPE RR LYRAE VARIABLES

Parameter	Variable			
	XZ Cyg	RR Lyr	X Ari	SU Dra
P (day)	0.467	0.567	0.651	0.660
$\Delta R/R$	...	0.13	0.17	0.13
(24/17) ΔV_{rad} (km s^{-1})	85:	85	75	85
ΔM_{vis}	1.2	1.0	1.0	1.0
Asymmetry (vel.)	3:	4	4	6
Asymmetry (lum.)	6	6	6	6
ϕ_v	1.6:	1.6	1.6	1.6
References	3, 4	1, 2, 5, 6, 7, 14	9, 12, 15	8, 10, 11, 13

References. -- (1) Sanford 1935, 1949; (2) Struve and Blaauw 1948; (3) Struve and van Hoof 1949; (4) Muller 1953; (5) Hardie 1955; (6) Abt 1959; (7) Oke and Bonsack 1960; (8) Varsavsky 1960; (9) Preston 1961; (10) Spinrad 1961; (11) Oke, Giver, and Searle 1962; (12) Preston and Paczynski 1964; (13) Preston 1965; (14) Preston, Smak, and Paczynski 1965; (15) Oke 1966.

velocity amplitudes quoted in the references have been multiplied by the fraction 24/17 to correct for limb darkening and for geometric projection. Observed radial velocities are derived using the metal and hydrogen lines of the stellar spectra. The metal lines reflect better the overall motion of the atmosphere. Therefore, these velocities are integrated into the present comparisons. Since two of the stars (XZ Cyg and RR Lyr) exhibit a Blazhko effect in their light curves only the largest amplitude cycles have been listed in Table 10. None of the theoretical models show any long-term variation with time.

Within the grid of stellar models, the standard model for the fundamental mode shows exceptional agreement with the overall observed characteristics of the *ab*-type variables, especially in connection with the phase of the secondary bump. When the theoretical results listed in Table 8 are compared with the corresponding observed values in Table 10 the models with high and low mass as well as the high helium model star (models #1, #3, and #7, respectively) may be ruled out as viable candidates for RR Lyrae stars. Observational errors in measuring the phase of the secondary bump on the descending surface velocity curve are quite small. The phase φ_s of the low mass model is about 1.5, and about 1.8 for the high mass and high helium models. The large differences of these phases from the observed phase value of ~1.6 warrants the exclusion of $M \sim 0.4\ M_\odot$ and $\sim 0.7\ M_\odot$ and $Y = 0.50$ as stellar parameters for RR Lyrae stars, leaving the standard model as the remaining viable model.

The phase difference between mean light and mean velocity somewhat mitigates the happy observational accord shown for the secondary bump. The phase lag for *ab*-type RR Lyrae variables is observed to be +0.01 P (Preston and Paczynski 1964). The $\delta\varphi$(mean) value for the standard model is +0.06, which is a comparatively significant deviation from the observed value. An improved radiative transfer theory may decrease the calculated phase lag but Stothers (1981) suspects on the basis of radiative transfer calculations by Hill (1972) that this does not sufficiently decrease the discrepancy. Further discussion will continue in connection with the first overtone models.

As a summary statement for the nonlinear *ab*-type models, the following characteristics may be accepted for RR Lyrae stars: M/M* = 0.55 - 0.65, Y = 0.2 - 0.3, and log (L/L*) = 1.6 - 1.7. Other methods of mass determination (Stothers 1981) produce values within this range which are similar but not more definitive. It is expected that the first overtone survey and/or linear survey comparison with observation will provide additional improvements.

It can now be demonstrated that the nonlinear program can reproduce optical observations well enough to permit differentiation within the adopted grid, even for the relatively bland *c*-type model stars. Lub (1977) presents light curves for thirteen *c*-type RR Lyrae stars ranging in period from $0^d.254$ to $0^d.406$. These curves are symmetrical and have a preliminary hump that may appear as a slight shoulder before maximum light (BY Eri, T Sex, V487 Sco) or

may occur very close to maximum light producing a double peak (DH Peg, YZ Cap, CG Lib, AU Vir). This first peak is not as broad as the second one nor does it exceed the magnitude of the second peak, though it may closely approach its height. As evident in Figure 24 the theoretical light curves reproduce all of these observed features quite closely.

There are two stars in Table 11 that match well two of the first overtone models. The light curve of model #3 for which M = 0.578 M*, log (L/L*) = 1.585, and log T_e = 3.869 with a period of $0^d.262$ is very similar to the visual light curve of DH Peg ($P = 0^d.256$) (Tifft 1964, Paczynski 1965). In addition to the agreement in period ($P \sim 0^d.26$) the shape of the curve is the same; the rise time of the light curve of the model and DH Peg is ~ 0.42 P and the difference in phase between the two peaks is about 0.12 P. Preston and Paczynski (1964, hereafter PP) give a temperature range of log T_e from 3.864 to 3.876 for DH Peg which coincides nicely with the temperature of this model. Another satisfactory match up is between model #5 and T Sex. Besides agreement in period ($P \sim 0^d.32$), the rise time, the short preliminary peak and broad secondary peak resemble the same structure of T Sex (Tifft and Smith 1958, PP, Radziszewski 1965). The temperature range for this star given by PP to be log T_e = 3.857 - 3.876 similarly includes the temperature of model #5 (log T_e = 3.869).

As important as the light curve maxima are in matchups, the calculated phase difference, $\delta\varphi$(mean), shows less good agreement with the stars of Table 11. The

TABLE 11

OBSERVED PROPERTIES OF FOUR C-TYPE RR LYRAE VARIABLES

	Variable			
Parameters	DH Peg	YZ Cap	RZ Cep	T Sex
P (days)	0.256	0.274	0.309	0.325
ΔV_r (Km/s)	30		36	30;22
$(\frac{24}{17})\ \Delta V_r$ (Km/s)	42		51	42
ΔM_{vis}	0.048		0.54	0.45
$\delta\phi$	-0.18	-0.14		-0.19
Sp (Ca I)	A2-A7		A2	A2-A4
Sp (H)	A5		A9	A9-F4
ΔS	1.2	3	7	5.3
References	1,2,6,7	1,7,8	3,5,7	1,2,4,7

References -- (1) Preston and Paczynski 1964; (2) Tifft 1964; (3) Paczynski 1965; (4) Tifft and Smith 1958; (5) Epps and Sinclair 1973; (6) Bonsack 1957; (7) Butler 1975; (8) Kinman 1961

discrepancy in $\delta\varphi$(mean) between the observed and calculated values is the same in magnitude and direction as found for the *ab*-type models. This may be due to a systematic error in the calculations or it may warrant an improvement over the radiative diffusion approximation to be employed in the stellar equations which will remove some of the differences (Stothers 1981, Hill 1972).

Another possibility is voiced by PP. They discovered that for Christy's models the calculated phase lags for the *a*-types did not agree with observations. In fact, these lags are on the order of magnitude of the $\delta\varphi$(mean) for our *ab*-type models. Closer examination of the models revealed a continuing decrease in the phase lag difference as the theoretical model continued to pulsate even though full amplitude was achieved. The calculation of the nonlinear models of this survey was usually stopped when full amplitude was first reached. The criterion for terminating the model calculation was the leveling off to zero of kinetic energy growth. A longer time integration past full amplitude might result in an improved phase lag value.

We summarize the foregoing mass and luminosity properties of the *c*-type models succinctly: As discussed in an earlier section the "standard" model and the high mass model (#6) at low effective temperature were found to be unsuitable on the basis of the $\delta\varphi$(mean) values (+0.0, +0.015, respectively). The phase values for the rest of the models are of the right order of magnitude and are not as useful in differentiating further the values for the mass and luminosity. By relying on the shapes of the

light curves to complete the deductive process, the models suggest a mass of 0.6 M* and a luminosity of log (L/L*) ~1.7, though ~1.6 is also acceptable. As expected (and somewhat reassuringly) these nonlinear first harmonic models substantiate the conclusions based on the fundamental mode models.

5.2 Comparison with observation (linear survey)

The linearized models complement and extend our nonlinear models, and suggest an independent method of verification. The method we use follows that of Cox, Hodson, and Clancy (1983, hereafter CHC). The following is our summation of part one of the CHC method. The ratio of the first overtone period to the fundamental period is sensitive to mass. CHC reanalyzed the RR Lyrae stars in M15 observed by Sandage, Katem, and Sandage (1981, hereafter SkS) and found seven double mode pulsators suitable for pulsation theory analysis. The periods and period ratios derived from the present linear models are plotted in Figure 30 for constant mass, with the observed values for the double mode stars superimposed. The lines of constant mass were calculated using the formula derived in Chapter 3:

$$P_1/P_0 = -0.059P_0 + 0.067\log(M/M*) + 0.03Y^{0.6} - 0.06Z^{0.4} + 0.776$$

which is a mean analytical expression fitted to the Carson opacity results. This formula is used instead of the raw data because of the scatter in the period ratios due to

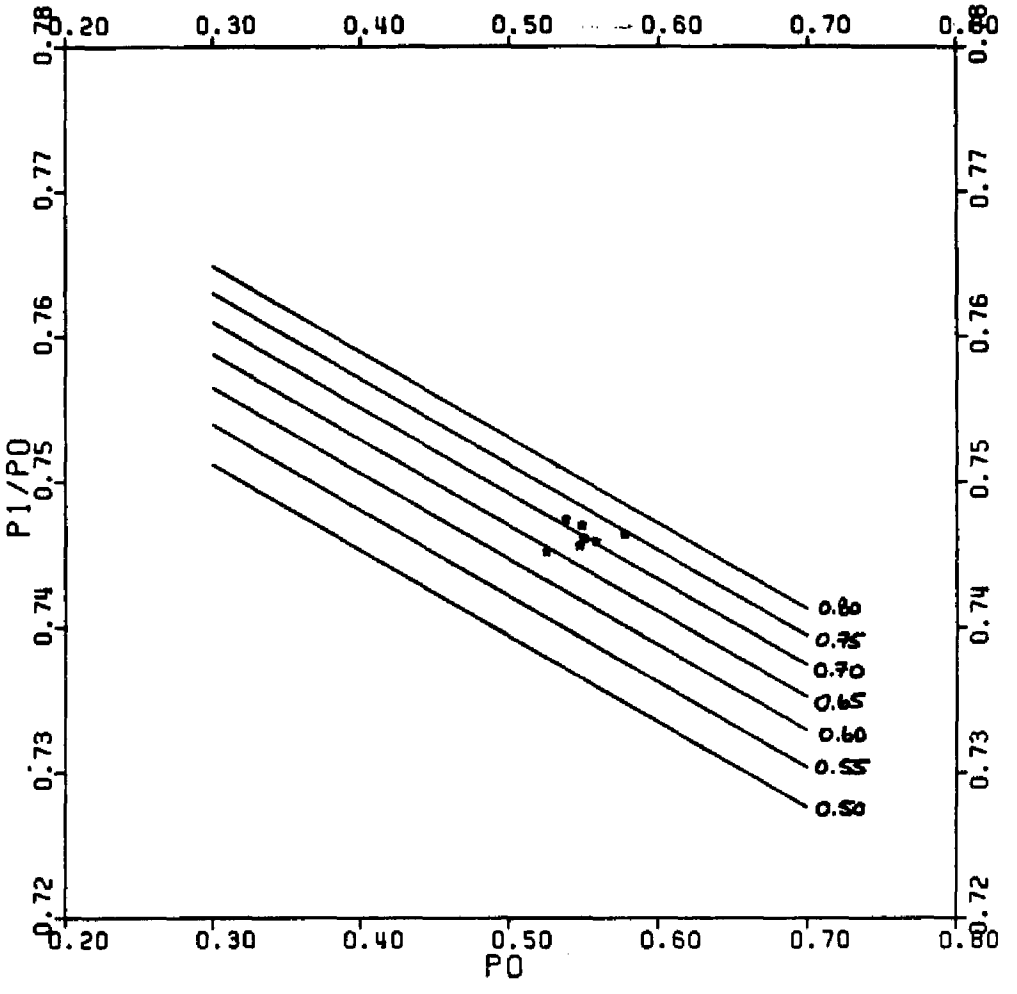

FIGURE 30

LOCATION OF OBSERVED DOUBLE-MODE STARS
ON THE PERIOD RATIO DIAGRAM

luminosity (as was discussed in Chapter 3). These lines were plotted for a chemical composition of (Y,Z) = (0.25,0.00). A value of zero for the metal content is a reasonable approximation here since a very low metal abundance is characteristic of globular clusters. Though the double mode star masses evidently extend from 0.65 M* to 0.75 M* it is easily seen that they aggregate around 0.7 M*. This value for the mass is higher than expected on the basis of the results of the nonlinear models.

It is important to keep in mind that the period ratio lines are derived only from the theoretical models, and they are not a function of mass alone. The effect of the chemical composition on the period ratios is significant. Therefore, the period ratio method of determining the mass for these double mode stars is dependent on the adopted chemical composition. The interplay between the mass and Y can be easily demonstrated. Within the restriction that the period be 0.55 and the period ratio remains 0.746 (the average observed value for the seven mixed mode stars), the constant mass lines in Figure 30 could be translated so that the stars clump around the 0.6 M* line when Y = 0.29. Similarly, for a helium content of Y = 0.26 this type of analysis would yield 0.65 M*. Therefore, the method for determination of the mass cannot converge on unique values, though it is strongly suggestive of a mass range of 0.60 M* to 0.65 M* (coupled to a range in Y of 0.29 to 0.26).

Another method afforded to us to determine mass and helium content comes from the knowledge that the transition edge as defined by Christy probably does not

exist (Cox, 1980A). The star pulsating in the fundamental mode presumably will switch to the first overtone mode at the fundamental blue edge for blueward evolution. Stobie (1971) reported that the shortest average period for RR Lyrae *ab*-type stars is $0^d.45$ for the Oosterhoff type I clusters and $0^d.55$ for the type II clusters. The intersection of the constant period line corresponding to the cluster transition period and the fundamental blue edge can easily be calculated and applied to determining values for the basic stellar parameters of RR Lyrae stars.

The effective temperature of the fundamental blue edge for the Carson opacity models in the mass range from 0.4 M* to 0.8 M*, and for log (L/L*) = 1.6-2.0, Y = 0.25-0.75, and Z = 0.00, can be represented by the following analytical expression:

$$\log T_e = -0.071\log(L/L*) + 0.0867(M/M*) - 0.500(M/M*)^2 + 0.1550Y - 0.0907Y^2 + 3.915 \qquad (12)$$

Using the PTLM relation (equation 10) log T_e may be eliminated. This leaves an equation (quadratic in Y) relating M, L, Y, and P_0. The scatter in P_1/P_0 values (see Figure 4a) due to luminosity is not as small as with the Los Alamos opacities (see Figure 4c). Therefore, by including the luminosity dependence the same quantities can be connected more accurately through a period ratio equation. This "expanded" period ratio equation is

$$P_1/P_0 = -0.059P_0 + 0.067\log(M/M*) - 0.02\log(L/L*) + 0.03Y^{0.6} + 0.810 \qquad (13)$$

The calculated values differ from the raw values by at most 0.001 for the following parameter ranges: M = 0.4 M* - 0.8 M*; Y = 0.25 - 0.50; log (L/L*) = 1.6 - 1.8; P = 0.45 - 0.55; Z = 0.00. For a particular transition period (i.e. Oosterhoff group) and an assumed value of mass, the simultaneous soulution of the above system of equation will yield values for the helium content and luminosity of RR Lyrae stars.

Table 12 lists the series of solutions of these equations. (It should be noted that in solving for Y in the quadratic equation, it always turned out that one of the roots had an unphysical value; for instance, Y = 0.25, 1.46.) The inconsistency between the coupled values of mass and Y in Table 12 and the values discussed in connection with Figure 30 is evident, to say the least. In addition, the high luminosity for the Oosterhoff group II stars is unsatisfactory. A probable explanation is that the equations used are sensitive to the helium content so that a small divergence in log (L/L*) will result in a large divergence in Y. This is particularly true in the case of the equation fitted to the theoretical fundamental blue edge. In the case of the Oosterhoff type I globular clusters, however, the range of parameters is closer to the results of the nonlinear survey. Further examination of this problem is necessary.

Another way of making the comparison is to superimpose the observed data and the theoretical blue edges on the HR diagram with the lines of constant period marked off (as in Figure 4 of CHC). Our construction of

TABLE 12

CALCULATED PARAMETERS FOR RR LYRAE STARS

Oosterhoff Group	Mass	Y	log L/L*	$\log T_e$	P0
II	0.60	0.48	1.85	3.868	0.55
II	0.65	0.40	1.86	3.864	0.55
II	0.70	0.32	1.86	3.858	0.55
II	0.75	0.30	1.94	3.872	0.55
I	0.55	0.24	1.68	3.860	0.45
I	0.60	0.16	1.67	3.850	0.45

Figure 31 begins with an input of the luminosity at the intersection point of the constant transition period line with the fundamental blue edge. This luminosity is converted to an absolute bolometric magnitude and is initially applied in the subsequent calculations as an average. Using the apparent bolometric magnitudes of RR Lyrae stars belonging to a globular cluster having the above transition period, an average distance modulus is calculated. Substituting for each star its rederived individual luminosity, its observed period, and an assumed mass into the PTLM relation (equation 10) log T_e is evaluated for each star, and all the observed stars are plotted on the HR diagram.

Figure 31 is the result of the application of this process to the M15 data given by SKS. The Carson fundamental blue edge for M = 0.65 M* and (Y,Z) = (0.25,0.00) is also plotted. (This mass was chosen because it is the one used by CHC.) The point of intersection with the line P = $0^d.55$ is log (L/L*) ~ 1.83 for this type II cluster. Assuming next the mass to be 0.55 M* (as do CHC), the data for M3 (Sandage 1981) yield the result illustrated in Figure 32. The luminosity at the intersection point is log (L/L*) ~ 1.69. Though the luminosity for the M15 stars is higher than predicted by the nonlinear, models it is as high as that derived by CHC.

In Figure 31 there is an overlap region where different variables are pulsating in the fundamental, first overtone, and mixed modes. The fundamental blue edge passes through the midst of this overlap region and

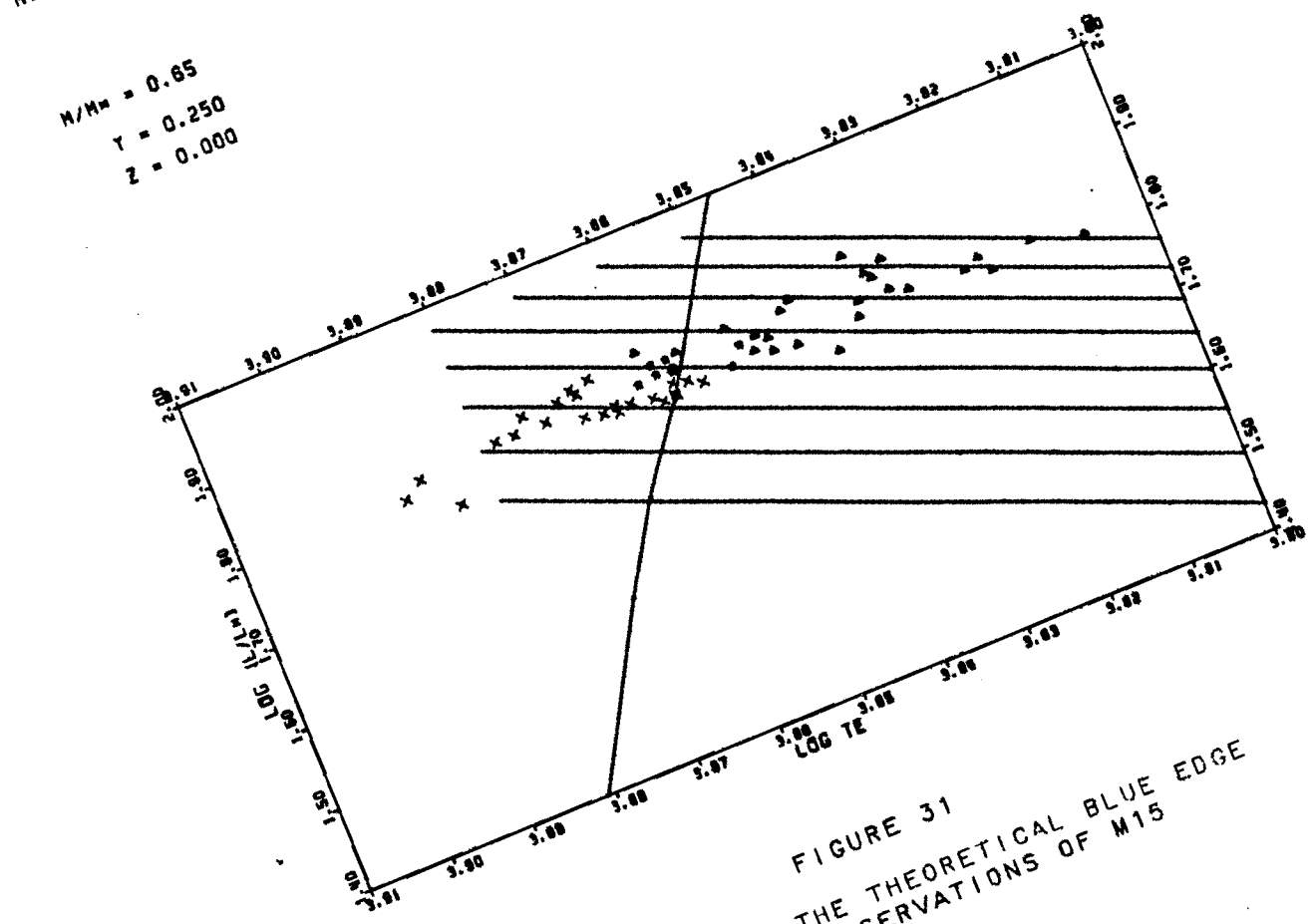

FIGURE 31

COMPARISON OF THE THEORETICAL BLUE EDGE WITH THE OBSERVATIONS OF M15

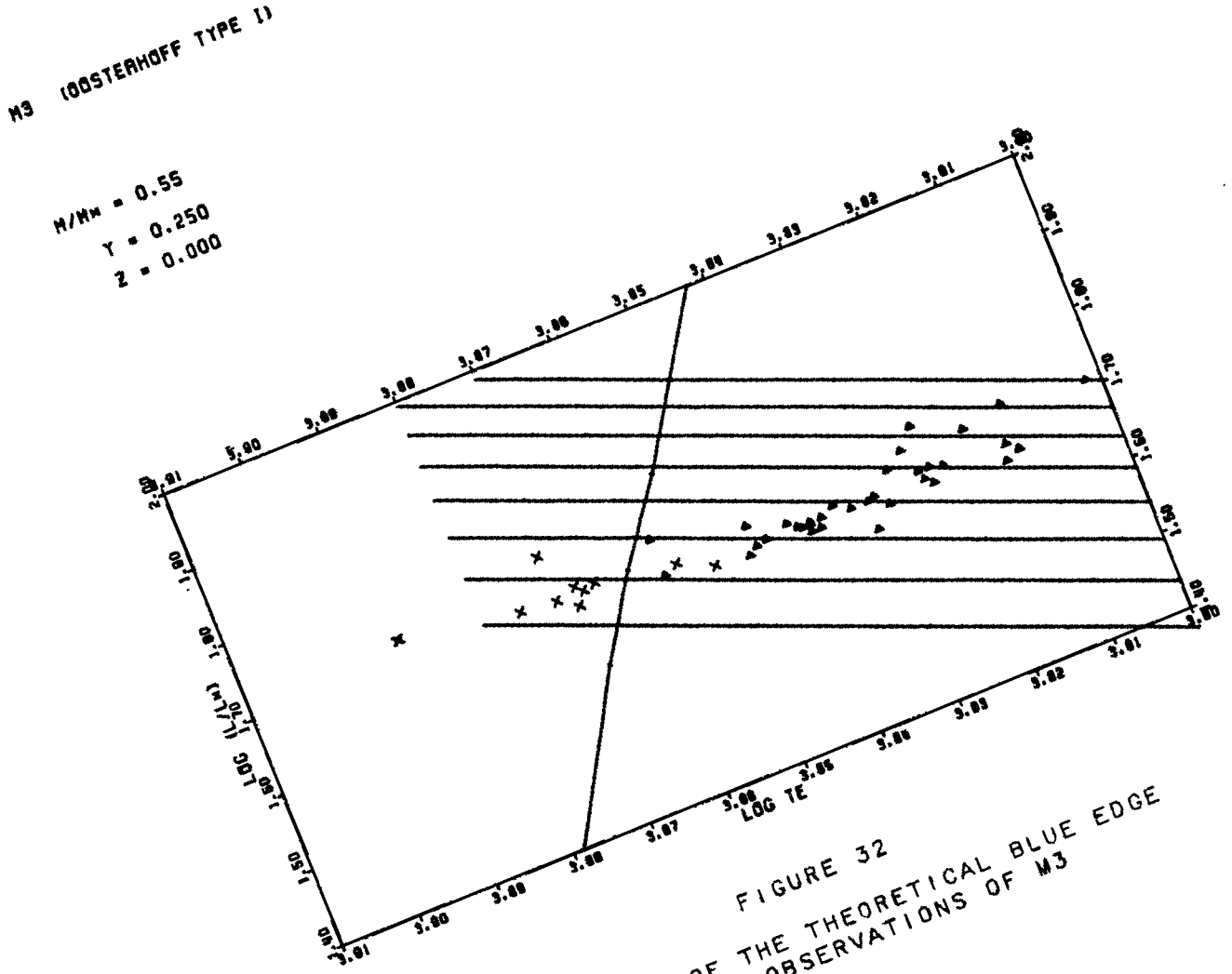

FIGURE 32
COMPARISON OF THE THEORETICAL BLUE EDGE WITH THE OBSERVATIONS OF M3

supports the assumption that this transition occurs at the fundamental blue edge. Of course, a different mass and/or helium content will somewhat shift the position of the fundamental blue edge in this diagram.

CHC claim that this is a method of determining the helium content. It was shown by us, when the linear results were reported, that the mass effects on the fundamental blue edge is small, particularly in the 0.6 M* - 0.8 M* mass range. The effect of the helium content, however, is more significant. Any comparison incorporating the fundamental blue edge will be a good indicator of helium abundance. However, it appears that this is a more subtle differentiator of opacity.

When CHC made their comparison using blue edges for Y = 0.299, the overlap region was situated to the right of the fundamental blue edge. Decreasing the helium content to Y = 0.279 naturally moves the fundamental blue edge redward. However, it is important to keep in mind that the basis for these comparisons is the assumed luminosity at the intersection of the P = 0.55 (or 0.45) line with the fundamental blue edge. If the blue edge is simply translated in the redward or blueward direction the P = 0.55 (or 0.45) point on the fundamental blue edge is altered. This intersection point changes with mass and Y as illustrated in Figure 33 for the two Oosterhoff groups in the mass range 0.4 M* to 0.8 M* (in intervals of 0.05 M*) and for helium abundances of Y = 0.20, 0.25, and 0.30. Therefore, if the initial input luminosity is not varied as the fundamental blue edge is shifted the result will be inconsistent.

INTERSECTION POINT BEHAVIOR
FBE - P=CONSTANT
BOSTERHOFF TYPE 1

LOG (L/Lo) - M/Mo AT P= 0.45

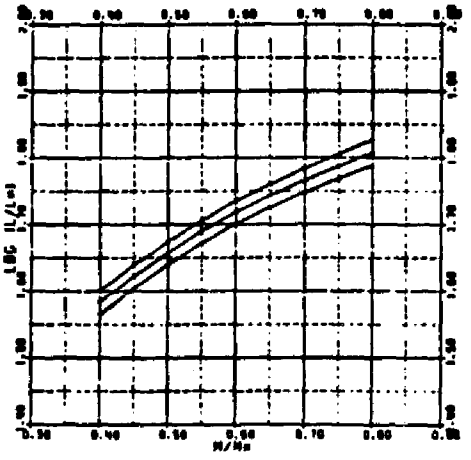

LOG TE - M/Mo AT P= 0.45

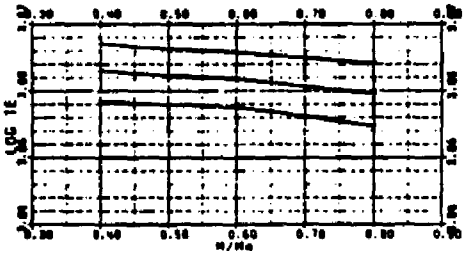

INTERSECTION POINT BEHAVIOR
FBE - P=CONSTANT
BOSTERHOFF TYPE 2

LOG (L/Lo) - M/Mo AT P= 0.55

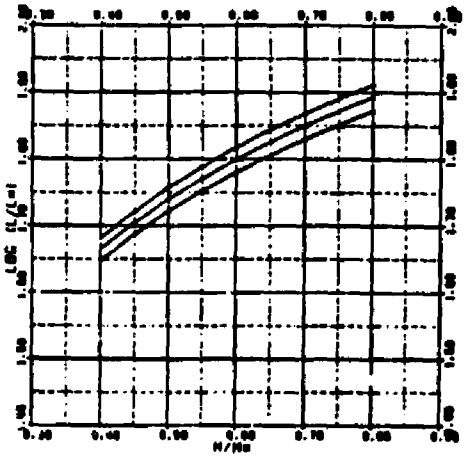

LOG TE - M/Mo AT P= 0.55

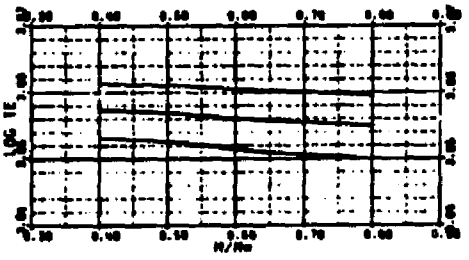

FIGURE 33

BEHAVIOR OF THE INTERSECTION POINT AS
MASS AND HELIUM CONTENT IS VARIED

The same M15 data are plotted in Figures 34a, b with fundamental blue edges corresponding to two different combinations of mass and helium abundance. In the CHC plots the fundamental blue edge for Y = 0.299 is to the left of the overlap region and it moves redward when the graph is redrawn using the fundamental blue edge for Y = 0.279. As clearly seen in Figures 34a,b, decreasing or increasing the mass and/or Y does not significantly shift the fundamental blue edge relative to the data. The reason for this is the strong playoff between Y and M. The only difference in the graphs is the luminosity moving the data up or down. This type of plot would give specific values for M and Y if the luminosities of RR Lyrae stars in globular clusters were known by some independent method. As already described, this type of comparison graph is solidly based on pulsation theory. The fundamental blue edge is consistently situated in the midst of the mixed mode variables. Since the only difference between the CHC models and the ones in the Carson survey is the opacities used for the calculations it may be possible to interpret these graphs as differentiators of the opacity. In that case the models using Carson opacities more closely resemble observations. A similar diagram for the M3 data, presented in Figures 35a,b, shows the theoretical fundamental blue edge falling between the ab- and c-type variables. Interestingly, the corresponding CHC plot for the same M and Y is similar to Figure 32, with respect to the relative positions of the fundamental blue edge and the observed stars.

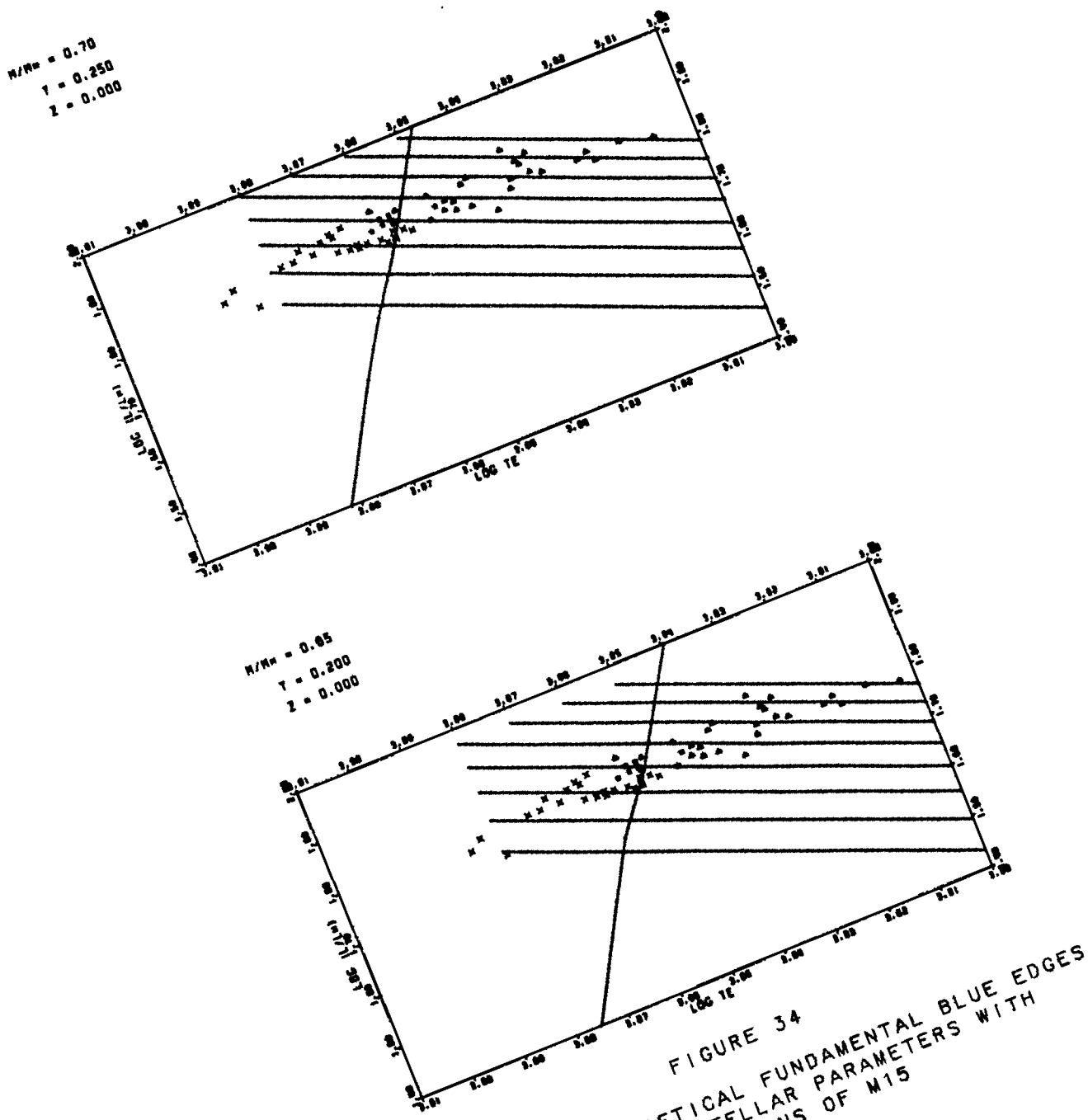

FIGURE 34

COMPARING THEORETICAL FUNDAMENTAL BLUE EDGES FOR DIFFERENT STELLAR PARAMETERS WITH OBSERVATIONS OF M15

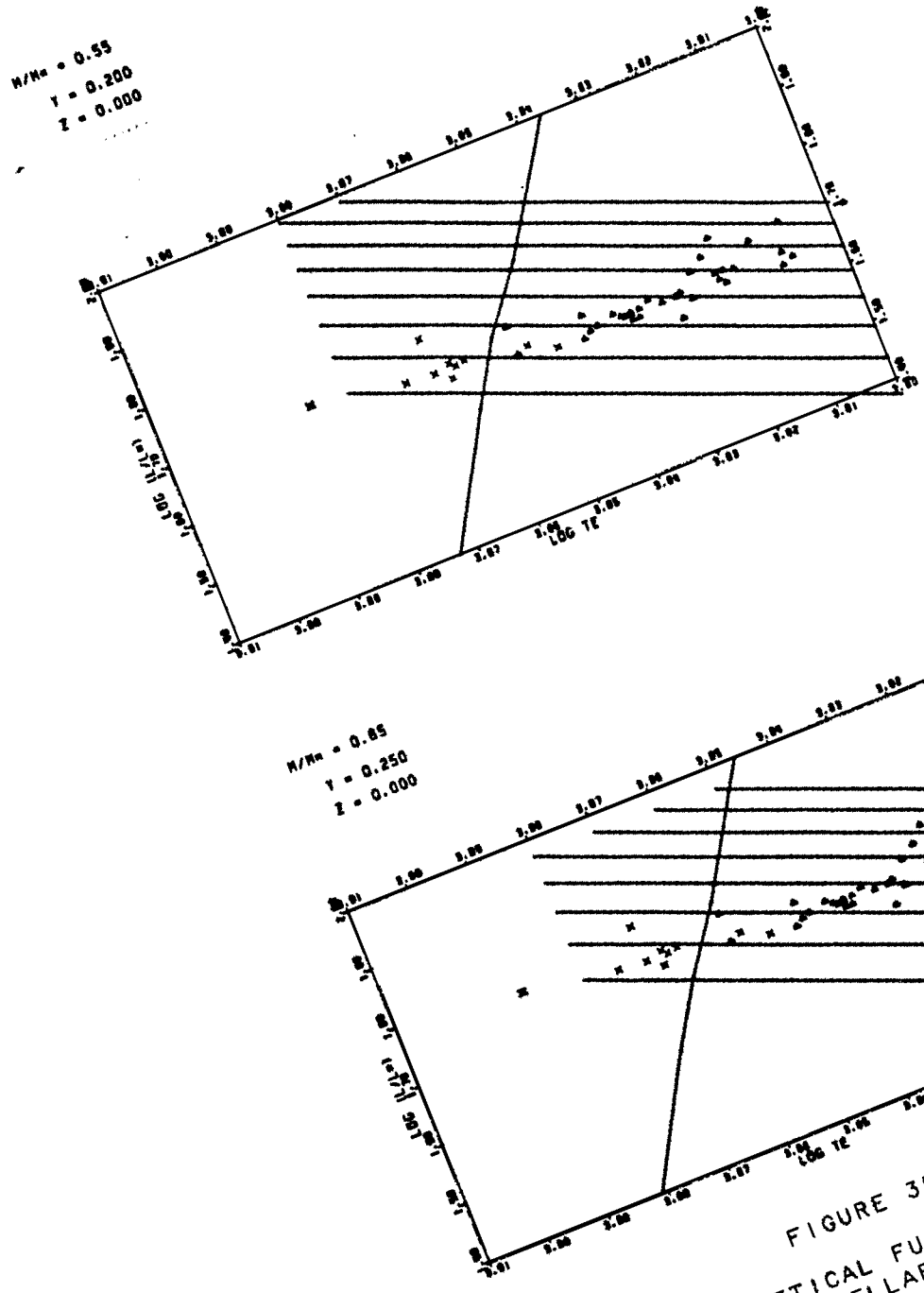

FIGURE 35

COMPARING THEORETICAL FUNDAMENTAL BLUE EDGES FOR DIFFERENT STELLAR PARAMETERS WITH OBSERVATIONS OF M3

Observations of the blue edges of the globular clusters can now be used in a third, independent derivation of the masses and helium abundances. This approach has rarely been invoked in model comparisons, and no previous investigator has attempted to reach this level of model justification. Specifically, the unreddened colors of the shortest period RR Lyrae stars have been collected from papers by Sandage and coworkers (1981, 1982) and Deupree (1977). These colors have then been converted to effective temperatures using the Bell calibration (Butler, Dickens, and Epps 1978). Other color - temperature conversions were considered (Oke, Giver, and Searle 1962, Dickens 1970), but the Bell calibration was chosen since Sandage, Cox, and respective workers applied this calibration in their studies. When the unreddened colors were applied to the Dickens calibration the difference in log T_e from the Bell values was at most ~ 0.01. The converted color data are here superimposed on plots of the Carson first overtone blue edges for varying parameters in Figure 36.

Surprisingly, given the uncertainties which attend the processing of the raw colors, and those involved in the conversion to effective temperatures, the temperature span of the observed blue edges is quite small. The upper and lower limits to the observed luminosities are taken from Sandage (1970), who states that $\langle M_v \rangle \sim +0.6$ 0.2 for the RR Lyrae stars in M3, M15, and M92. A rectangular error box is drawn in Figure 36 (dashed lines); the width corresponds to the temperature range of the observed blue edges and the length corresponds to the span in

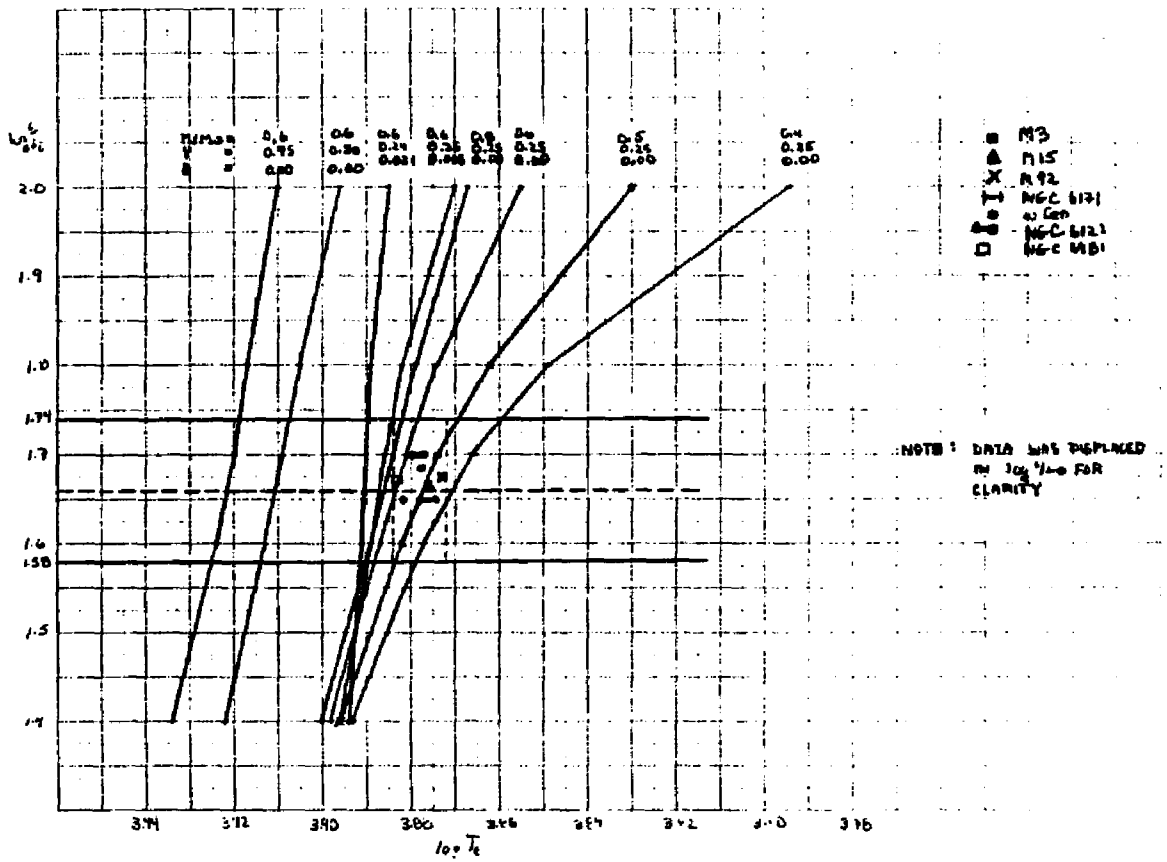

FIGURE 36

COMPARISON OF OBSERVATIONAL AND THEORETICAL BLUE EDGES

more precise values of basic parameters than those derived from the nonlinear survey. However, it did provide several methods of approach and the possibility of achieving more exact RR Lyrae parameters in the future. It also established that the Carson blue edges for models with M = 0.6 M*, Y = 0.25, and log (L/L*) ~ 1.7 are easily compatible with observed blue edges.

5.3 Concluding Remarks

By means of bumps, humps, shoulders, and other related quantities, light and velocity curves of RR Lyrae stars have been theoretically and observationally studied. The main purpose of this thesis was to obtain better understanding of the nature of these variables. In studying the fine details it was simple to put aside the importance of variable stars on the grander scale in astronomy.

Knowing the helium abundance of RR Lyrae stars in globular clusters, cosmologists will have a better value for the primordial helium content of our galaxy. By also knowing the luminosities of these stars, the galactic distance scale can be determined more accurately. RR Lyrae stars have been observed through Baade's window in the galactic nucleus. Moreover, the distribution of the globular clusters around the galactic bulge can also be calculated if reliable distances to the cluster RR Lyrae stars are available. Therefore, the distance to the galactic center can be determined if we have full knowledge of these pulsating stars.

Combining the luminosities and helium abundences of

RR Lyrae stars with results of stellar evolution calculations for horizontal branch stars, the ages of Population II stars are derived, and hence the age of the Universe. It is clear that the pursuit of the details of pulsating stars should be continued since these are important in developing our knowledge about the Universe.

REFERENCES

Abt, H. A. 1959, *Ap. J.*, 130, 824.

Baker, N. H., and Kippenhahn, R. 1962, *Zs. f. Ap.*, 54, 114.

. 1965, *Zs. f. Ap.*, 62, 868.

Baker, N. H., and von Sengbusch, K. 1969, *Mitt. Astr. Gesellschaft*, No. 27, p.162.

Bohm-Vitense, E., Szkody, P., Wallerstein, G., and Iben, I., Jr. 1974, *Ap. J.*, 194, 125.

Bonsack, W. K. 1957, *Ap. J.*, 126, 291.

Butler, D. 1975, *Ap. J.*, 200, 68.

Butler, D., Dickens, R. J., and Epps, E. 1978, *Ap. J.*, 225,148.

Carson, T. R. 1976, *Ann. Rev. of Astr. and Ap.*, 14, 95.

Carson, T. R., Mayers, D. F., and Stibbs, D. W. N. 1968, *M.N.R.A.S.*, 140, 483.

Carson, T. R., and Stothers, R. 1976, *Ap. J.*, 204, 461.

Carson, T. R., and Stothers, R., and Vemury, S. K. 1978, *Ap. J.*, 225, 939.

. 1981, *Ap. J.*, 244, 230.

Castor, J. I. 1971, *Ap. J.*, 166, 109.

Christy, R. F. 1964, *Rev. Mod. Phys.*, 36, 555.

. 1966, *Ap. J.*, 144, 108.

. 1967, In *Methods of Computational Physics*, ed. B. Adler (London: Academic Press), p. 191.

. 1968, *Quart. J. R. A. S.*, 9, 13.

Cox, A. N. 1980A, *Spa. Sci. Rev.*, 27, 475.

Cox, A. N., Hodson, S. W., and Clancy, S. P. 1983, preprint.

Cox, A. N., King, D. S., and Hodson, S. W. 1980, *Ap. J.*, 236, 219.

Cox, A. N., and Stewart, J. N. 1965, *Ap. J. Suppl.*, 94, 1.

. 1971, private communication with Tuggle and Iben (1972)

Cox, J. P. 1963, *Ap. J.*, 138, 487.

. 1964, *Ap. J.*, 140, 485.

. 1974, *Rep. Prog. Phys.*, 37, 563.

. 1980J, *Theory of Stellar Pulsation* (Princeton: Princeton University Press)

Cox, J. P., and Guili, R. T. 1968, *Principles of Stellar Structure* (New York: Gordon and Breach).

Deupree, R. G. 1977, *Ap. J.*, 214, 502.

Dickens, R. J. 1970, *Ap. J. Suppl.*, 22, 249.

Eddington, A. S. 1926, *The Internal Constitution of the Stars*, (Cambridge: Cambridge University Press; also available as a Dover paperback, 1959)

. 1941, *M.N.R.A.S.*, 101, 182.

. 1942, *M.N.R.A.S.*, 102, 154.

Epps, E., and Sinclair, J. 1973, *Obs.*, 93, 78.

Hardie, R. H. 1955, *Ap. J.*, 122, 256.

Hill, S. J. 1972, *Ap. J.*, 178, 793.

Iben, I. Jr. 1971a, *Ap. J.*, 166, 131.

. 1971b, *Pub. A. S. P.*, 83, 697.

Iben, I, Jr., and Huchra, J. 1971, *Astr. and Ap.*, 14, 293.

Kaplan, W. 1964, *Elements of Ordinary Differential Equations* (Reading, Mass: Addison - Wesley).

Kinman, T. D., 1959, *M.N.R.A.S.*, 119, 538.

. 1961, *R.O.B.*, 37, 151.

Ledoux, P., and Walraven, Th. 1958, *Handbuch der Physik*, ed. S. Flugge (Berlin: Springer - Verlag), 51, 353.

Lub, J. 1977, *Astr. and Ap. Suppl.*, 29, 345.

Muller, A. B. 1953, *Bull. Astr. Inst. Netherlands*, 12, 11.

Oke, J. B. 1966, *Ap. J.*, 145, 418.

Oke, J. B., and Bonsack, W. 1960, *Ap. J.*, 132, 417.

Oke, J. B., Giver, L. P., and Searle, L. 1962, *Ap. J.*, 136, 393.

Oosterhoff, P. Th. 1939, *Observatory*, 62, 104.

Paczynski, B. 1965, *ACTA Astr.*, 15, 115.

Preston, G. W. 1961, *Ap. J.*, 134, 633.

. 1965, *Ap. J.*, 142, 1262.

Preston, G. W., and Paczynski, B. 1964, *Ap. J.*, 140, 181.

Preston, G. W., Smak, J. I., and Paczynski, B. 1965, *Ap. J. Suppl.*, 12, 99.

Radziszewski, W. 1965, *ACTA Astr.* 15, 253.

Rood, R. T. 1971, *Ap. J.*, 169, 191.

Sandage, A. 1970, *Ap. J.*, 162, 841.

. 1981, *Ap. J.*, 248, 161.

Sandage, A., Katem, B. N., and Sandage, M. 1981, *Ap. J. Suppl.*, 46, 41.

Sanford, R. F. 1935, *Ap. J.*, 81, 149.

. 1949, *Ap. J.*, 109, 208.

Simon, N. R., and Schmidt, E. G. 1976, *Ap. J.*, 205, 162.

Spinrad, H. 1961, *Ap. J.*, 133, 479.

Stellingwerf, R. F. 1975, *Ap. J.*, 195, 441.

Stobie, R. S. 1969, *M.N.R.A.S.*, 144, 461.

. 1971, *Ap. J.*, 168, 381.

Stothers, R. 1974, *Ap. J.*, 194, 695.

. 1981, *Ap. J.*, 247, 941.

Struve, O., and Blaauw, A. 1948, *Ap. J.*, 108, 60.

Struve, O., and van Hoof, A. 1949, *Ap. J.*, 109, 215.

Tifft, W. G. 1964, *Ap. J.*, 139, 451.

Tifft, W. G., and Smith, H. J. 1958, *Ap. J.*, 127, 591.

Tuggle, R. S., and Iben, I. Jr. 1972, *Ap. J.*, 178, 455.

van Albada, T. S., and Baker, N. H. 1971, *Ap. J.*, 169, 311.

. 1973, *Ap. J.*, 185, 477.

Varsavsky, C. M. 1960, *Ap. J.*, 131, 623.

Vemury, S. K., and Stothers, R. 1978, *Ap. J.*, 225, 939.

Young, D. M., and Gregory, R. T. 1972, *A Survey of Numerical Mathematics* (Reading, Mass: Addison - Wesley).

Zhevakin, S. A. 1952, *Russ. Astron. J.*, 29, 37.

. 1963, *Ann. Rev. of Astr. and Ap.*, ed. L. Goldberg, 1, 367.